ABSTRACT

BODLE, JOSEPHINE CHENOA. Mechanisms of Adipose Stem Cell Differentiation: from Primary Cilia to Donor Populations. (Under the direction of Dr. Elizabeth Loboa).

Adipose-derived stem cells have recently emerged as a promising, abundant cell source for tissue replacement therapies for a wide range of applications, particularly in the area of musculoskeletal tissue engineering. In spite of recent research advancements towards developing stem cell therapies, there have been few successfully translated adult stem technologies to date. The goal of this research is to elucidate fundamental processes of human adipose-derived stem cell (hASC) differentiation, from the sub-cellular level, up to global changes in age and donor specific cell populations, with a particular focus on osteogenic differentiation. Though hASC are well established to differentiate into osteogenic cells types, exhibiting calcium accretion, an upregulation of osteogenic gene markers and an increase in alkaline phosphatase activity, the underlying mechanisms of these processes remain elusive. We hypothesized that an organelle known as the primary cilium plays an integral role in mediating hASC lineage specification. Primary cilia are composed of nine microtubule doublets arranged concentrically forming the axoneme of the cilium structure, however over 1000 proteins are estimated to be associated with the cilium. We have identified two particular cilia-associated proteins to play a role in hASC osteogenesis: polycystin-1 (PC1) and intraflagellar transport-88 (IFT88). Using siRNA knockdown techniques, we established that IFT88 expression was required to upregulate Runx2, an early gene marker of osteogenesis. Further, we established that knockdown of PC1 conferred reduced expression of later gene markers as well as a marked decrease in calcium accretion and endogenous alkaline phosphatase activity, indicators of osteogenic differentiation.

Following the study on chemically induced hASC differentiation, we generalized our hypothesis to explore the broader role of the primary cilium in hASC lineage specification. Previous reports from our group have identified 10% cyclic tensile strain to enhance hASC osteogenesis and we hypothesize the primary cilium functions in part as a mechanosensor in this process. To understand the cilium structure as a mechanosesnsor, we first wanted to analyze its morphology on the hASC population as well as on the osteogenically and adipogenically differentiated hASC populations. We found that in as few as three days of chemical stimulation, differentiating hASCs exhibited differential cilia expression. Cilia generally tended to be more prevalent in more committed cell types, however their expression was somewhat temporal during the differentiation process. Gene expression analysis of cilia-associated genes also suggested that cyclic tensile strain affects ciliary gene expression in addition to the frequency of expression of the cilia structure. In our efforts to uncover the fundamental mechanisms of hASC differentiation, we observed a persistent experimental challenge throughout a majority our studies: donor-to-donor variation. Behavior predictability is critical to the success of applying hASC technologies in the clinic, and without consistent cell behavior and predictable physiological profiles, hASC will not emerge as a reliable treatment method for tissue replacement therapies. The final study of this dissertation examines the degree of donor-to-donor variability within our lab's cell bank. Based on the observations in our cell lines, we hope that our findings may be extrapolated into the larger pool of information on hASCs. We highlight age-related changes in osteogenic and adipogenic differentiation and draw attention to important considerations for designing bench top experiments as well as creating clinically relevant technologies. Taken together, this dissertation addresses fundamental areas of research in adipose stem cell differentiation

towards improving knowledge of their *in vitro* behavior for bench top studies, as well as furthering our knowledge of patient-specific information to facilitate their future clinical application.

Mechanisms of Adipose Stem Cell Differentiation from Primary Cilia to Donor Populations

by
Josephine Chenoa Bodle

A dissertation submitted to the Graduate Faculty of
North Carolina State University
in partial fulfillment of the
requirements for the degree of
Doctor of Philosophy

Biomedical Engineering

Raleigh, North Carolina

2014

APPROVED BY:

Elizabeth G Loboa, PhD Committee Chair	Greg McCarty, PhD
Lola M Reid, PhD	Susan H Bernacki, PhD

Albert J Banes, PhD

DEDICATION

This dissertation is dedicated to my parents, John and Elberta Bodle, for without their support and guidance I never would have pursued science, to my big brothers Ethan and Tristan Bodle who inspire me to be better at what I do everyday and Titus for being my best bud throughout graduate school.

BIOGRAPHY

Josie Bodle was born in Kentfield, California on January 31st, 1984. She attended Northgate High School in Walnut Creek, CA and went on to UC Berkeley. In 2005 she graduated with a B.S. In Bioengineering and continued her studies at Cornell University where she received an M. Eng. in Biomedical Engineering in 2008 under the direction of Dr. Cynthia Reinhart-King. During her undergraduate and masters studies, Josie was also an active participant on the UC Berkeley and Cornell University Intercollegiate Figure Skating Teams. In the fall of 2008 she joined Dr. Elizabeth Loboa's Cell Mechanics Lab in the Joint Department of Biomedical Engineering at the University of North Carolina and North Carolina State University as a PhD student.

ACKNOWLEDGEMENTS

I would like to genuinely acknowledge all who have helped me in completing this body of work. I would like to thank my committee for their invaluable guidance through my tenure as a PhD student. I would like to thank Dr. Loboa for giving me the opportunity to be a part of this fantastic lab group, for her unwavering support, guidance, patience and critical discussion and evaluation of my work. I would like to thank Dr. Susan Bernacki for always having the time to answer even the most minute scientific questions and for her overall mentorship. I would like to thank Dr. Greg McCarty for our technical discussions on experiments and general career advice. I would like to thank Dr. Albert Banes for providing the platform and facilities for which we initiated this cilia project. I would like to thank Dr. Lola Reid for her guidance and unique perspectives on the field of tissue engineering stem cell differentiation.

Additionally, I would like to acknowledge the undergraduates that contributed to the success of this research: Candace Rubenstein, Ramey Williams, Michelle Phillips, Mehdi Hamouda, Leigh Atchison and Ashwin Sakhare. I would also like to thank Andrew DiMeo for his teaching mentorship. Further, I would like to acknowledge Dr. Lars Allan Larsen, Dr. Søren Christensen, and Dr. Lotte Pedersen for hosting me as a visiting graduate student in their labs at the University of Copenhagen and Dr. Cynthia Reinhart-King for continuing to support my research career. I would like to recognize my CML labmates, Audrey Charoenpanich, Mahsa Mohiti-Asli, Pattie Mathieu, Stephanie Teeter, Carla Haslauer, Wayne Pfeiler, Stephen Tuin, Liliana Mellor and Sonya Sonnenberg for insightful scientific

discussions and friendships. Lastly, I am so grateful to the following people for their unending support throughout my time in grad school; through proofreading, helping with graphics, listening to me discuss data or to just go for a run, sit down for a lunch or a cold beer: Big thanks to Brett Hartsfield, Erin Jerkins, Ryan Boehm, Chris Grigsby, Lani Chan, Eric Morrow, Achiamar Lee, Titus Bodle and Shasta Grigsby.

TABLE OF CONTENTS

LIST OF TABLES

LIST OF FIGURES

Chapter 1 Introduction

1.1 Objectives

Research in tissue engineered cell-based therapies has shown great promise over recent years, though as a field it has largely failed to deliver many impactful clinical treatments, particularly for critical defect musculoskeletal injuries. Current barriers to clinical success include issues of construct size, mechanical integrity, biocompatibility, immunogenicity, cell source and cell phenotype. The issue of cell source is particularly critical for generating autologous tissue-based therapies and human adipose-derived adult stem cells (hASC) have proven to be an abundant candidate for such therapies (*1*-*3*). However, when working with any stem cells, it is necessary to consider the methods used to differentiate the stem cell into the desired cell phenotype, and how that phenotype will be defined in the context of a functional tissue construct. For the purposes of this study we will be focusing primarily on bone and fat tissue phenotypes. These tissue types are not only defined by their distinct biochemical make up, but also their distinctly different tissue mechanical properties. From the perspective of providing an hASC-derived tissue construct to emulate the native environment of bone or fat, it is critical to understand how the biochemical and mechanical environment is sensed by hASC and how this affects the differentiated hASC phenotype. Understanding the cellular mechanisms of hASC chemically and mechanically induced differentiation will further our progress towards producing optimally autologous, functional tissue engineered replacements to improve treatments of critical defect injuries.

In this dissertation we focus on one such sensing mechanism via an organelle known as the primary cilium. Primary cilia are organelle structures present on a variety of mammalian cell types and are thought to be both chemo- and mechanosensors (*4*). Additionally, they are known to be integral signaling structures in the process of cellular differentiation in the developing embryos. This study aims to elucidate how the dynamic primary cilium structure functions in hASC lineage specification. This project focuses on three specific cilia proteins: Intraflagellar transport-88 (IFT88), polycystin-1 (PC1) and polycystin-2 (PC2). IFT88 is important in generating the structure of the primary cilium and has been implicated in controlling stem cell differentiation (*5*). PC1 and PC2 are the proteins associated with the development of autosomal polycystic kidney disease and the loss of mechanosensitivity in kidney epithelial cells (*6*). Based on our knowledge of the primary cilium as a chemo and mechanosensor, this study aims to systematically tease out its chemical, mechanical and combined synergistic sensing/signaling mechanisms involved in hASC differentiation. To that end, our approach utilizes siRNA transient knockdown methods and physical abrogation methods to disrupt the primary cilia in hASC in a variety of culture systems. Static two-dimensional (2D) culture in standard tissue culture plastic, static 2D culture on substrates of varying stiffness, dynamic 2D culture on collagen I-coated silicone membranes and dynamic 3D culture in collagen I gels. Our dynamic culture system uses 10% cyclic tensile strain, based on our previous evidence of enhanced hASC osteogenesis under this loading modality. Each of these four culture methods isolates different external effectors of hASC lineage specification moving from the most simplistic 2D model, to the 3D model simulating a rudimentary in vivo environment. The systematic

four-model approach will facilitate teasing out the multi-facet mechanisms of the complex primary cilium organelle and improve our ability to optimize hASC phenotypic commitment in autologous tissue engineered constructs.

1.2. Human Adipose Stem Cells

Adipose stem cells (ASC) are stem cells derived and isolated from fat pads that can be removed from almost any site of the body. Human adipose-derived adult stem cells (hASC) have emerged as an attractive multipotent cell population for use in tissue replacement therapies. As a potentially autologous cell source, they show great promise as a more abundant alternative to human bone marrow-derived mesenchymal stem cells (hMSC).

Purification techniques yielding hASC range from selection by adherent culture to rigorous surface marker cell sorting techniques and clonal culture (*2*, *7-9*). The most widely utilized method to isolate ASC is simply to propagate the adherent cell fraction from adipose tissue without surface marker selection, particularly in the context of tissue engineering applications. Despite the use cell surface marker enrichment techniques, it has been demonstrated that adherent cell populations isolated from adipose tissue tend toward a characteristic surface marker expression profile after propagation in culture (*10*). Nonetheless, the surface profile is not necessarily an indicator of ASC potency.

In the clinical setting, not only do hASC present advantages due to their autologous potential to overcome issues of immunogenicity and host rejection, they also present a number of advantages over other stem cell types. As compared to their bone marrow-derived hMSC counterparts, not only are they more abundant, they also do not have the yield and scalability issues associated with hMSC isolation and culture. This unique attribute is

particularly important when using them as a primary cell source for autologous tissue replacement applications. Population heterogeneity and donor-to-donor variation in potency still remain common challenges in most adult stem cell types and these issues need to be further investigated when manipulating hASC.

However, hASC are relatively easy to maintain in culture as they readily self-renew and have the ability to commit to a range of lineages including adipogenic (Figure 1.1a), osteogenic (Figure 1.1b), chondrogenic (*2*), myogenic, neuronal (*11*), cardiomyogenic (*12*), and endothelial (*13*) with the addition of chemical induction factors. Due to their versatility, we aim to explore and elucidate their mechanisms of differentiation to efficiently harness their potential use as a cell source for engineered musculoskeletal tissue replacements.

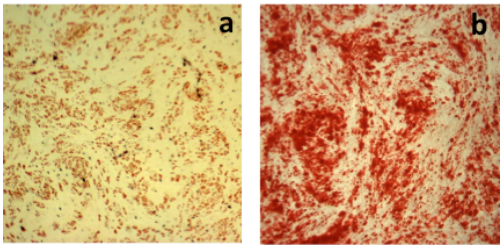

Figure 1.1 Adipogenic and osteogenic differentiation of hASC. a) Oil Red O staining of ASC cultured in adipogenic media for 14 days; presence of cherry red oil droplets indicate adipogenic differentiation. b) Alizarin Red staining of ASC cultured in osteogenic media for 14 days; presence of dark red calcium deposits indicates osteogenic differentiation.

1.3 Mechanical Environment and Stem Cell Differentiation

While chemical induction is the principal approach to stem cell differentiation, modulating the physical and mechanical environment is also now understood to be an integral part of stem cell lineage specification, particularly in musculoskeletal lineages (*14-18*). The physical culture environment can be modulated through a variety of "passive" and/or "active" culture modalities. For the basis of this dissertation we focus on application of cyclic tensile strain as an active application of mechanical stimulation and culture

dimensionality; and modulation of substrate stiffness as a form of passive mechanical stimulation. Early work by Thomas and El Haj in 1996 and Yoshikawa et al. in 1997 demonstrated some of the first evidence of in vitro mechanosensitivity in MSC, implicating the role of tensile strain for MSC osteogenic specification (*19*, *20*). Further, stemming from in vivo work with distraction osteogenesis (*21*, *22*), cyclic tensile strain has been shown to establish successfully enhanced osteogenic induction of bone marrow-derived MSC in vitro (*14*, *23-25*). Extending the optimal in vivo distraction osteogenesis parameters to an in vitro model, Sumanasinghe et al. found that even in the absence of osteogenic differentiation medium (i.e. cells maintained in complete growth medium) 10% cyclic tensile strain, applied at a frequency of 1 Hz, for 4 hours/day, resulted in an upregulation of BMP-2 in MSC seeded in a three-dimensional collagen I matrix after 1 week, a significant 4-fold increase over unstrained samples (Loboa et al., 2004). Likewise, Ignatius et al. reported that cyclic tensile strain (1% at 1 Hz for 1800 cycles/day) applied to osteoblastic precursor cells for 3 weeks resulted in slight increases of histone H4, alkaline phosphatase, CBFα1 (runx2), and osteopontin compared to unstrained controls (*26*). Lower frequencies of strain (2.5% at 0.17 Hz) have also been shown to enhance osteogenesis in MSC and reduce their proliferation rate, hinting at the relationship between mechanically signaled proliferation and differentiation (*27*).

The role of mechanical stimulation in ASC differentiation is following in the stride of MSC, though the mechanotransduction mechanisms in both cell types remain an active area of investigation. In hASC, we have demonstrated enhanced osteogenesis when exposed to 10% cyclic tensile strain, though the mechanism to this process has remained largely elusive

(*15*). The basis for mechanically directed differentiation is increasingly supported through the evidence of behavioral changes in bone tissue and cells (osteoblasts, osteoclasts and osteocytes) in response to mechanical signals such as fluid flow and tensile strain in committed cell types, and provides support for exploring the role of mechanical stimulation in hASC osteogenic differentiation.

1.4 Primary Cilia

Discovered over a century ago, non-motile primary cilia were largely regarded as vestigial organelles, despite their prevalence on a variety of mammalian cell types (*4*). More recently, they have been implicated as critically important chemo- and mechanoresponsive cell surface structures, hinting at their role in functional phenotypic maintenance in a variety of mammalian cell types (*28*, *29*). Kidney, bone, fat and cardiac cells, have been identified as having dynamic, multifunctional primary cilium organelles (*6*, *30-32*). Emerging evidence from our group and others suggests in addition to tissue homeostasis, they may also be involved in signaling stem cell lineage commitment in embryonic development as well as in adult stem cells, in the in vivo and in vitro environment (*33-35*).

The non-motile primary cilia axoneme projects from the apical cell surface, consisting of a set of nine peripheral microtubule doublets arranged in a 9 + 0 configuration (Fig. 3). This is in contrast to motile cilia, which have a 9 + 2 arrangement, to include a doublet pair of microtubules in the center. Assembly of the primary cilia is cell cycle dependent and most mammalian cells types express primary cilia at some point during the cell cycle (*29*). The scope of the primary cilium's function remains largely elusive, though evidence suggests that

its function is complex, acting as an important site for intracellular signaling (*35*) as well as detecting external chemical and mechanical changes in the extracellular environment (*33*).

Non-motile primary cilia have been most thoroughly studied in kidney epithelial cells under the autosomal polycystic kidney disease model. The loss of cilia, and associated proteins polycystin-1 (PC1) and polycystin-2 (PC2), in the kidney epithelial cells is associated with the loss of epithelial cell mechanosensitivity, leading to development of cysts and deregulation of tissue morphogenesis (*6*, *36*). Polycystin-1 and polycystin-2 are colocalized to the primary cilium and are thought to have a large part of their functional activity at the site of the cilium (*37*). In the primary cilium, PC1 is thought to be involved in cell-cell and cell-matrix interactions and PC2, when associated with PC1 forms a stretch activated calcium channel (*37*, *38*). Additionally, polycystin-1 localizes to other subcellular compartments including the apical cell membrane. Polycystin-2 is found in the plasma membrane and the membrane of the endoplasmic reticulum (*37*).

IFT88 is a critical intraflagellar transport protein necessary to support ciliary structure and protein transport (*35*). IFT88 knockout mouse models generate a polycystic phenotype, similar to those observed with dysfunctional PC1/PC2, suggesting IFT88 plays a critical role in supporting cilia functionality (*39*). Malone et al. showed that siRNA knockdown of intraflagellar transport-88 (IFT88) reduced the frequency of primary cilia observed on osteoblastic cell lines. Subsequently they also showed reduced expression of osteogenic gene markers known to be upregulated with fluid shear stimulation, indicating a suppression of functional osteogenic phenotype (*30*). This work demonstrated some compelling in vivo

evidence of primary cilia modulated mechanosensitivity to fluid flow in osteogenic cell types.

As introduced previously the primary cilium is a complex organelle having chemosensory, mechanosensory and structural roles in cell signaling. Primary cilia generation corresponds to the cell cycle and is the site of hedgehog (Hh) signaling, an important regulator of proliferation and associated cell cycle control (*40*). Knockdown of cilia proteins IFT88 and IFT20 in pluripotent embryonic stem cells disrupts Hh signaling in the cilium, preventing cardiogenesis (*32*). Further, siRNA knockdown of IFT88 in bone marrow-derived mesenchymal stem cells (MSCs) downregulated gene expression in early gene markers in osteogenesis, chondrogenesis and adipogenesis (*41*). These data suggest the cilium architecture may critically modulate control between proliferation and differentiation signaling.

Each of these three key ciliary proteins (PC1, PC2, IFT88) crucially defines the structural and functional properties in the cilia, and they are the proteins of interest in this hASC. The goal of this project is to explore the role of the primary cilium as a "master switch" controlling hASC differentiation and implications for hASC approaches in generating autologous tissue replacement therapies. The background data on primary cilia as dynamic chemo- and mechanosensors in a variety of tissues as well as their role in the developing embryo provides compelling evidence that they play an important role in hASC differentiation.

1.5 Clinical Significance

Tissue engineering has the potential to revolutionize the way we treat a wide demographic of patients, ranging from the severe limb injuries of our wounded warriors to myocardial infarction of the standard heart attack patient. However, host rejection and immunogenicity remain key barriers to the widespread application of tissue-engineered treatments generated from allograft cell sources. Human adipose-derived adult stem cells, (hASC) are an attractive, potentially autologous, multipotent cell population for use in tissue replacement therapies, making them an ideal cell source population for tissue engineering applications. Due to their vast clinical potential in treating critical defect injuries, ASC have gained popularity in cartilage and bone tissue engineered constructs (*3*). Despite these advantages, it is necessary to fully understand the mechanisms controlling hASC differentiation, to best harness their potential, though the mechanisms of the differentiation process remain elusive.

Interestingly, hASC possess primary cilia, unique chemo- and mechanosensing organelles, that may be a key regulators in this process of hASC differentiation. Though at first thought it would seem that studying one specific cell organelle process may not have significant clinical impact, tightly controlling stem cell fate would tremendously affect the efficacy of a potential autologous tissue replacement. In studying primary cilia-mediated hASC differentiation, we hope to uncover key mechanisms behind chemically and mechanically induced lineage specification processes. In turn, this understanding will aid in optimizing culture methods, both for directing hASC cell phenotype from the bottom up, and for creating and maintaining functional cell phenotype within an entire tissue construct.

Mechanistic understanding can help overcome some major barriers plaguing the use of stem cells in clinical applications for critical defect tissue replacements, particularly in mechanical tissue such as bone.

1.6 Specific Aims

Aim 1: Primary cilia chemosensing. Evaluate and establish the basic mechanisms of primary cilia chemosensing in hASC chemically induced osteogenic lineage specification. Cilia structure and function was disrupted using siRNA cilia abrogation techniques.

> *Hypothesis: siRNA knockdown of cilia-associated proteins PC1, PC2 and IFT88 during chemically-induced hASC leads to disruption of hASC osteogenic and adipogenic differentiation as measured by diminished expression of osteogenic gene expression markers as well as diminished end product expression.*

The goal of this aim was to establish the baseline the chemosensory behavior of primary cilia and to establish whether disruption of this structure affected hASC osteogenesis in the static culture environment.

Aim 2: Cilia Mechanosensing in 2D. Evaluate and analyze the effect of cyclic tensile strain on primary cilia structural conformation and subsequently its functional activity in mechanically induced hASC differentiation in 2D culture.

> *Hypothesis: A structurally and/or functionally intact primary cilia is critical in signaling and mediating mechanically enhanced hASC osteogenesis through cyclic tensile strain.*

Based on previous work in our lab, we had established the mechanosensitivity of hASCs undergoing osteogenesis, but had very limited data on the mechanisms transducing these

processes. The goal of aim 2 was to establish the role of the hASC primary cilium, if any, under a mechanically stimulated growth environment. The long-term objective of this was to determine whether the primary cilium may be a novel target in manipulating hASC phenotype.

Aim 3: Understanding Donor-to-Donor Variability in hASCs. Systematically characterize the baseline differentiation behavior of age-clustered donor cell populations to validate the use of pooled donor superlots.

Hypothesis: Pooled donor cell superlots will represent average differentiation behaviors of each individual donor cell line and may also provide average consensus hASC behavior for a particular age group.

In our efforts to study fundamental mechanisms of chemically and mechanically-induced hASC differentiation, we, as investigators skew our own data by pre-selecting cell lines that have similar levels of multipotency, while excluding other hASC lines. When working with primary hASC populations, our worked is plagued with a high level of donor-to-donor variability. The goal of aim 3 was to take a step back from answering fundamental questions about hASC differentiation and to address more global feasibility issues in understanding hASC physiology and differentiation behavior with clinical translation applications in mind.

CHAPTER 2 Adipose-Derived Stem Cells in Functional Bone Tissue Engineering: Lessons from Bone Mechanobiology

This chapter has been published in the Journal of Tissue Engineering Part B: Reviews under the following citation:

Bodle JC, Hanson AD, Loboa EG.
Adipose-derived stem cells in functional bone tissue engineering: lessons from bone mechanobiology.
Tissue Eng Part B Rev. 2011 Jun;17(3):195-211. doi: 10.1089/ten.TEB.2010.0738. Epub 2011 Apr 8. Review.
PMID: 21338267

TISSUE ENGINEERING: Part B
Volume 17, Number 3, 2011

DOI: 10.1089/ten.teb.2010.0738

Adipose-Derived Stem Cells in Functional Bone Tissue Engineering: Lessons from Bone Mechanobiology

Josephine C. Bodle, M.Eng.,[1] Ariel D. Hanson, M.S.,[1] and Elizabeth G. Loboa, Ph.D.[1,2]

This review aims to highlight the current and significant work in the use of adipose-derived stem cells (ASC) in functional bone tissue engineering framed through the bone mechanobiology perspective. Over a century of work on the principles of bone mechanosensitivity is now being applied to our understanding of bone development. We are just beginning to harness that potential using stem cells in bone tissue engineering. ASC are the primary focus of this review due to their abundance and relative ease of accessibility for autologous procedures. This article outlines the current knowledge base in bone mechanobiology to investigate how the knowledge from this area has been applied to the various stem cell-based approaches to engineering bone tissue constructs. Specific emphasis is placed on the use of human ASC for this application.

Introduction

Adipose-derived stem cells (ASC) have become an attractive multipotent cell population for use in tissue replacement therapies. They are a rapidly emerging alternative to the traditional bone marrow-derived mesenchymal stem cells (MSC), though the two cell types have many phenotypic similarities. As an abundant and autologous cell source, use of ASC in tissue-engineered constructs minimizes immunogenicity concerns associated with allograft-based methods. ASC are relatively easy to maintain in culture as they readily self-renew and have the ability to commit to a range of lineages including adipogenic (Fig. 1a), osteogenic (Fig. 1b), chondrogenic, myogenic, neuronal,[1,2] cardiomyogenic,[3] and endothelial.[4] Due to their vast clinical potential in treating critical defect injuries, ASC have gained popularity in cartilage and bone tissue engineering constructs.[5]

It has long been established that bone responds to changes in its mechanical environment. Documented observations date back to the development of Wolff's Law, in the late 19th century, which described loading induced architectural adaptations in bone, remodeling its structure through a feedback system.[6] In later years, these ideas were expanded further by Harold M. Frost, who proposed that a minimum effective strain, or "set point," determined the remodeling process; when strains in the bone exceed the set point, mechanically controlled remodeling acts to increase bone mass and the reverse occurs with strains below the set point.[7]

Much of the contemporary evidence of bone mechanosensitivity has derived from a multitude of disuse osteoporosis studies[8] and microgravity experiments,[9] as well as exercise and loading studies.[10,11] This body of work provided substantial evidence that increased loading conditions induced bone formation, and reduced loading conditions induced osteoporotic phenotypes, leading to exploration of these patterns in *in vitro* experimental models. Corresponding work demonstrated that bone cells in culture exhibit mechanosensitivity, and upregulate genes associated with bone formation, in response to mechanical strain and fluid shear, as previously reviewed by Ehrlich and Lanyon.[12] Given the wealth of *in vivo* and *in vitro* evidence, mechanical forces are considered increasingly crucial for success of current bone tissue engineering methods,[13] and are of particular interest in the context of directing ASC osteogenic differentiation.

In 2001 Zuk *et al.* were the first to establish ASC as a multipotent stem cell population, with the ability to assume osteogenic as well as chondrogenic, adipogenic, and neurogenic phenotypes, through chemically induced differentiation.[1,14] Zuk *et al.* found that when ASC were cultured in osteogenic differentiation media for 2–6 weeks, osteogenic specification was detected by increases in alkaline phosphatase activity, calcium accretion, and upregulation of bone specific gene markers.[1] In general, chemical induction of lineage specification has been the most prevalent method used to direct stem cells for tissue engineering applications. However, it is now understood that functional tissue engineering of load bearing tissues likely requires additional physical stimuli (mechanical or electrical) concurrently with chemical stimuli.[15–23]

A quickly emerging scheme in stem cell differentiation for tissue engineering applications involves simulating a

[1]Joint Department of Biomedical Engineering, University of North Carolina at Chapel Hill and North Carolina State University, Raleigh, North Carolina.
[2]Department of Materials Science and Engineering, North Carolina State University, Raleigh, North Carolina.

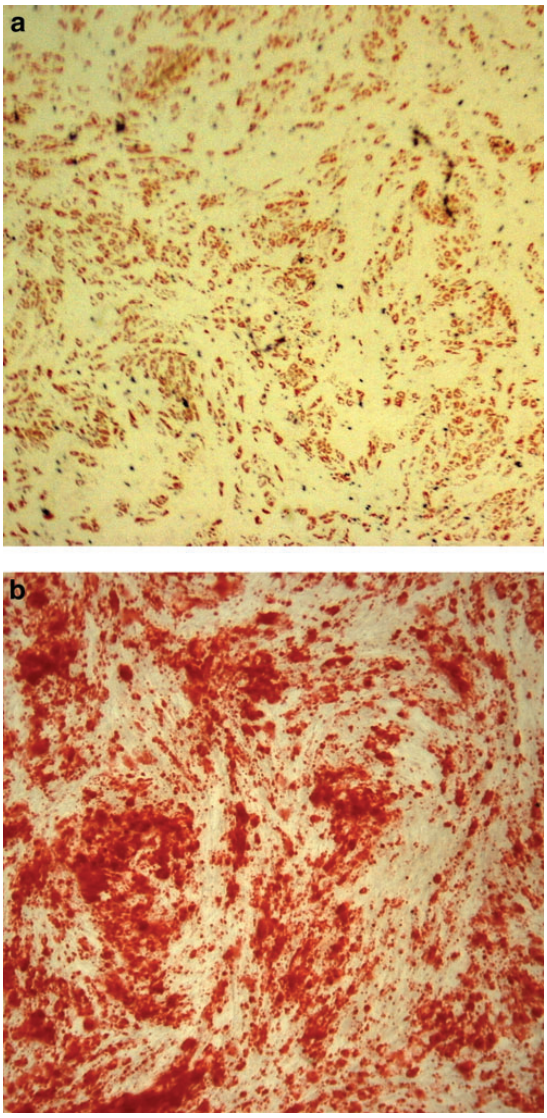

FIG. 1. Adipogenic and osteogenic differentiation of ASC. **(a)** Oil Red O staining of ASC cultured in adipogenic media for 14 days; presence of cherry red oil droplets indicates adipogenic differentiation. **(b)** Alizarin Red staining of ASC cultured in osteogenic media for 14 days; presence of dark red calcium deposits indicates osteogenic differentiation. ASC, adipose-derived stem cell. Color images available online at www.liebertonline.com/teb

physiologically relevant growth environment for the generated tissue construct. A large part of this effort includes emulating the *in vivo* mechanical environment experienced by the cells in an *in vitro* culture. Two major approaches have been used to modulate the mechanical environment of cells and/or tissue-engineered constructs in culture: (1) bioreactors applying "active" mechanical signals such as fluid shear, electrical stimulation, tensile, or compressive strain[13,15,24–26] and (2) somewhat "passive" signaling applied through modulation of substrate biochemical composition and stiffness.[27–30] A number of custom-designed[31–34] and commercially available bioreactor systems[15,21,22] are used to apply the signaling modalities discussed in this article, though the versatility of each system is often constrained by design criteria. Bioreactor development remains an active area of research, as bioreactors have become increasingly relevant to overcoming common challenges in tissue engineering. They are also emerging as tools to seed cells throughout three-dimensional (3D) scaffold materials,[31,35] as well as devices to validate mechanical and electrochemical properties of a construct.[36] As bone functions largely as structural support for the body, construct mechanical integrity is tantamount to applying physiological loading regimes in an *in vitro* culture environment to generate the construct. Both substrate properties and bioreactors have proven to be an integral part of mechanical approaches to directing ASC lineage specification toward an osteogenic phenotype.[21,30,34,37]

To create an ASC-derived functional tissue-engineered bone construct for regenerative medicine applications, the construct must carry out the necessary biochemical processes characteristic of healthy bone. To that end, it must emulate the morphology and mechanical behavior of native bone tissue. We refer to this tissue-level construct design approach as a "Top-Down" approach to creating ASC-derived tissue-engineered bone constructs. In contrast, we refer to cell-level approaches as "Bottom-Up." On a cellular level, the construct should contain cells of an osteogenic phenotype, which respond appropriately to physiologically relevant biochemical and mechanical stimuli. The successful generation of these functional constructs relies on the intersection of Top-Down and Bottom-Up approaches, thoroughly elucidating how mechanical signals affect ASC fate and behavior, in the context of synthesized tissue-level replacements.

This review aims to summarize the current knowledge of mechanotransduction in ASC lineage specification and how this information has been used in bone tissue engineering with ASC. We will begin by briefly reviewing relevant current knowledge of the mechanical environment and mechanotransduction processes in bone. The knowledge in this area has built the foundation for understanding appropriate physical stimuli and growth environments for the creation of stem cell-derived bone tissue engineering constructs. Framed through the context of bone mechanobiology, we will discuss current mechanobiological approaches applied in ASC osteogenic differentiation and methods in bone tissue engineering. Additionally, we will discuss some of the major studies involving bone marrow-derived MSC as a basis for comparison with ASC, though we will not cover MSC in depth. For a comprehensive review of mechanical control of MSC differentiation to osteochondral tissues, we refer the reader to a recent review by Knothe Tate *et al.*[29] We will conclude with a general summary of the field and comments on its future directions. A schematic illustrating the progression of the field and the topics covered in the article is provided in Figure 2.

Mechanosensitivity of Bone

To determine appropriate mechanical loads for functional bone tissue engineering using ASC, we must first understand

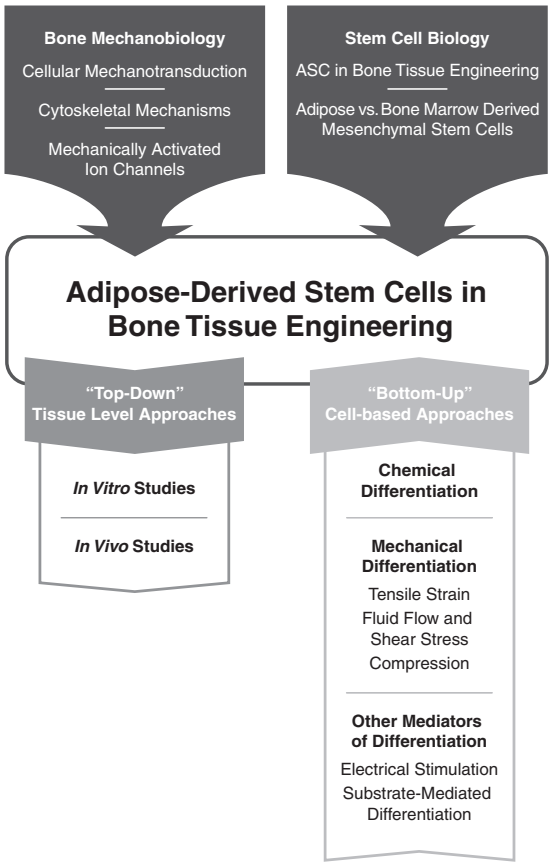

FIG. 2. General schematic illustrating the flow of information provided in this review describing the development and progression of the field. The field of stem-cell-derived bone tissue engineering emerged as a marriage of approaches from bone mechanobiology and stem cell biology. The combination of these two fields has now developed into two different approaches to creating a bone tissue construct: "Top-Down" approaches utilizing the more traditional cell and scaffold tissue level approach meant for immediate translation from bench-to-bedside, and "Bottom-Up" cell-level approaches to characterize the cell population behavior for construct component-level optimization.

the typical mechanical environment experienced by bone cells *in vivo.* From the cellular perspective *in vivo,* active mechanical loading of bone translates into either strain through small deformation of the calcified matrix, or fluid shear stress produced by interstitial fluid movement in the osteocyte canaliculi.[33] When bone is loaded, both bending and compressive forces create degrees of strain on the bone surface[38] and concurrently, on the osteocytes and bone-lining cells.[5] The tensile strain imposed on the osteocytes and bone lining cells leads to a change in cytoskeletal conformation. This change is associated with induced activation of stretch-activated ion channels,[38,39] voltage sensitive channels via an influx of calcium and shift in membrane potential,[38,40] and stretch-activated cation channels.[38]

Additionally, the resulting compressive strain from external loading causes an increase in interstitial fluid pressure, forcing the fluid to flow from regions of high pressure to regions of lower pressure[33,41] within the bone matrix. However, because the matrix is so stiff, the deformation as a result of physiological loads is very small (on the order of 0.2%).[42,43] This leads to the canalicular fluid flow hypothesis, which proposes that these small strains impose a local force that initiates fluid flow between thin layers of non-mineralized matrix surrounding the osteocytes' bodies and processes, thus creating a shear stress (8–30 dyn/cm^2) at the osteocyte cell membrane.[44,45]

This section provides a brief overview citing some of the major studies in bone mechanotransduction. All current work in ASC osteogenesis builds off of the basis of bone's chemical, electrical, and mechanical environments, and we will limit the discussion to the relevant mechanisms currently applied in directing ASC differentiation. For thorough reviews on the current state of bone mechanobiology and its implications in tissue engineering applications, we refer the reader to reviews by Riddle and Donahue[46] and Allori *et al.*[47]

Cellular mechanotransduction in bone

Osteocytes and bone-lining cells are presently thought to be the primary mechanosensory cells responsible for interpreting mechanical forces in bone tissue and translating them to osteoblasts and osteoclasts for bone remodeling.[33,45,48,49] Multiple investigators report evidence supporting the key mechanosensory role of osteocytes in bone formation as detected by changes in matrix protein expression, and production of nitric oxide (NO) and prostaglandin E_2 (PGE_2), a potent stimulator for bone formation.[50,51] Osteocytes have been found to be more mechanically sensitive to pulsatile fluid flow (PFF) than osteoblasts and periosteal fibroblasts, as only osteocytes increase production of PGE_2 in response to such mechanical stimulation.[51] These findings have been further validated by increased NO production in osteocytes in response to PFF, with increases not exhibited by periosteal fibroblasts.[45,51] More recent studies using microarray analysis have also identified the mechanosensitivity of osteoblasts to PFF. Thi *et al.* identified the upregulation of vascular endothelial growth factor and other associated genes in MC3T3E1 cells, an osteoblastic cell line, in response to PFF.[52] That work suggested that PFF stimulates signaling pathways crucial to the bone healing and remodeling processes, and identifying these markers of osteogenic healing is of particular relevance in ASC osteogenic lineage transition.

Osteoblasts, perhaps the most relevant cell type to the ASC-derived osteogenic phenotype, have also demonstrated sensitivity to oscillatory fluid flow (OFF), believed by some to be a more physiologically relevant mode of mechanical stimulation in bone.[52,53] OFF has been shown to affect osteoblasts: calcium mobilization, mitogen-activated protein kinase activity, and expression of osteopontin (OPN), a bone-specific matrix protein.[53] Increases in these metabolic bone markers have been reported to occur in minutes to hours after continuous exposure to OFF.[53] Subsequent studies have reported differences in osteoblast

behavior in response to continuous OFF and rest-inserted OFF, manifested in changes in intracellular calcium and OPN expression.[54] Qin *et al.* illustrated an analogous mechanosensitivity *in vivo* through oscillating the intramedullary pressure in the marrow cavity of functionally isolated ulnae in adult turkeys. The adaptive response of the bone was observed after 4 weeks of disuse. The disuse ulna exposed to 10 minutes of OFF per day exhibited increased bone formation on both the endosteal and periosteal surfaces as compared to the control, an ulna not exposed to fluid shear.[55] Additional work has suggested osteoblast and osteocyte behavioral response to fluid flow is further modulated by the surface micro-architecture of the cell substrate.[56] Generally, in both *in vitro* and *in vivo* studies, bone cells have shown sensitivity to dynamic fluid shear, which has led directly to its exploration as a mechanical stimulation modality in ASC, as discussed in section Fluid flow and shear stress.[34]

Uniaxial tensile strain has been used as another mode of mechanical stimulation to successfully induce bone regeneration *in vivo* via distraction osteogenesis.[57–62] Buchman *et al.* developed a rat model establishing specific parameters, including critical bone defect size as greater than 3 mm to sufficiently study the mechanisms of distraction osteogenesis and provide a quantitative distinction from conventional bone fracture healing.[59] Following this work, in an *in vivo* study utilizing rat models, Loboa *et al.*[63] reported that gradual distraction of the hemi-mandible (0.25 mm every 12 h) over 8 days, followed by 28 days of rest resulted in periosteal bone formation by postoperative day 7 and a full bridge of new bone spanning the width of the distraction gap by postoperative day 41.[57] Our empirical and computational investigations of the regions with the highest rate of new bone formation indicated that tensile strains in the range of 10%–12.5% appeared to optimally induce the highest rate of bone regeneration in the distraction callus.[57,63] A similar study by Meyer *et al.* reported that distraction osteogenesis of the mandible under physiological magnitudes (2000 microstrain) resulted in woven bone formation and some lamellar ossification after 14 days. Over the same time period, a magnitude of 20,000 microstrains resulted in thin trabecular bone formation over the entire gap, and active osteoblasts could be seen on a layer of primary bone.[62] These *in vivo* strain-stimulated bone formation studies have provided the parameter basis adapted to *in vitro* cyclic strain systems to stimulate osteogenesis in ASC.[21] Taken together, these studies provide convincing evidence that osteoblasts and osteocytes are highly mechanosensitive cells capable of differentially sensing mechanical deformation. Harnessing these sensing mechanisms is likely significant for ASC osteogenic lineage specification.

Cytoskeletal mechanisms of mechanotransduction in bone

There are many possible mechanisms by which bone cells interpret external mechanical loads and transmit them via biochemical signals. One such method involves the extracellular matrix-integrin-cytoskeleton network.[38,50,64,65] Transmission of mechanical stimulation across the cell surface is modulated by transmembrane receptors (i.e., integrins, cell adhesion molecules, and cadherins) that connect the cytoskeleton to an external substrate.[66] This connection provides a molecular pathway for mechanical signals to be passed across the cell surface, allowing focal adhesion molecules to act as mechanoreceptors.

The transmission of mechanical signaling via the connection between integrins and the cytoskeleton has been linked to intracellular pathways that dictate cell viability,[67] proliferation,[68–70] morphology,[67,70] and differentiation.[65,68,69,71,72] Tong *et al.* reported evidence of mechanically transduced signaling as mediated by integrins and focal adhesion kinase in critical defect healing during distraction osteogenesis. Further, they suggested that the mechanical signals were specifically inducing bone formation as detected by bone sialoprotein mRNA expression patterns.[65] Mechanistic studies report that PFF results in fluid shear stress-induced reorganization of actin, concurrent with actin-dependent increases in cyclooxygenase-2 (COX-2), c-Fos expression, and PGE_2 release, important markers of mechanically induced bone formation.[50,73] Together, these results demonstrate the critical role that actin stress fibers and their anchorage to the substrate via focal adhesions have on the mechanotransduction of external mechanical loads and subsequent bone formation.

Similarly, cell–cell interactions and connections have been implicated as a mechanism in transmitting intercellular mechanical signals in bone cells. This cell–cell signaling is associated with the initiation of bone formation and has been suggested to occur via a network of gap junctions and cadherins connecting osteocytes to osteoblasts and osteoclasts.[49,74–76] Osteocytes, exposed to a fluid shear stress of 4.4 dyn/cm^2 in an osteocyte–osteoblast co-culture system, mediate the upregulated alkaline phosphatase activity response in osteoblasts, as evidenced by Taylor *et al.* in 2007.[76] Although not immediately relevant to the current state of ASC osteogenic work, this study brings up an important point relating the dynamic process of mechanical signaling in bone. The intercellular transmission of mechanical signals among different osteogenic cell types will be directly relevant to the functionality of an ASC-derived bone construct in the future.

More recently, primary cilia have been implicated in the mechanosensitivity and transduction of mechanical signals in bone cells.[32,77] The primary cilium, present on most mammalian cell types, was previously believed to be a vestigial organelle. It was later characterized as a mechanosensing organelle in kidney epithelial cells with its dysfunctionality linked to development of polycystic kidney diseases.[78] Similarly, its role as a mechanosensor on osteoblasts has been characterized through physical abrogation of the primary cilia as well as siRNA knockdown of ciliary proteins. Malone *et al.* illustrated significant reduction in gene expression of PGE_2 and OPN in primary cilia-free MC3T3E1 cells, as compared to MC3T3E1 cells with intact primary cilia. The reduction in expression was consistent for both siRNA protein knockdown and physical removal of the cilia.[32] The role of primary cilia in bone mechanotransduction is under active investigation, as more knowledge is needed to truly understand its role in bone mechanotransduction and its mechanism of action. However, this emerging evidence along with preliminary work in our group hints that it may be a potential mechanistic mediator of osteogenic differentiation in adult stem cells.[79]

Mechanisms of mechanically activated ion channels

Although they are not extensively studied in mechanically mediated ASC osteogenesis, mechanically sensitive channels such as stretch-activated ion channels,[80–83] L-type voltage-sensitive calcium channels,[80,84] and potassium-selective channels also play a role in mechanotransduction signaling. Work by Rawlinson *et al.* suggests the importance of stretch-sensitive channels in mechanically transduced signals. They demonstrated that tensile strain in a rat ulna resulted in activation of stretch/shear-sensitive nonselective cation channels and L-type voltage-dependent calcium channels, involved in osteogenic potential and metabolic activity.[80] Li *et al.* further demonstrated that blocking L-type voltage-sensitive calcium channels *in vivo* significantly reduced the mechanical loading-induced increase in mineralizing surface, mineral apposition rate, and bone formation rate.[84] It is apparent that these calcium channels are significantly involved in bone adaptation and mechanical response *in vivo*, and elucidating their role in osteogenesis will play a future role in validating the functional ASC osteogenic phenotype.

For a comprehensive review of mechanotransduction and the effects of biomechanical stimulation in bone, please refer to reviews by Riddle and Donahue[46]and Allori *et al.*[47] For the remainder of the discussion, we will primarily focus on the current understanding of ASC and how they have been incorporated into the field of bone tissue engineering.

ASC in Bone Tissue Engineering

Adult stem cells such as ASC and MSC demonstrate vast potential in regenerative medicine applications. Traditional methods of treating degenerative skeletal diseases and wounds include use of allografts, autografts, or artificial implants; however, for some types of injuries these treatments are not an option.[85] These techniques often present complications such as donor site morbidity, low tissue availability, immunogenicity, or loosening of the implant.[30,86–89] The use of autologous ASC for tissue replacement treatments minimizes immunogenic response, and yields a more abundant cell source than bone marrow-derived MSC.

As previously mentioned, the general top-down approach to creating a generic tissue-engineered construct has two primary components: (1) tissue-specific cells and (2) a biocompatible, mechanically appropriate scaffold on which cells can adhere to produce extracellular matrix and encourage regeneration at the defect site.[21,87,90,91] A tissue-engineered construct using the general cell-seeded scaffold of the top-down tissue-level approach has been utilized by researchers and physicians for tissue replacement therapies in: (1) tendon[92–94]; (2) cartilage[95–99]; and (3) bone[100–105] repairs. With increasing use of ASC and other types of stem cells as the primary cell source in an implanted tissue-engineered construct, a second cell-based bottom-up approach has emerged. The bottom-up approach has begun to elucidate the cellular behavior and function within the construct, providing knowledge on how to optimize the scaffold environment. To discuss the ASC approaches currently used in the creation of living bone tissue equivalents, it is important to briefly delineate the current knowledge on the differences between MSC and ASC.

Adipose-derived versus bone marrow-derived MSC

As much of the ASC tissue engineering work to date has arisen from foundational MSC studies, we would be remiss to exclude MSC from the discussion. The majority of stem cell-based tissue replacement efforts to date have typically used bone marrow-derived MSC.[18,92,95,100–103,106,107] However, the limited supply of these cells constrains the feasibility of using them in large commercial applications. This constraint has led to the study of stem cells derived from adipose tissue. In contrast to bone marrow, adipose tissue is an abundant and more readily available source of cells.[108] In a study performed by De Ugarte *et al.*, ASC showed a similar capacity for adherent cell yield per gram tissue, cell expansion, growth kinetics, and differentiation as that of MSC.[109] It should be noted that investigators have reported scalability issues with large volume bone marrow aspirates as peripheral blood contamination reduces MSC cell yields.[110] Scalability is not an issue with large ASC isolates and comparisons of cell yield per gram of tissue correspond to optimized volumes for MSC isolation.[109] Studies involving ASC, including investigations from our group, have demonstrated their MSC-like multipotency by inducing these cells down osteogenic, myogenic, adipogenic, and chondrogenic lineages.[1,109,111–115] Moreover, with few exceptions the surface marker expression profile of ASC seems to generally align with MSC.[14,116] However, the use of ASC as a substitute for MSC in certain applications has stimulated controversy due to inconsistent reports of ASC differentiation potential.

While some investigators have reported that there are no differences between the potential for MSC and ASC to differentiate into multiple lineages,[109,114,117] others report that ASC are inferior to MSC with respect to their ability to differentiate down particular pathways.[1,118–122] De Ugarte *et al.* examined the multilineage potential of bone marrow-derived MSC to ASC and found that under chemically induced differentiation, there was no difference between the two cell types in their ability to undergo osteogenic and adipogenic differentiation, express neuron-like morphology, or express discrepancies in growth kinetics.[109] Likewise, Hattori *et al.* reported that both MSC and ASC cultured in osteogenic medium expressed similar quantities of calcium phosphate deposition and osteocalcin secretion.

However, studies by Im *et al.* and Mehlhorn *et al.* argue that these two cell types do not have the same potential to differentiate down osteogenic or chondrogenic lineages. Im *et al.* found that the level of mineralization and alkaline phosphatase activity in MSC was significantly greater than that in ASC after 2 and 3 weeks of differentiation, and likewise reported consistent data with specific markers for chondrogenesis.[120] The results of a study by Mehlhorn *et al.* focusing on chondrogenesis agreed with the Im *et al.* study. MSC cultured in TGF-β1-supplemented medium showed an increase expression of chondrogenic gene markers collagen type II, type X, cartilage oligomeric matrix protein, and aggrecan at least three times higher than expression levels in ASC.[118]

While some comparisons among different studies have led to a suspicion that ASC may exhibit reduced stem cell potency as compared to MSC, it is important to note that the consensus data are generally inconclusive. Other distinctions between ASC and MSC such as their expression of different

surface markers,[1,109] requirements of additional medium supplements to differentiate down specific lineages,[123–125] and upregulation in different genes during differentiation[122] all suggest that ASC are, in fact, not less potent but simply behave differently than MSC. Recently, an in-depth comparison between the gene expression profiles of ASC and MSC demonstrated distinct and unique differences inherent to the specific cell populations.[126] Despite emerging evidence supporting inherent differences between ASC and MSC, further characterization of the cell populations remains a critical step in their effective use in tissue engineering applications.

ASC isolation

ASC can be derived from fat pads removed from almost any site of the body, though studies suggest variation in ASC potency as dependent on their derived body location and among donors.[127] Generally, ASC are isolated from adipose tissue using a collagenase (most commonly Type I) tissue digest and a series of centrifugation steps to separate the pelleted stromal cell fraction from the red blood cells, adipocyte and adipogenic progenitor fraction.[14,128] Final culture selection procedures range from culturing cells that adhere to the culture surface to rigorous cell sorting techniques and clonal culture.[1,128–130] General ASC cell surface marker profiles have been characterized, though specific marker discrepancies regarding the surface expression of Stro-1, CD34, and VCAM (CD106) have been reported among ASC population studies from different groups.[14,116,129] In spite of these discrepancies, for the most part adherent cells isolated from adipose tissue generally have a defined surface marker expression profile, and Katz *et al.* suggest that differences are likely related to variations in isolation procedure, propagation time in culture, and exposure to tissue culture plastic. The most widely utilized method to isolate ASC is simply to propagate the adherent cell fraction from adipose tissue without surface marker selection. Consistent reports of the surface expression profiles emerging from different research groups have validated this method.[14,116,129] Taken together, this evidence suggests that exposure and adherence to tissue culture plastic may play an important role in defining the ASC immunophenotype. Nonetheless, the surface profile is not necessarily an indicator of ASC potency. Population heterogeneity and donor-to-donor variation still remain challenges that need to be further investigated when manipulating ASC.

Top-Down ASC Living Tissue Equivalent Approaches

We refer to the top-down approach as a primarily tissue level approach, which has rapidly advanced the development of bone tissue constructs, generating potentially implantable living tissue equivalents. The top-down approach has provided the quickest path to usable implants, translating bench-top work by researchers to bedside application by clinicians. However, their success has largely been validated through characterizing tissue-level morphology with some limited evaluation of *in vivo* functionality. To date, the validation has focused primarily on the performance of the entire construct emulating basic tissue level organization, exhibiting a simplified version of native tissue morphology, with limited understanding of cellular activity and phenotype. *In vitro* and *in vivo* top-down approaches to creating living bone tissue equivalents have been largely similar for ASC and MSC and below is a brief summary highlighting some key ASC studies.

In vitro *studies*

Clinically, autologous bone grafts can provide a treatment method for critical defect repair, but the quantity of donor tissue is limited and there is potential for donor-site morbidity. Tissue engineering using ASC combined with a biocompatible scaffold is emerging as a novel approach for bone tissue replacements in repair of critical defect injuries.[22,31,131–134] Work by Hattori *et al.* demonstrated the osteogenic potential of ASC cultured on β-tricalcium phosphate (TCP) scaffolds with osteogenic media *in vitro*. Osteocalcin secretion and histology demonstrated an acquired osteogenic phenotype within these constructs.[135] Similarly, our group has recently shown that ASC-seeded composite TCP/poly (L-lactic acid) (PLA) scaffolds enhance cell-mediated mineralization and alkaline phosphatase activity in osteogenic media, as compared to the same growth conditions on a purely PLA scaffold.[131] This suggests that biochemical composition of the scaffold can play a significant role in directing ASC differentiation and enhancing functionality of the tissue engineered construct.

More recently, decellularized bone scaffolds derived from native bone have shown significant promise as a viable and instructive scaffold material for ASC due to their biochemical and mechanical properties. Fröhlich *et al.* have presented an approach using ASC seeded on a decellularized bone matrix and reported cell survival, mineral deposition, and expression of bone-specific markers (collagen, bone sialoprotein, and OPN) in histological sections, up to 5 weeks in culture.[31] That comparative study showed ASC-seeded bone matrices supported osteogenic differentiation of ASC under static and perfusion culture. Perfusion culture improved cellular distribution throughout the scaffold, thus enhancing the potential three-dimensionality of the construct, a consistent challenge in creating tissue constructs.[31]

A wide variety of scaffold materials, derived from both natural and synthetic sources, have been used as a platform for ASC growth and induction toward an osteogenic phenotype in two-dimensional and 3D culture. We and others have shown that ASC acquire an osteogenic phenotype *in vitro* when grown on collagen scaffolds in 3D,[37,136] decellularized bone scaffolds,[31] PLA scaffolds,[132] β-TCP,[131,137] bioceramics,[138] and composite scaffolds containing the aforementioned materials,[131,134,135,139,140] among others. In general, most top-down *in vitro* approaches apply similar methodologies with ASC and simply vary the scaffold type, but all focus on tissue level resolution and function. The cell-level effects of scaffold variation will be further discussed in the section exploring bottom-up approaches.

In vivo *studies*

In 2005, a study by Cowan *et al.* reported successful calvarial critical defect healing by 12 weeks in mice with implantation of ASC-seeded, apatite-coated poly(lactic-co-glycolic acid) (PLGA) scaffolds.[141] The cell-seeded scaffolds were biochemically stimulated with bone morphogenetic protein-2 (BMP-2) and retinoic acid for 4 weeks *ex vivo* before implantation.[141] Although the mechanism was not understood and the differentiation process not optimized, this was

one of the initial studies reporting the potential use of ASC in healing a critical bone defect. In 2006, Conejero *et al.* reported successful repair of surgically created palatal bone defects in rats using osteogenically differentiated ASC on a PLA scaffold. After 12 weeks, the osteogenically differentiated ASC produced osseous regeneration of bone, calcium accretion, and positive staining for osteocalcin, a bone matrix protein, at the defect site. Defect sites implanted with PLA alone, PLA seeded with undifferentiated ASC, or left implant free exhibited only fibrous tissue production with little evidence of bone formation.[142] Similarly, Yoon *et al.* implanted osteogenically differentiated ASC-seeded scaffolds into critical-sized rat calvarial defects and observed robust bone regeneration after 12 weeks.[143]

These studies suggest that the osteogenic phenotype of pre-differentiated ASC is functionally maintained *in vivo* and that they can operate in a regenerative capacity at a bone defect site. Work by Jeon *et al.* further evaluated the ability of ASC to differentiate *in vivo* through BMP-2 stimulation, without the need for an *in vitro* pre-differentiation step.[144] It is important to highlight that this study directly evaluated *in vivo* differentiation capacity only in the sub-cutaneous space, and did not evaluate its performance within a critical bone defect. ASC seeded on PLGA/hydroxyapatite scaffolds loaded with BMP-2 and implanted subcutaneously into athymic mice generated bone formation and calcification after 8 weeks. The phenotype of the explanted cell population was confirmed through upregulation in bone genetic markers after 8 weeks.[144]

Further, a comparative study explored the osteogenic potential of BMP-4 retrovirally transduced ASC and MSC and their capacity to ossify a calvarial defect. The transduced ASC and MSC embedded in fibrin gel both formed bone when implanted in the calvarial defect with no significant differences between the groups, though the ASC deposited a higher amount of calcified matrix.[145] Similarly, gene therapy approaches using ASC transduced to express BMP-7 derived from rats[146] and humans[147] have shown evidence for enhanced bone formation *in vitro* and *in vivo.* The BMP-7 was encased in a collagen I gel and implanted subcutaneously into rats[146] or SCID mice,[147] respectively, and caused an increase in mineralization, alkaline phosphatase activity, and osteocalcin expression.[146,147] Taken together, these transduction results are consistent with an *in vitro* study by Dragoo *et al.* showing increased frequency of a BMP-2-transduced ASC-derived osteoblastic phenotype comparable to exogenous BMP-2 stimulation.[148] Another transduction study inducing overexpression of osterix, an important transcription factor in bone development, also produced similar results and differentiation of ASC into an osteoblastic phenotype.[149] Gene therapy techniques show promise as an *in vivo* single-step alternative to chemically induced differentiation before and/or during implantation, minimizing the complexity of the construct components. This body of work suggests feasible techniques for *in vivo* differentiation of ASC, potentially simplifying therapeutic procedures.

ASC Differentiation: Bottom-Up Cell-Based Approaches

With the emergence of ASC and other stem cell types as a cell source in tissue constructs, a more cell-based, mechanistic, bottom-up approach has led to extensive study on the mechanisms of differentiation. This more basic science approach focuses largely on characterizing cell behavior, phenotype, and the cell-level activity as it contributes to the potential function of a tissue-engineered construct. Such cell-level understanding is becoming particularly important following the increasing popularity of stem cells as cell sources in tissue engineering (Fig. 2). With the growing evidence supporting that chemical, mechanical, and electrical environments all significantly affect ASC differentiation and behavior, the bottom-up approach has generated more rigorous validation methods to understand cell activity. This allows researchers to best optimize tissue-construct design, leading to in-depth study of the differentiation process. Table 1 highlights the major studies applying bottom-up approaches modifying the physical environment, for using ASC in bone tissue engineering.

Differentiation via chemical stimulation

As stem cell-based tissue engineering technology continues to progress, it is imperative to establish techniques yielding a well characterized and consistent cell population following the differentiation process. The most prevalent bottom-up approach to creating tissue engineering therapeutics operates in the realm of *in vitro* expansion of the stem cells and subsequent induction of differentiation before implantation into the defect or disease site. ASC can be differentiated by chemical stimulation using media supplements and growth factors to induce lineage specification. Typically, osteogenesis can be obtained by treating ASC with dexamethasone or 1,25-dihydroxyvitamin D3, ascorbic acid, and β-glycerolphosphate in the standard cell growth/expansion media.[1,14,115,150] Additional components and growth factors such as BMP-2 and retinoic acid,[141] tumor necrosis factor-α,[151] growth and differentiation factor-5,[152] and histone deacetylase inhibitor valproic acid[153] among others have also been studied as osteogenic enhancers. Much of the differentiation media formulation has been based on previous work with pre-osteoblasts and MSC osteogenic differentiation media.[154–156]

To evaluate the level of osteogenic differentiation response, differentiated cells are characterized using histological stains, protein and gene markers, and morphological properties specific to the osteogenic lineage. Typically, the most straightforward test for differentiation is the Alizarin Red stain for calcium deposits (Fig. 1b), indicating the presence of an osteogenic phenotype.[1,115,122,157] Osteogenesis can also be quantified nonspecifically by measuring calcium content using a colorimetric assay or specifically by the upregulation of osteogenic gene and protein markers such as BMP-2, collagen I, alkaline phosphatase, osteocalcin, OPN (SPP1), bone sialoprotein (IBSP), and runt-related transcription factor-2 (Runx2 also known as CBFα1).[1,28,31,113,115,156,157] Chemically induced differentiation still remains the gold standard to produce an osteogenic phenotype from ASC, though it has become quite clear that chemical signals are certainly not the only mediators in that process.

Differentiation via mechanical stimulation

While chemical differentiation methods are generally effective at inducing osteogenesis and production of bone ECM products, studies including mechanical stimulation[15,21,158–161] are proving to be more appropriate

Table 1. Major Studies Utilizing Bottom-Up Physical Approaches in the Generation of Adipose Stem Cell-Derived Osteogenic Tissue Constructs

Author	*External mechanical load*	*Medium*	*Substrate*	*Evidence of differentiation*	*Conclusions*
Wall *et al.*[113]	Cyclic tensile strain	ODM	3D culture in Collagen I in Tissue Train strain culture system. (Flexcell Int.)	Alizarin Red Staining Opn protein expression	Palladin expression is upregulated with chemically induced osteogenesis and tensile strain.
Hanson *et al.*[21]	Cyclic tensile strain	ODM	2D culture on Col I-coated Bioflex membrane™ (Flexcell Int.)	Quantified calcium accretion	Continuous and rest-inserted cyclic tensile strain enhances osteogenic differentiation.
Huang *et al.*[167]	Cyclic tensile strain	ODM	2D culture on Col I-coated Bioflex membrane™ (Flexcell Int.)	Quantified calcium deposition Alizarin Red Staining	Proliferative capacity of ASC is reduced with age, but restored with tensile strain stimulation. Osteogenic potential is unchanged with age.
Knippenberg *et al.*[34]	PFF	ODM	Polylysine-coated glass	NO production *cox-2* gene expression	PFF upregulates NO production and *cox-2* gene expression in osteogenically differentiated ASC.
Tjabringa *et al.*[171]	PFF	ODM	Polylysine-coated glass	NO production, *cox-2, runx2* and poly-amine associated *SSAT* gene expression	PFF upregulates *SSAT* gene expression. Polyamines mediate mechanically induced upregulation of NO activity and *cox-2* gene expression.
Fröhlich *et al.*[31]	Continuous flow	ODM	3D culture in decellularized bone matrix scaffold	Histological and Immunostaining detection of Col I, BSP, and Opn SEM detection of mineralization	Perfusion culture of ASC on 3D deceullarized bone scaffolds improves cellular distribution and enhances mass transport through the scaffold. ODM in perfusion culture system enhances expression of bone specific markers throughout the construct.
Hammerick *et al.*[25]	Electrical stimulation (DC field)	ODM	Tissue culture plastic	Gene expression of *ALP, Opn, Col I, Runx2 and Osc* Atomic force microscopy ALP activity Cytosolic calcium Immunostaining	*ALP, Opn, Col I,* and *Runx2* gene expression is upregulated with DC field exposure. DC field exposure increases cytoskeletal tension Increase in cytoskeletal tension is not necessary for DC field induced differentiation.
McCullen *et al.*[26]	Electrical stimulation (AC field)	ODM	Glass slides	Intracellular calcium Mineralized calcium accretion	AC field exposure induces intracellular calcium signaling and increases mineralized calcium accretion.

ODM, osteogenic differentiation medium; 3D, three-dimensional; 2D, two-dimensional; ASC, adipose-derived stem cell; OPN, osteopontin; PFF, pulsatile fluid flow; NO, nitric oxide; cox-2, cyclo-oxygenase-2; SSAT, spermidine/spermine N (1)-acetyltransferase; BSP, bone sialoprotein; Runx2, runt-related transcription factor-2; SEM, scanning electron microscope; ALP, alkaline phosphatase; OSC, osteocalcin; DC, direct current; AC, alternating current.

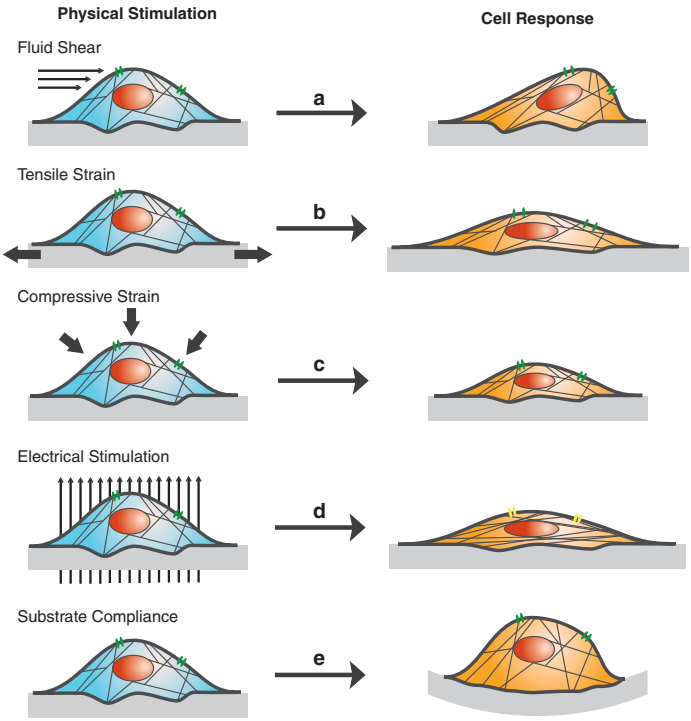

FIG. 3. Schematic of ASC responses to physical stimulation in 2D culture. Each type of stimulation results in physical changes in cell morphology, alignment, conformation of actin cytoskeleton, and ion channel activity. **(a)** Fluid shear deforms the apical surface of the cell when sensed by cytoskeletal proteins and activation of stretch-activated ion channels. **(b)** Tensile strain elongates the basal surface of the cell through stretching of the substrate. Cytoskeletal proteins sense the cellular deformation via connections to integrin–substrate adhesions. Strain applied to the basal surface also induces activation of stretch-activated ion channels. **(c)** Compressive strain applies pressure to the apical surface of the cell leading to compaction of the cytoplasm and cytoskeleton. **(d)** Electrical stimulation results in cellular and cytoskeletal alignment perpendicular to the direction of the electric field. Ion channel activity changes, though the mechanism is not clear. **(e)** Substrate compliance alters the cell's ability to form focal adhesions, limiting cell spreading and causing integrin-cytoskeleton mediated changes in cell behavior. 2D, two-dimensional. Color images available online at www.liebertonline.com/teb

for creation of functional tissue-engineered constructs. Further knowledge on the native mechanical environments cells experience *in vivo* has suggested an entirely different mode of differentiation signaling from the physical environment (Fig. 3).

The role of mechanical stimulation in ASC differentiation is following in the stride of MSC, though the mechanotransduction mechanisms in both cell types remain an active area of investigation. However, the basis for mechanically directed differentiation is increasingly supported through the evidence of behavioral changes in bone tissue and cells (osteoblasts, osteoclasts, and osteocytes) in response to mechanical signals such as fluid flow and tensile strain in committed cell types, as discussed previously.

Tensile strain. Early work by Thomas and El Haj in 1996 and Yoshikawa *et al.* in 1997 demonstrated some of the first evidence of *in vitro* mechanosensitivity in MSC, implicating the role of tensile strain for MSC osteogenic specification.[162,163] Further, stemming from *in vivo* work with distraction osteogenesis,[57,59] cyclic tensile strain has been shown to establish successfully enhanced osteogenic induction of bone marrow-derived MSC *in vitro*.[15,39,162–166] Extending the optimal *in vivo* distraction osteogenesis parameters to an *in vitro* model, Sumanasinghe *et al.* found that even in the absence of osteogenic differentiation medium (i.e., cells maintained in complete growth medium) 10% cyclic tensile strain, applied at a frequency of 1 Hz, for 4 h/day, resulted in an upregulation of BMP-2 in MSC seeded in a 3D collagen I matrix after 1 week, a significant fourfold increase over unstrained samples.[15] Likewise, Ignatius *et al.* reported that cyclic tensile strain (1% at 1 Hz for 1800 cycles/day) applied to osteoblastic precursor cells for 3 weeks resulted in slight increases of histone H4, alkaline phosphatase, CBFα1 (runx2), and OPN compared to unstrained controls.[19] Lower frequencies of strain (2.5% at 0.17 Hz) have also been shown to enhance osteogenesis in MSC and reduce their proliferation rate, hinting at the relationship between mechanically signaled proliferation and differentiation.[20] Additionally, that mechanistic study demonstrated the critical role of stretch activated cation channels and kinases such as ERK, p38, and PI3K in mediating the mechanically transduced differentiation signals.[20]

Subsequent work with ASC has similarly demonstrated mechanosensitivity during osteogenic differentiation, though the specific mechanisms of the process are less clear. We have shown that ASC exhibit enhanced osteogenic differentiation when exposed to both continuous (10% strain, 1 Hz) and rest inserted strain (10% strain, 1 Hz, 10 rest between each cycle).[21] That particular study specifically compared ASC from two different donors: one line with high mineralization potential in response to chemical stimulation with osteogenic supplements and the other with low mineralization potential. Both modalities of tensile strain enhanced cell-mediated calcium accretion in both ASC lines; however, the ASC with a predisposition to greater calcium accretion expressed a relatively higher osteogenic response to tensile strain, suggesting increased mechanical sensitivity in this line.[21] Differences in the observed osteogenic response support the idea that all ASC do not always behave the same way. Just as human ASC from different donors vary in their chemical differentiation potential, so do they in

their mechanosensitivity and differentiation potential. Much investigation is still needed to understand the underlying mechanisms of these predispositions and how they are related.

Our group has published a mechanistic study with the goal of elucidating proteins and mechanisms associated with mechanically induced osteogenic differentiation of ASC. We have described the upregulation of palladin expression, an actin-associated cytoskeletal protein, during chemically induced osteogenesis and under cyclic tensile strain.[37] That study identified a mechanosensitive protein associated with both osteogenesis and signaling transduction of tensile strain, though it is unclear whether this protein is crucial to mechanically enhanced osteogenesis.

Very recent work with mouse-derived ASC has shown that tensile strain can mechanically mediate age-related variations in ASC proliferation and differentiation potential, altering their cell fate in a magnitude and frequency-dependent fashion.[167] However, that study reported significant age and strain-related differentiation effects only in ASC adipogenesis and no significant age and strain related differences in osteogenesis.[167] Characteristics such as magnitude,[15] number of cycles,[168] and frequency[168] of strain have been shown to be important variables for optimal tissue regeneration. It is apparent that mechanical signals differentially affect cell behavior more widely than initially hypothesized. Elucidating this process will allow researchers to better harness these characteristics for optimal ASC differentiation.

Fluid flow and shear stress. As stated previously, interstitial fluid flow is believed to impose a physical signal on osteocytes altering their proliferation and metabolic activity.[33,50,55,72,73] Empirical and computational studies on the effects of fluid flow signaling osteogenic proliferation and differentiation in MSC[16,17,169,170,172] have opened the door for similar studies in ASC.[31,34,35,171] Fluid perfusion has also been used as a culture tool to increase dimensionality and cellular distribution throughout a scaffold material, enhancing nutrient transport, to create a more functional construct.[35,172] Direct osteogenic signaling via fluid shear in ASC has been primarily PFF, though constant flow perfusion culture regimes have been specifically used to promote 3D cell seeding.[31,173]

Knippenberg *et al.* harnessed this principle in an attempt to enhance ASC osteogenesis. ASC differentiation was chemically initialized with 1,25-dihydroxyvitamin D3 and subsequently the cells were cultured under PFF. They reported significant differences in phenotypic behavior between ASC-derived osteogenic cells cultured under PFF and those in static culture. Osteogenic ASC cultured under PFF showed increases in production of NO and upregulation of *cox-2* gene expression. This suggests functional validation and enhancement of the osteogenic phenotype through application of physiologically relevant mechanical stimulation, and further demonstrates the innate mechanosensitivity of ASC.[34] A subsequent study from the same group identified the role of polyamines in the process of fluid shear-enhanced differentiation in ASC.[171] They reported that PFF also led to increased gene expression of spermidine/spermine N (1)-acetyltransferase (*SSAT*), an enzyme associated with polyamine activity, suggesting that PFF affected polyamine levels. Furthermore, the authors showed that the addition of polyamine spermine inhibited mechanically induced NO-production and *cox-2* gene expression.[171] These data imply that polyamines play a role in modulating ASC response to mechanical stimulation, which may have a profound effect on ASC approaches to bone tissue engineering and potential therapeutic uses for polyamines in skeletal disorders.

Additionally, studies by Grayson *et al.* and Li *et al.* have utilized a perfusion culture system with steady fluid flow to distribute MSC throughout 3D scaffold materials.[35,172] Grayson *et al.* reported substantial cellular penetration and distribution throughout a decellularized bone matrix scaffold and enhanced expression of specific bone matrix markers, concluding flow rate alone can directly control the quality of an MSC-derived bone construct.[172] Likewise Li *et al.* achieved cell survival and shear stress-level dependent osteogenic differentiation and matrix mineralization throughout a TCP scaffold in perfusion culture.[35]

Following the Grayson *et al.* article, the same group applied their perfusion culture system to ASC seeded on decellularized bone scaffolds for a comparative investigation, using the same parameters as their MSC study and other static culture methods (study also discussed in "*In vitro* studies").[31] Similar to the MSC study, ASC also achieved improved 3D cellular distribution and expression of bone specific markers, validating the perfusion culture method for creating a 3D ASC-derived bone construct.[31] In general, a variety of fluid flow modalities are proving to provide directive mechanical cues for ASC differentiation as well as cell-seeding methods and improved nutrient delivery within a 3D construct.

Unconfined and confined compression. Cyclic compression has been shown to stimulate osteoblast differentiation and bone formation *in vitro* and *in vivo*.[36,174,175] Although there has been little work to date on the effect of compression on ASC osteogenic differentiation, it has been implicated in MSC osteogenesis and thus likely is another important mediator of ASC lineage specification. A majority of the work in MSC suggests that cyclic compressive loading leads to a chondrogenic phenotype,[176,177] though there is some evidence it may also enhance osteogenic differentiation.[174,175] However, it is unclear whether it is the compressive force initiating the mechanically transduced signal, or rather the tensile force acting along the unconfined axis, orthogonally to the direction of compression.

Other environmental mediators of differentiation

Electrical stimulation. Electrical stimulation has been used clinically as a therapeutic procedure to stimulate bone growth and enhance healing of nonunion bone fractures, though some argue the evidenced benefits of the procedure.[178] Regardless, the effect of various modalities of electrical stimulation on osteoblast,[179] MSC,[180–182] and ASC[25,26] osteogenic differentiation remains an active area of research. Tsai *et al.* demonstrated enhanced early osteogenic induction in MSC via application of low-frequency (7.5 Hz) pulsed electromagnetic fields as determined by an increase in alkaline phosphatase activity and upregulation of *Runx2* and *ALP* gene expression.[180] Hammerick *et al.* used pulsed direct current (DC) at a higher frequency (50 Hz) applied to ASC and likewise observed enhanced osteogenic differentiation via upregulation of *Opn, Col I,* and *Runx2* gene expression as

well as an increase in cytoskeletal tension, as measured by atomic force microscopy.[25] Interestingly, this study reported an important mechanistic finding: the addition of an inhibitor disrupting the tensional action of the cytoskeleton did not yield an apparent decrease in osteogenesis, suggesting that electric field effects are not mediated by mechanical changes in cytoskeletal tension, but rather through another pathway.[25] Similarly, active research in our group has observed enhanced osteogenesis and intracellular calcium activity in ASC when exposed to low frequency alternating current (AC) fields via ASC growth and stimulation on interdigitated electrodes.[26] Further understanding of this process is needed to fully harness the potential of using electrical stimulation as a tool in creating tissue-engineered bone constructs.

Substrate-mediated differentiation. Another development in directing stem cell differentiation has come out of investigating cell–substrate interactions. Substrate biochemical composition, stiffness, and surface morphology can greatly affect ASC and MSC adhesion, proliferation, migration, and differentiation.[28,131–134,183–189] Engler *et al.* demonstrated distinct morphological, gene, and protein differences among MSC cultured on collagen-coated polyacrylamide gels with elastic moduli of 0.1–1 kPa, 8–17 kPa, and 25–40 kPa. These values were predicted to emulate the tissue compliance of brain, muscle, and collagenous bone, respectively.[28] They described synergistic lineage specification effects when combining chemical differentiation media with the appropriate substrate stiffness for the target phenotype. Following that study, work by Rowlands *et al.* described the interplay between substrate stiffness and surface ligand properties, through testing various ECM coatings. This group reported greatest osteogenic differentiation of MSC on the stiffest (80 kPa) collagen I-coated substrate through expression of *Runx2* as compared to other ECM coatings. Interestingly, MSC showed peak expression of myogenic marker MyoD1 at varying moduli depending on type of ECM coating.[188]

In addition to these mechanistic studies, others have explored the use of bioinstructive materials to direct functional differentiation through inducing characteristic metabolic activities. A study by Au *et al.* used a well-defined protein peptide for cellular adhesion (GRGDSPY) and a peptide derived from bone sialoprotein (FHRRIKA) to observe integrin-mediated processes in MSC osteogenic differentiation and alkaline phosphatase activity.[183] Although much of the work on substrate-mediated differentiation has characterized MSC behavior, our group has shown similar findings of substrate-mediated differentiation with ASC. Studies in our lab have shown that incorporating TCP into electrospun PLA scaffolds enhances ASC endogenous alkaline phosphatase activity and cell-mediated calcium accretion.[131] These results were consistent with a similar study conducted by Haimi *et al.* confirming that PLA/TCP composite scaffolds significantly enhance osteogenic differentiation of ASC.[140] These studies suggest that the biochemical composition of the substrate can provide important environmental cues to direct lineage specification of ASC and MSC, particularly for osteogenesis. Although there are fewer studies on substrate-controlled differentiation of ASC, there is substantial evidence that ASC may have similar mechanosensing properties to MSC.

Conclusions

From the development of Wolff's law in the late 19th century to the principles of mechanobiology applied to stem cell osteogenic differentiation, the field has made huge strides toward engineering bone tissue replacements. Mechanical stimulation is now a well-established inducer of osteogenesis in native bone and its role in ASC and MSC osteogenic differentiation is relatively undeniable. Creating a viable tissue-engineered bone construct derived from ASC is truly a multifaceted process necessitating a multidisciplinary approach to optimize the culture environment, as discussed in various sections of this review. Although ASC are a relatively abundant cell source, they are not as well characterized as their MSC counterparts. Further understanding of both of these cell populations will improve our understanding of their multipotency and their limitations for use in bone tissue engineering. Additionally, development of consensus in ASC isolation procedures, though not emphasized in this article, is a necessary step for an accurate characterization definition of the ASC population, as some studies have a more stringent and specific selection process for their ASC population than others.

Most importantly, the crux of this review aimed to explore the current knowledge base in ASC mechanobiology as framed through established principles in bone, though a thorough mechanistic understanding of mechanotransduction processes in these cells remains elusive. It is quite clear that mechanical forces, particularly tensile strain and fluid shear among others, are crucial signals in ASC osteogenic differentiation. Emerging evidence of hypothesized mediators such as the cytoskeletal proteins, primary cilia, and ion channels shows great promise in elucidating the mechanisms behind mechanotransduction in these cells. As we expand our understanding of the ASC mechanosensing process, we can better optimize the chemical, mechanical, and electrical culture environment, as well as the properties of the culture substrate, to direct ASC toward the specified osteogenic phenotype. ASC continue to show great promise as a cell source for autologous bone replacement and regeneration procedures, and as each facet of bone tissue engineering advances in conjunction with further understanding of the ASC populations, they will very likely be cell source candidates in these future therapeutic constructs.

Acknowledgments

This work was supported by NIH/NCRR 10KR51023(EGL), NIH/NIBIB R03Eb008790(EGL) and the NSF Graduate Research Fellowship Program (JCB). We thank B. Hartsfield for his artwork design guidance & E.D. Jerkins for her critical comments on this review.

Disclosure Statement

No competing financial interests exist.

References

1. Zuk, P., Zhu, M., Ashjian, P., De Ugarte, D., Huang, J., Mizuno, H., *et al.* Human adipose tissue is a source of multipotent stem cells. Mol Biol Cell **13,** 4279, 2002.
2. Gimble, J., and Guilak, F. Adipose-derived adult stem cells: isolation, characterization, and differentiation potential. Cytotherapy **5,** 362, 2003.

3. Strem, B., Zhu, M., Alfonso, Z., Daniels, E., Schreiber, R., Begyui, R., *et al.* Expression of cardiomyocytic markers on adipose tissue-derived cells in a murine model of acute myocardial injury. Cytotherapy **7,** 282, 2005.
4. Dimuzio, P., and Tulenko, T. Tissue engineering applications to vascular bypass graft development: The use of adipose-derived stem cells. J Vasc Surg **45,** A99, 2007.
5. Rada, T., Reis, R., and Gomes, M. Adipose tissue-derived stem cells and their application in bone and cartilage tissue engineering. Tissue Eng Part B Rev **15,** 113, 2009.
6. Frost, H.M. Skeletal structural adaptations to mechanical usage (SATMU): 1. Redefining Wolff's law: the bone modeling problem. Anat Rec **226,** 403, 1990.
7. Frost, H.M. Bone "mass" and the "mechanostat": a proposal. Anat Rec **219,** 1, 1987.
8. Schneider, V., and McDonald, J. Skeletal calcium homeostasis and countermeasures to prevent disuse osteoporosis. Calcif Tissue Int **36,** 151, 1984.
9. Morey, E., and Baylink, D. Inhibition of bone formation during space flight. Science **201,** 1138, 1978.
10. Robling, A., Hinant, F., Burr, D., and Turner, C. Improved bone structure and strength after long-term mechanical loading is greatest if loading is separated into short bouts. J Bone Miner Res **17,** 1545, 2002.
11. Greene, D.A., and Naughton, G.A. Adaptive skeletal responses to mechanical loading during adolescence. Sports Med **36,** 723, 2006.
12. Ehrlich, P., and Lanyon, L. Mechanical strain and bone cell function: a review. Osteoporos Int **13,** 688, 2002.
13. van Griensven, M., Diederichs, S., Roeker, S., and Boehm, S. Mechanical strain using 2D and 3D bioreactors induces osteogenesis: implications for bone tissue engineering. Adv Biochem Eng Biotechnol **112,** 95, 2008.
14. Zuk, P., Zhu, M., Mizuno, H., Huang, J., Futrell, J., Katz, A., *et al.* Multilineage cells from human adipose tissue: implications for cell-based therapies. Tissue Eng **7,** 211, 2001.
15. Sumanasinghe, R.D., Bernacki, S.H., and Loboa, E.G. Osteogenic differentiation of human mesenchymal stem cells in collagen matrices: effect of uniaxial cyclic tensile strain on bone morphogenetic protein (BMP-2) mRNA expression. Tissue Eng **12,** 3459, 2006.
16. Arnsdorf, E.J., Tummala, P., Kwon, R.Y., and Jacobs, C.R. Mechanically induced osteogenic differentiation - the role of RhoA, ROCKII and cytoskeletal dynamics. J Cell Sci **122,** 546, 2009.
17. Arnsdorf, E.J., Tummala, P., and Jacobs, C.R. Non-canonical Wnt signaling and N-cadherin related beta-catenin signaling play a role in mechanically induced osteogenic cell fate. PLoS ONE **4,** e5388, 200.
18. Lee, W., Maul, T., Vorp, D., Rubin, J., and Marra, K. Effects of uniaxial cyclic strain on adipose-derived stem cell morphology, proliferation, and differentiation. Biomech Model Mechanobiol **6,** 265, 2007.
19. Ignatius, A., Blessing, H., Liedert, A., Schmidt, C., Neidlinger-Wilke, C., Kaspar, D., *et al.* Tissue engineering of bone: effects of mechanical strain on osteoblastic cells in type I collagen matrices. Biomaterials **26,** 311, 2005.
20. Kearney, E.M., Farrell, E., Prendergast, P.J., and Campbell, V.A. Tensile strain as a regulator of mesenchymal stem cell osteogenesis. Ann Biomed Eng **38,** 1767, 2010.
21. Hanson, A., Marvel, S., Bernacki, S.H., Banes, A., Aalst, J., and Loboa, E.G. Osteogenic effects of rest inserted and continuous cyclic tensile strain on hASC lines with disparate osteodifferentiation capabilities. Ann Biomed Eng **37,** 955, 2009.
22. Sumanasinghe, R., Osborne, J., and Loboa, E. Mesenchymal stem cell-seeded collagen matrices for bone repair: effects of cyclic tensile strain, cell density, and media conditions on matrix contraction *in vitro*. J Biomed Mater Res **88,** 778, 2009.
23. Ozcivici, E., Luu, Y.K., Adler, B., Qin Y-X, Rubin, J., Judex, S., *et al.* Mechanical signals as anabolic agents in bone. Nat Rev Rheumatol **6,** 50, 2010.
24. Altman, G., Lu, H., Horan, R., Calabro, T., Ryder, D., Kaplan, D., *et al.* Advanced bioreactor with controlled application of multi-dimensional strain for tissue engineering. J Biomech Eng **124,** 742, 2002.
25. Hammerick, K.E., James, A.W., Huang, Z., Prinz, F.B., and Longaker, M.T. Pulsed direct current electric fields enhance osteogenesis in adipose-derived stromal cells. Tissue Eng Part A **16,** 917, 2010.
26. McCullen, S., McQuilling, J., Grossfeld, R., Lubischer, J., Clarke, L., and Loboa, E. Application of low frequency AC electric fields via interdigitated electrodes: effects on cellular viability, cytoplasmic calcium, and osteogenic differentiation of human adipose-derived stem cells. Tissue Eng Part C Methods **16,** 1377, 2010.
27. Discher, D.E., Janmey, P., and Wang, Y.L. Tissue cells feel and respond to the stiffness of their substrate. Science **310,** 1139, 2005.
28. Engler, A.J., Sen, S., Sweeney, H.L., and Discher, D.E. Matrix elasticity directs stem cell lineage specification. Cell **126,** 677, 2006.
29. Knothe Tate, M., Falls, T., McBride, S., Atit, R., and Knothe, U. Mechanical modulation of osteochondroprogenitor cell fate. Int J Biochem Cell Biol **40,** 2720, 2008.
30. McCullen, S.D., Haslauer, C.M., and Loboa, E.G. Musculoskeletal mechanobiology: Interpretation by external force and engineered substratum. J Biomech **43,** 119, 2010.
31. Fröhlich, M., Grayson, W.L., Marolt, D., Gimble, J.M., Kregar-Velikonja, N., and Vunjak-Novakovic, G. Bone grafts engineered from human adipose-derived stem cells in perfusion bioreactor culture. Tissue Eng Part A **16,** 179, 2010.
32. Malone, A.M., Anderson, C.T., Tummala, P., Kwon, R.Y., Johnston, T.R., Stearns, T., *et al.* Primary cilia mediate mechanosensing in bone cells by a calcium-independent mechanism. Proc Natl Acad Sci U S A **104,** 13325, 2007.
33. Klein-Nulend, J., Semeins, C., Burger, E., Plas, A.V.d., Ajubi, N., and Nijweide, P. Response of isolated osteocytes to mechanical loading *in vitro*. In: Odgaard, A., and Weinans, H., eds. Bone Structure and Remodeling. Singapore: World Scientific Publishing Co. Pvt. Ltd., 1994, pp. 37–49.
34. Knippenberg, M., Helder, M., Zandieh Doulabi, B., Semeins, C., Wuisman, P., and Klein-Nulend, J. Adipose tissue-derived mesenchymal stem cells acquire bone cell-like responsiveness to fluid shear stress on osteogenic stimulation. Tissue Eng **11,** 1780, 2005.
35. Li, D., Tang, T., Lu, J., and Dai, K. Effects of flow shear stress and mass transport on the construction of a large-scale tissue-engineered bone in a perfusion bioreactor. Tissue Eng Part A **15,** 2773, 2009.
36. David, V., Guignandon, A., Martin, A., Malaval, L., Lafage-Proust, M.-H., Rattner, A., *et al.* Ex vivo bone formation in bovine trabecular bone cultured in a dynamic 3D bioreactor is enhanced by compressive mechanical strain. Tissue Eng Part A **14,** 117, 2008.

37. Wall, M., Rachlin, A., Otey, C., and Loboa, E. Human adipose-derived adult stem cells upregulate palladin during osteogenesis and in response to cyclic tensile strain. Am J Physiol Cell Physiol **293,** C1532, 2007.
38. Duncan, R.L., and Turner, C.H. Mechanotransduction and the functional response of bone to mechanical strain. Calcif Tissue Int **57,** 344, 1995.
39. Carter, D.R., Beaupre, G.S., Giori, N.J., and Helms, J.A. Mechanobiology of skeletal regeneration. Clin Orthop Relat Res **355 Suppl,** S41, 1998.
40. Rubin, J., Rubin, C., and Jacobs, C.R. Molecular pathways mediating mechanical signaling in bone. Gene **367,** 1, 2006.
41. Knothe Tate, M.L. "Whither flows the fluid in bone?" An osteocyte's perspective. J Biomech **36,** 1409, 2003.
42. Rubin, C.T., and Lanyon, L.E. Regulation of bone formation by applied dynamic loads. J Bone Joint Surg Am **66,** 397, 1984.
43. Cowin, S.C., Moss-Salentijn, L., and Moss, M.L. Candidates for the mechanosensory system in bone. J Biomech Eng **113,** 191, 1991.
44. Weinbaum, S., Cowin, S.C., and Zeng, Y. A model for the excitation of osteocytes by mechanical loading-induced bone fluid shear stresses. J Biomech **27,** 339, 1994.
45. Burger, E.H., and Klein-Nulend, J. Mechanotransduction in bone—role of the lacuno-canalicular network. Faseb J **13 Suppl,** S101, 1999.
46. Riddle, R., and Donahue, H. From streaming-potentials to shear stress: 25 years of bone cell mechanotransduction. J Orthop Res **27,** 143, 2009.
47. Allori, A., Sailon, A., Pan, J., and Warren, S. Biological basis of bone formation, remodeling, and repair—part III: biomechanical forces. Tissue Eng Part B: Rev **14,** 285, 2008.
48. Burger, E.H., and Klein-Nulend, J. Responses of bone cells to biomechanical forces *in vitro*. Adv Dental Res **13,** 93, 1999.
49. Sikavitsas, V.I., Temenoff, J.S., and Mikos, A.G. Biomaterials and bone mechanotransduction. Biomaterials **22,** 2581, 2001.
50. Ajubi, N.E., Klein-Nulend, J., Nijweide, P.J., Vrijheid-Lammers, T., Alblas, M.J., and Burger, E.H. Pulsating fluid flow increases prostaglandin production by cultured chicken osteocytes—a cytoskeleton-dependent process. Biochem Biophys Res Commun **225,** 62, 1996.
51. Klein-Nulend, J., Semeins, C.M., Ajubi, N.E., Nijweide, P.J., and Burger, E.H. Pulsating fluid flow increases nitric oxide (NO) synthesis by osteocytes but not periosteal fibroblasts—correlation with prostaglandin upregulation. Biochem Biophys Res Commun **217,** 640, 1995.
52. Thi, M., Iacobas, D., Iacobas, S., and Spray, D. Fluid shear stress upregulates vascular endothelial growth factor gene expression in osteoblasts. Ann N Y Acad Sci **1117,** 73, 2007.
53. You, J., Reilly, G.C., Zhen, X., Yellowley, C.E., Chen, Q., Donahue, H.J., *et al.* Osteopontin gene regulation by oscillatory fluid flow via intracellular calcium mobilization and activation of mitogen-activated protein kinase in MC3T3-E1 osteoblasts. J Biol Chem **276,** 13365, 2001.
54. Batra, N., Li, Y., Yellowley, C., You, L., Malone, A., Kim, C., *et al.* Effects of short-term recovery periods on fluid-induced signaling in osteoblastic cells. J Biomech **38,** 1909, 2005.
55. Qin, Y., Kaplan, T., Saldanha, A., and Rubin, C. Fluid pressure gradients, arising from oscillations in intramedullary pressure, is correlated with the formation of bone and inhibition of intracortical porosity. J Biomech **36,** 1427, 2003.
56. Schwartz, Z., Denison, T., Bannister, S., Cochran, D., Liu, Y., Lohmann, C., *et al.* Osteoblast response to fluid induced shear depends on substrate microarchitecture and varies with time. J Biomed Mater Res **83A,** 20, 2007.
57. Loboa, E.G., Fang, T.D., Warren, S.M., Lindsey, D.P., Fong, K.D., Longaker, M.T., *et al.* Mechanobiology of mandibular distraction osteogenesis: experimental analyses with a rat model. Bone **34,** 336, 2004.
58. Richards, M., Goulet, J.A., Weiss, J.A., Waanders, N.A., Schaffler, M.B., and Goldstein, S.A. Bone regeneration and fracture healing. Experience with distraction osteogenesis model. Clin Orthop Relat Res **355 Suppl,** S191, 1998.
59. Buchman, S.R., Ignelzi, M.A., Radu, C., Wilensky, J., Rosenthal, A.H., Tong, L., *et al.* Unique rodent model of distraction osteogenesis of the mandible. Ann Plast Surg **49,** 511, 2002.
60. Waanders, N.A., Richards, M., Steen, H., Kuhn, J.L., Goldstein, S.A., and Goulet, J.A. Evaluation of the mechanical environment during distraction osteogenesis. Clin Orthop Relat Res **349,** 225, 1998.
61. Smith-Adaline, E.A., Volkman, S.K., Ignelzi, M.A., Jr., Slade, J., Platte, S., and Goldstein, S.A. Mechanical environment alters tissue formation patterns during fracture repair. J Orthop Res **22,** 1079, 2004.
62. Meyer, U., Wiesmann, H.P., Kruse-Losler, B., Handschel, J., Stratmann, U., and Joos, U. Strain-related bone remodeling in distraction osteogenesis of the mandible. Plast Reconstr Surg **103,** 800, 1999.
63. Loboa, E., Fang, T., Parker, D., Warren, S., Fong, K., Longaker, M., *et al.* Mechanobiology of mandibular distraction osteogenesis: finite element analyses with a rat model. J Orthop Res **23,** 663, 2005.
64. Plotkin, L.I., Mathov, I., Aguirre, J.I., Parfitt, A.M., Manolagas, S.C., and Bellido, T. Mechanical stimulation prevents osteocyte apoptosis: requirement of integrins, Src kinases, and ERKs. Am J Physiol Cell Physiol **289,** C633, 2005.
65. Tong, L., Buchman, S.R., Ignelzi, M.A., Rhee, S., and Goldstein, S.A. Focal adhesion kinase expression during mandibular distraction osteogenesis: evidence for mechanotransduction. Plast Reconstr Surg **111,** 211, 2003.
66. Ingber, D.E. Tensegrity: the architectural basis of cellular mechanotransduction. Annu Rev Physiol **59,** 575, 1997.
67. Ingber, D.E., and Folkman, J. Mechanochemical switching between growth and differentiation during fibroblast growth factor-stimulated angiogenesis *in vitro*: role of extracellular matrix. J Cell Biol **109,** 317, 1989.
68. Rana, B., Mischoulon, D., Xie, Y., Bucher, N.L., and Farmer, S.R. Cell-extracellular matrix interactions can regulate the switch between growth and differentiation in rat hepatocytes: reciprocal expression of C/EBP alpha and immediate-early growth response transcription factors. Mol Cell Biol **14,** 5858, 1994.
69. Mooney, D., Hansen, L., Vacanti, J., Langer, R., Farmer, S., and Ingber, D. Switching from differentiation to growth in hepatocytes: control by extracellular matrix. J Cell Physiol **151,** 497, 1992.
70. Hansen, L.K., Mooney, D.J., Vacanti, J.P., and Ingber, D.E. Integrin binding and cell spreading on extracellular matrix act at different points in the cell cycle to promote hepatocyte growth. Mol Biol Cell **5,** 967, 1994.
71. McGarry, J.G., Klein-Nulend, J., and Prendergast, P.J. The effect of cytoskeletal disruption on pulsatile fluid flow-induced nitric oxide and prostaglandin E2 release in

osteocytes and osteoblasts. Biochem Biophys Res Commun **330,** 341, 2005.
72. Mullender, M., El Haj, A.J., Yang, Y., van Duin, M.A., Burger, E.H., and Klein-Nulend, J. Mechanotransduction of bone cells *in vitro*: mechanobiology of bone tissue. Med Biol Eng Comput **42,** 14, 2004.
73. Pavalko, F., Chen, N., Turner, C., Burr, D., Atkinson, S., Hsieh, Y., *et al.* Fluid shear-induced mechanical signaling in MC3T3-E1 osteoblasts requires cytoskeleton-integrin interactions. Am J Physiol Cell Physiol **275,** 1591, 1998.
74. Liedert, A., Kaspar, D., Blakytny, R., Claes, L., and Ignatius, A. Signal transduction pathways involved in mechanotransduction in bone cells. Biochem Biophys Res Commun **349,** 1, 2006.
75. Jiang, J.X., Siller-Jackson, A.J., and Burra, S. Roles of gap junctions and hemichannels in bone cell functions and in signal transmission of mechanical stress. Front Biosci **12,** 1450, 2007.
76. Taylor, A.F., Saunders, M.M., Shingle, D.L., Cimbala, J.M., Zhou, Z., and Donahue, H.J. Mechanically stimulated osteocytes regulate osteoblastic activity via gap junctions. Am J Physiol Cell Physiol **292,** C545, 2007.
77. Whitfield, J. The solitary (primary) cilium–A mechanosensory toggle switch in bone and cartilage cells. Cell Signal **20,** 1019, 2008.
78. Zhou, J. Polycystins and primary cilia: primers for cell cycle progression. Ann Rev Physiol **71,** 83, 2009.
79. Tummala, P., Arnsdorf, E.J., and Jacobs, C.R. The role of primary cilia in mesenchymal stem cell differentiation: a pivotal switch in guiding lineage commitment. Cell Mol Bioeng **3,** 207, 2010.
80. Rawlinson, S.C., Pitsillides, A.A., and Lanyon, L.E. Involvement of different ion channels in osteoblasts' and osteocytes' early responses to mechanical strain. Bone **19,** 609, 1996.
81. Charras, G.T., Williams, B.A., Sims, S.M., and Horton, M.A. Estimating the sensitivity of mechanosensitive ion channels to membrane strain and tension. Biophys J **87,** 2870, 2004.
82. Davidson, R.M. Membrane stretch activates a high-conductance K+ channel in G292 osteoblastic-like cells. J Membr Biol **131,** 81, 1993.
83. Davidson, R.M., Tatakis, D.W., and Auerbach, A.L. Multiple forms of mechanosensitive ion channels in osteoblast-like cells. Pflugers Arch **416,** 646, 1990.
84. Li, J., Duncan, R.L., Burr, D.B., and Turner, C.H. L-type calcium channels mediate mechanically induced bone formation *in vivo*. J Bone Miner Res **17,** 1795, 2002.
85. Khan, Y., Yaszemski, M.J., Mikos, A.G., and Laurencin, C.T. Tissue engineering of bone: material and matrix considerations. J Bone Joint Surg **90 Suppl 1,** 36, 2008.
86. Younger, E.M., and Chapman, M.W. Morbidity at bone graft donor sites. J Orthop Trauma **3,** 192, 1989.
87. Ringe, J., Kaps, C., Burmester, G.R., and Sittinger, M. Stem cells for regenerative medicine: advances in the engineering of tissues and organs. Naturwissenschaften **89,** 338, 2002.
88. Moore, W.R., Graves, S.E., and Bain, G.I. Synthetic bone graft substitutes. ANZ J Surg **71,** 354, 2001.
89. Hui, J.H., Ouyang, H.W., Hutmacher, D.W., Goh, J.C., and Lee, E.H. Mesenchymal stem cells in musculoskeletal tissue engineering: a review of recent advances in National University of Singapore. Ann Acad Med Singapore **34,** 206, 2005.
90. Bonassar, L.J., and Vacanti, C.A. Tissue engineering: the first decade and beyond. J Cell Biochem Suppl **30–31,** 297, 1998.
91. Vacanti, C.A., and Vacanti, J.P. The science of tissue engineering. Orthop Clin North Am **31,** 351, 2000.
92. Young, R.G., Butler, D.L., Weber, W., Caplan, A.I., Gordon, S.L., and Fink, D.J. Use of mesenchymal stem cells in a collagen matrix for Achilles tendon repair. J Orthop Res **16,** 406, 1998.
93. Juncosa-Melvin, N., Shearn, J.T., Boivin, G.P., Gooch, C., Galloway, M.T., West, J.R., *et al.* Effects of mechanical stimulation on the biomechanics and histology of stem cell-collagen sponge constructs for rabbit patellar tendon repair. Tissue Eng **12,** 2291, 2006.
94. Awad, H.A., Boivin, G.P., Dressler, M.R., Smith, F.N., Young, R.G., and Butler, D.L. Repair of patellar tendon injuries using a cell-collagen composite. J Orthop Res **21,** 420, 2003.
95. Wakitani, S., Goto, T., Pineda, S.J., Young, R.G., Mansour, J.M., Caplan, A.I., *et al.* Mesenchymal cell-based repair of large, full-thickness defects of articular cartilage. J Bone Joint Surg Am **76,** 579, 1994.
96. Liu, Y., Shu, X.Z., and Prestwich, G.D. Osteochondral defect repair with autologous bone marrow-derived mesenchymal stem cells in an injectable, *in situ*, cross-linked synthetic extracellular matrix. Tissue Eng **12,** 3405, 2006.
97. Yan, H., and Yu, C. Repair of full-thickness cartilage defects with cells of different origin in a rabbit model. Arthroscopy **23,** 178, 2007.
98. Kuroda, R., Ishida, K., Matsumoto, T., Akisue, T., Fujioka, H., Mizuno, K., *et al.* Treatment of a full-thickness articular cartilage defect in the femoral condyle of an athlete with autologous bone-marrow stromal cells. Osteoarthritis Cartilage **15,** 226, 2007.
99. Wakitani, S., Imoto, K., Yamamoto, T., Saito, M., Murata, N., and Yoneda, M. Human autologous culture expanded bone marrow mesenchymal cell transplantation for repair of cartilage defects in osteoarthritic knees. Osteoarthritis Cartilage **10,** 199, 2002.
100. Endres, M., Hutmacher, D.W., Salgado, A.J., Kaps, C., Ringe, J., Reis, R.L., *et al.* Osteogenic induction of human bone marrow-derived mesenchymal progenitor cells in novel synthetic polymer-hydrogel matrices. Tissue Eng **9,** 689, 2003.
101. Bruder, S.P., Kraus, K.H., Goldberg, V.M., and Kadiyala, S. The effect of implants loaded with autologous mesenchymal stem cells on the healing of canine segmental bone defects. J Bone Joint Surg Am **80,** 985. 1998.
102. Arinzeh, T.L., Peter, S.J., Archambault, M.P., van den Bos, C., Gordon, S., Kraus, K., *et al.* Allogeneic mesenchymal stem cells regenerate bone in a critical-sized canine segmental defect. J Bone Joint Surg Am **85A,**1927, 2003.
103. Schantz, J.T., Hutmacher, D.W., Lam, C.X., Brinkmann, M., Wong, K.M., Lim, T.C., *et al.* Repair of calvarial defects with customised tissue-engineered bone grafts II. Evaluation of cellular efficiency and efficacy *in vivo*. Tissue Eng **9 Suppl 1,** S127, 2003.
104. Quarto, R., Mastrogiacomo, M., Cancedda, R., Kutepov, S.M., Mukhachev, V., Lavroukov, A., *et al.* Repair of large bone defects with the use of autologous bone marrow stromal cells. N Engl J Med **344,** 385, 2001.
105. Kon, E., Muraglia, A., Corsi, A., Bianco, P., Marcacci, M., Martin, I., *et al.* Autologous bone marrow stromal cells loaded onto porous hydroxyapatite ceramic accelerate bone repair in critical-size defects of sheep long bones. J Biomed Mater Res **49,** 328, 2000.

106. Park, J.S., Chu, J.S., Cheng, C., Chen, F., Chen, D., and Li, S. Differential effects of equiaxial and uniaxial strain on mesenchymal stem cells. Biotechnol Bioeng **88,** 359, 2004.
107. Endres, M., Hutmacher, D.W., Salgado, A.J., Kaps, C., Ringe, J., Reis, R.L., Sittinger, M., Brandwood, A., and Schantz, J.T. Osteogenic induction of human bone marrow-derived mesenchymal progenitor cells in novel synthetic polymer-hydrogel matrices. Tissue Eng **9,** 689, 2003.
108. Aust, L., Devlin, B., Foster, S.J., Halvorsen, Y.D., Hicok, K., du Laney, T., *et al.* Yield of human adipose-derived adult stem cells from liposuction aspirates. Cytotherapy **6,** 7, 2004.
109. De Ugarte, D.A., Morizono, K., Elbarbary, A., Alfonso, Z., Zuk, P.A., Zhu, M., *et al.* Comparison of multi-lineage cells from human adipose tissue and bone marrow. Cells Tissues Organs **174,** 101, 2003.
110. Batinić, D., Marusić, M., Pavletić, Z., Bogdanić, V., Uzarević, B., Nemet, D., *et al.* Relationship between differing volumes of bone marrow aspirates and their cellular composition. Bone Marrow Transplant **6,** 103, 1990.
111. Guilak, F., Lott, K.E., Awad, H.A., Cao, Q., Hicok, K.C., Fermor, B., *et al.* Clonal analysis of the differentiation potential of human adipose-derived adult stem cells. J Cell Physiol **206,** 229, 2006.
112. Weinzierl, K., Hemprich, A., and Frerich, B. Bone engineering with adipose tissue derived stromal cells. J Craniomaxillofac Surg **34,** 466, 2006.
113. Halvorsen, Y.D., Franklin, D., Bond, A.L., Hitt, D.C., Auchter, C., Boskey, A.L., *et al.* Extracellular matrix mineralization and osteoblast gene expression by human adipose tissue-derived stromal cells. Tissue Eng **7,** 729, 2001.
114. Hattori, H., Sato, M., Masuoka, K., Ishihara, M., Kikuchi, T., Matsui, T., *et al.* Osteogenic potential of human adipose tissue-derived stromal cells as an alternative stem cell source. Cells Tissues Organs **178,** 2, 2004.
115. Wall, M., Bernacki, S.H., and Loboa, E.G. Effects of serial passaging on the adipogenic and osteogenic differentiation potential of adipose-derived human mesenchymal stem cells. Tissue Eng **13,** 1291, 2007.
116. Gronthos, S., Franklin, D.M., Leddy, H.A., Robey, P.G., Storms, R.W., and Gimble, J.M. Surface protein characterization of human adipose tissue-derived stromal cells. J Cell Physiol **189,** 54, 2001.
117. Mauney, J.R., Nguyen, T., Gillen, K., Kirker-Head, C., Gimble, J.M., and Kaplan, D.L. Engineering adipose-like tissue *in vitro* and *in vivo* utilizing human bone marrow and adipose-derived mesenchymal stem cells with silk fibroin 3D scaffolds. Biomaterials **28,** 5280, 2007.
118. Mehlhorn, A.T., Niemeyer, P., Kaiser, S., Finkenzeller, G., Stark, G.B., Sudkamp, N.P., *et al.* Differential expression pattern of extracellular matrix molecules during chondrogenesis of mesenchymal stem cells from bone marrow and adipose tissue. Tissue Eng **12,** 2853, 2006.
119. Vidal, M.A., Kilroy, G.E., Lopez, M.J., Johnson, J.R., Moore, R.M., and Gimble, J.M. Characterization of equine adipose tissue-derived stromal cells: adipogenic and osteogenic capacity and comparison with bone marrow-derived mesenchymal stromal cells. Vet Surg **36,** 613, 2007.
120. Im, G.I., Shin, Y.W., and Lee, K.B. Do adipose tissue-derived mesenchymal stem cells have the same osteogenic and chondrogenic potential as bone marrow-derived cells? Osteoarthritis Cartilage **13,** 845, 2005.
121. Afizah, H., Yang, Z., Hui, J.H., Ouyang, H.W., and Lee, E.H. A comparison between the chondrogenic potential of human bone marrow stem cells (BMSC) and adipose-derived stem cells (ADSCs) taken from the same donors. Tissue Eng **13,** 659, 2007.
122. Liu, T.M., Martina, M., Hutmacher, D.W., Hui, J.H., Lee, E.H., and Lim, B. Identification of common pathways mediating differentiation of bone marrow- and adipose tissue-derived human mesenchymal stem cells into three mesenchymal lineages. Stem Cells **25,** 750, 2007.
123. Estes, B.T., Wu, A.W., and Guilak, F. Potent induction of chondrocytic differentiation of human adipose-derived adult stem cells by bone morphogenetic protein 6. Arthritis Rheum **54,** 1222, 2006.
124. Estes, B.T., Wu, A.W., Storms, R.W., and Guilak, F. Extended passaging, but not aldehyde dehydrogenase activity, increases the chondrogenic potential of human adipose-derived adult stem cells. J Cell Physiol **209,** 987, 2006.
125. Puetzer, J.L., Petitte, J.N., and Loboa, E.G. Comparative review of growth factors for induction of three-dimensional in vitro chondrogenesis in human mesenchymal stem cells isolated from bone marrow and adipose tissue. Tissue Eng Part B Rev **16,** 435, 2010.
126. Jansen, B.J., Gilissen, C., Roelofs, H., Schaap-Oziemlak, A., Veltman, J., Raymakers, R.A., *et al.* Functional differences between mesenchymal stem cell populations are reflected by their transcriptome. Stem Cells Dev **19,** 481, 2010.
127. Prunet-Marcassus, B., Cousin, B., Caton, D., André, M., Pénicaud, L., and Casteilla, L. From heterogeneity to plasticity in adipose tissues: site-specific differences. Exp Cell Res **312,** 727, 2006.
128. Bernacki, S., Wall, M., and Loboa, E. Isolation of human mesenchymal stem cells from bone and adipose tissue. Methods Cell Biol **86,** 257, 2008.
129. Katz, A.J., Tholpady, A., Tholpady, S.S., Shang, H., and Ogle, R.C. Cell surface and transcriptional characterization of human adipose-derived adherent stromal (hADAS) cells. Stem Cells **23,** 412, 2005.
130. Rada, T., Reis, R.L., and Gomes, M.E. Distinct stem cells subpopulations isolated from human adipose tissue exhibit different chondrogenic and osteogenic differentiation potential. Stem Cell Rev **7,** 64, 2011.
131. McCullen, S., Zhu, Y., Bernacki, S., Narayan, R., Pourdeyhimi, B., Gorga, R., *et al.* Electrospun composite poly (L-lactic acid)/tricalcium phosphate scaffolds induce proliferation and osteogenic differentiation of human adipose-derived stem cells. Biomed Mater **4,** 035002, 2009.
132. Hanson, A., Wall, M., Pourdeyhimi, B., and Loboa, E. Effects of oxygen plasma treatment on adipose-derived human mesenchymal stem cell adherence to poly (L-lactic acid) scaffolds. J Biomater Sci Poly Ed **18,** 1387, 2007.
133. Hyde, G., McCullen, S., Jeon, S., Stewart, S., Jeon, H., Loboa, E., *et al.* Atomic layer deposition and biocompatibility of titanium nitride nano-coatings on cellulose fiber substrates. Biomed Mater **4,** 025001, 2009.
134. McCullen, S., Stevens, D., Roberts, W., Clarke, L., Bernacki, S., Gorga, R., *et al.* Characterization of electrospun nanocomposite scaffolds and biocompatibility with adipose-derived human mesenchymal stem cells. Int J Nanomed **2,** 253, 2007.
135. Hattori, H., Masuoka, K., Sato, M., Ishihara, M., Asazuma, T., Takase, B., *et al.* Bone formation using human adipose tissue-derived stromal cells and a biodegradable scaffold. J Biomed Mater Res Part B Appl Biomater **76,** 230, 2006.
136. Kakudo, N., Shimotsuma, A., Miyake, S., Kushida, S., and Kusumoto, K. Bone tissue engineering using human

adipose-derived stem cells and honeycomb collagen scaffold. J Biomed Mater Res Part A **84,** 191, 2008.
137. Marino, G., Rosso, F., Cafiero, G., Tortora, C., Moraci, M., Barbarisi, M., *et al.* Beta-tricalcium phosphate 3D scaffold promote alone osteogenic differentiation of human adipose stem cells: *in vitro* study. J Mater Sci Mater Med **21,** 353, 2010.
138. Liu, Q., Cen, L., Yin, S., Chen, L., Liu, G., Chang, J., *et al.* A comparative study of proliferation and osteogenic differentiation of adipose-derived stem cells on akermanite and beta-TCP ceramics. Biomaterials **29,** 4792, 2008.
139. Hao, W., Pang, L., Jiang, M., Lv, R., Xiong, Z., and Hu, Y.-Y. Skeletal repair in rabbits using a novel biomimetic composite based on adipose-derived stem cells encapsulated in collagen I gel with PLGA-β-TCP scaffold. J Orthop Res **28,** 252, 2010.
140. Haimi, S., Suuriniemi, N., Haaparanta, A.M., Ellä, V., Lindroos, B., Huhtala, H., *et al.* Growth and osteogenic differentiation of adipose stem cells on PLA/bioactive glass and PLA/beta-TCP scaffolds. Tissue Eng Part A **15,** 1473, 2009.
141. Cowan, C.M., Aalami, O.O., Shi, Y.-Y., Chou, Y.-F., Mari, C., Thomas, R., *et al.* Bone morphogenetic protein 2 and retinoic acid accelerate *in vivo* bone formation, osteoclast recruitment, and bone turnover. Tissue Eng **11,** 645, 2005.
142. Conejero, J., Lee, J., Parrett, B., Terry, M., Wear-Maggitti, K., Grant, R., *et al.* Repair of palatal bone defects using osteogenically differentiated fat-derived stem cells. Plast Reconstr Surg **117,** 857, 2006.
143. Yoon, E., Dhar, S., Chun, D., Gharibjanian, N., and Evans, G. In vivo osteogenic potential of human adipose-derived stem cells/poly lactide-co-glycolic acid constructs for bone regeneration in a rat critical-sized calvarial defect model. Tissue Eng **13,** 619, 2007.
144. Jeon, O., Rhie, J., Kwon, I., Kim, J., Kim, B., and Lee, S. In vivo bone formation following transplantation of human adipose–derived stromal cells that are not differentiated osteogenically. Tissue Eng Part A **14,** 1285, 2008.
145. Lin, L., Shen, Q., Wei, X., Hou, Y., Xue, T., Fu, X., *et al.* Comparison of osteogenic potentials of BMP4 transduced stem cells from autologous bone marrow and fat tissue in a rabbit model of calvarial defects. Calcif Tissue Int **85,** 55, 2009.
146. Yang, M., Ma, Q.J., Dang, G.T., Ma, K.t., Chen, P., and Zhou, C.Y. *In vitro* and *in vivo* induction of bone formation based on *ex vivo* gene therapy using rat adipose-derived adult stem cells expressing BMP-7. Cytotherapy **7,** 273, 2005.
147. Kang, Y., Liao, W.-M., Yuan, Z.-H., Sheng, P.-Y., Zhang, L.-J., Yuan, X.-W., *et al. In vitro* and *in vivo* induction of bone formation based on adeno-associated virus-mediated BMP-7 gene therapy using human adipose-derived mesenchymal stem cells. Acta Pharmacol Sin **28,** 839, 2007.
148. Dragoo, J.L., Choi, J.Y., Lieberman, J.R., Huang, J., Zuk, P.A., Zhang, J., *et al.* Bone induction by BMP-2 transduced stem cells derived from human fat. J Orthop Res **21,** 622, 2003.
149. Wu, L., Wu, Y., Lin, Y., Jing, W., Nie, X., Qiao, J., *et al.* Osteogenic differentiation of adipose derived stem cells promoted by overexpression of osterix. Mol Cell Biochem **301,** 83, 2007.
150. Gupta, A., Leong, D.T., Bai, H.F., Singh, S.B., Lim, T.-C., and Hutmacher, D.W. Osteo-maturation of adipose-derived stem cells required the combined action of vitamin D3, beta-glycerophosphate, and ascorbic acid. Biochem Biophys Res Commun **362,** 17, 2007.
151. Cho, H.H., Shin, K.K., Kim, Y.J., Song, J.S., Kim, J.M., Bae, Y.C., *et al.* NF-kappaB activation stimulates osteogenic differentiation of mesenchymal stem cells derived from human adipose tissue by increasing TAZ expression. J Cell Physiol **223,** 168, 2010.
152. Zeng, Q., Li, X., Beck, G., Balian, G., and Shen, F.H. Growth and differentiation factor-5 (GDF-5) stimulates osteogenic differentiation and increases vascular endothelial growth factor (VEGF) levels in fat-derived stromal cells *in vitro*. Bone **40,** 374, 2007.
153. Cho, H.H., Park, H.T., Kim, Y.J., Bae, Y.C., Suh, K.T., and Jung, J.S. Induction of osteogenic differentiation of human mesenchymal stem cells by histone deacetylase inhibitors. J Cell Biochem **96,** 533, 2005.
154. Jørgensen, N.R., Henriksen, Z., Sørensen, O.H., and Civitelli, R. Dexamethasone, BMP-2, and 1,25-dihydroxyvitamin D enhance a more differentiated osteoblast phenotype: validation of an *in vitro* model for human bone marrow-derived primary osteoblasts. Steroids **69,** 219, 2004.
155. Karageorgiou, V., Meinel, L., Hofmann, S., Malhotra, A., Volloch, V., and Kaplan, D. Bone morphogenetic protein-2 decorated silk fibroin films induce osteogenic differentiation of human bone marrow stromal cells. J Biomed Mater Res Part A **71,** 528, 2004.
156. Jaiswal, N., Haynesworth, S.E., Caplan, A.I., and Bruder, S.P. Osteogenic differentiation of purified, culture-expanded human mesenchymal stem cells *in vitro*. J Cell Biochem **64,** 295, 1997.
157. Pittenger, M.F., Mackay, A.M., Beck, S.C., Jaiswal, R.K., Douglas, R., Mosca, J.D., *et al.* Multilineage potential of adult human mesenchymal stem cells. Science **284,** 143, 1999.
158. Raab-Cullen, D.M., Akhter, M.P., Kimmel, D.B., and Recker, R.R. Bone response to alternate-day mechanical loading of the rat tibia. J Bone Miner Res **9,** 203, 1994.
159. Zhao, F., Chella, R., and Ma, T. Effects of shear stress on 3-D human mesenchymal stem cell construct development in a perfusion bioreactor system: Experiments and hydrodynamic modeling. Biotechnol Bioeng **96,** 584, 2007.
160. Cartmell, S.H., Porter, B.D., Garcia, A.J., and Guldberg, R.E. Effects of medium perfusion rate on cell-seeded three-dimensional bone constructs *in vitro*. Tissue Eng **9,** 1197, 2003.
161. Goldstein, A.S., Juarez, T.M., Helmke, C.D., Gustin, M.C., and Mikos, A.G. Effect of convection on osteoblastic cell growth and function in biodegradable polymer foam scaffolds. Biomaterials **22,** 1279, 2001.
162. Thomas, G.P., and el Haj, A.J. Bone marrow stromal cells are load responsive *in vitro*. Calcif Tissue Int **58,** 101, 1996.
163. Yoshikawa, T., Peel, S.A., Gladstone, J.R., and Davies, J.E. Biochemical analysis of the response in rat bone marrow cell cultures to mechanical stimulation. Biomed Mater Eng **7,** 369, 1997.
164. Mauney, J., Sjostorm, S., Blumberg, J., Horan, R., O'leary, J., Vunjak-Novakovic, G., *et al.* Mechanical stimulation promotes osteogenic differentiation of human bone marrow stromal cells on 3-D partially demineralized bone scaffolds in vitro. Calcif Tissue Int **74,** 458, 2004.
165. Ward, D.F., Jr., Salasznyk, R.M., Klees, R.F., Backiel, J., Agius, P., Bennett, K., *et al.* Mechanical strain enhances extracellular matrix-induced gene focusing and promotes osteogenic differentiation of human mesenchymal stem cells through an extracellular-related kinase-dependent pathway. Stem Cells Dev **16,** 467, 2007.
166. Simmons, C., Matlis, S., Thornton, A., Chen, S., Wang, C., and Mooney, D. Cyclic strain enhances matrix mineraliza-

tion by adult human mesenchymal stem cells via the extracellular signal-regulated kinase (ERK1/2) signaling pathway. J Biomech **36,** 1087, 2003.
167. Huang, S.-C., Wu, T.-C., Yu, H.-C., Chen, M.-R., Liu, C.-M., Chiang, W.-S., *et al.* Mechanical strain modulates age-related changes in the proliferation and differentiation of mouse adipose-derived stromal cells. BMC Cell Biol **11,** 18, 2010.
168. Kaspar, D., Seidl, W., Neidlinger-Wilke, C., Beck, A., Claes, L., and Ignatius, A. Proliferation of human-derived osteoblast-like cells depends on the cycle number and frequency of uniaxial strain. J Biomech **35,** 873, 2002.
169. Gurkan, U.A., and Akkus, O. The mechanical environment of bone marrow: a review. Ann Biomed Eng **36,** 1978, 2008.
170. Loboa, E.G., Wren, T.A.L., Beaupré, G.S., and Carter, D.R. Mechanobiology of soft skeletal tissue differentiation—a computational approach of a fiber-reinforced poroelastic model based on homogeneous and isotropic simplifications. Biomech Model Mechanobiol **2,** 83, 2003.
171. Tjabringa, G., Vezeridis, P., Zandieh-Doulabi, B., Helder, M., Wuisman, P., and Klein-Nulend, J. Polyamines modulate nitric oxide production and Cox-2 gene expression in response to mechanical loading in human adipose tissue-derived mesenchymal stem cells. Stem Cells **24,** 2262, 2006.
172. Grayson, W.L., Bhumiratana, S., Cannizzaro, C., Chao, P.-H.G., Lennon, D.P., Caplan, A.I., *et al.* Effects of initial seeding density and fluid perfusion rate on formation of tissue-engineered bone. Tissue Eng Part A **14,** 1809, 2008.
173. Grayson, W.L., Martens, T.P., Eng, G.M., Radisic, M., and Vunjak-Novakovic, G. Biomimetic approach to tissue engineering. Semin Cell Dev Biol **20,** 665, 2009.
174. Sim, W.Y., Park, S.W., Park, S.H., Min, B.H., Park, S.R., and Yang, S.S. A pneumatic micro cell chip for the differentiation of human mesenchymal stem cells under mechanical stimulation. Lab Chip **7,** 1775, 2007.
175. Duty, A.O., Oest, M.E., and Guldberg, R.E. Cyclic mechanical compression increases mineralization of cell-seeded polymer scaffolds *in vivo*. J Biomech Eng **129,** 531, 2007.
176. Pelaez, D., Charles Huang, C.-Y., Cheung, H.S. Cyclic compression maintains viability and induces chondrogenesis of human mesenchymal stem cells in fibrin gel scaffolds. Stem Cells Dev **18,** 93, 2009.
177. Kisiday, J.D., Frisbie, D.D., McIlwraith, C.W., and Grodzinsky, A.J. Dynamic compression stimulates proteoglycan synthesis by mesenchymal stem cells in the absence of chondrogenic cytokines. Tissue Eng Part A **15,** 2817, 2009.
178. Goldstein, C., Sprague, S., and Petrisor, B.A. Electrical stimulation for fracture healing: current evidence. J Orthop Trauma **24 Suppl 1,** S62, 2010.
179. Tsai, M.-T., Chang, W.H.-S., Chang, K., Hou, R.-J., and Wu, T.-W. Pulsed electromagnetic fields affect osteoblast proliferation and differentiation in bone tissue engineering. Bioelectromagnetics **28,** 519, 2007.
180. Tsai, M.-T., Li, W.-J., Tuan, R.S., and Chang, W.H. Modulation of osteogenesis in human mesenchymal stem cells by specific pulsed electromagnetic field stimulation. J Orthop Res **27,** 1169, 2009.
181. Kim, I.S., Song, J.K., Song, Y.M., Cho, T.H., Lee, T.H., Lim, S.S., *et al.* Novel effect of biphasic electric current on *in vitro* osteogenesis and cytokine production in human mesenchymal stromal cells. Tissue Eng Part A **15,** 2411, 2009.
182. Aaron, R.K., and Ciombor, D.M. Acceleration of experimental endochondral ossification by biophysical stimulation of the progenitor cell pool. J Orthop Res **14,** 582, 1996.
183. Au, A., Boehm, C., Mayes, A., Muschler, G., and Griffith, L. Formation of osteogenic colonies on well-defined adhesion peptides by freshly isolated human marrow cells. Biomaterials **28,** 1847, 2007.
184. Chaubey, A., Ross, K., Leadbetter, R., and Burg, K. Surface patterning: tool to modulate stem cell differentiation in an adipose system. J Biomed Mater Res **84B,** 70, 2007.
185. Kim, T., Seong, J., Ouyang, M., Sun, J., Lu, S., Hong, J., *et al.* Substrate rigidity regulates Ca 2+oscillation via RhoA pathway in stem cells. J Cell Physiol **218,** 285, 2009.
186. Martino, M.M., Mochizuki, M., Rothenfluh, D.A., Rempel, S.A., Hubbell, J.A., and Barker, T.H. Controlling integrin specificity and stem cell differentiation in 2D and 3D environments through regulation of fibronectin domain stability. Biomaterials **30,** 1089, 2008.
187. Neal, R., McClugage, S., III., Link, M., Sefcik, L., Ogle, R., and Botchwey, E. Laminin nanofiber meshes that mimic morphological properties and bioactivity of basement membranes. Tissue Eng Part C: Methods **15,** 11, 2008.
188. Rowlands, A., George, P., and Cooper-White, J. Directing osteogenic and myogenic differentiation of MSC: interplay of stiffness and adhesive ligand presentation. Am J Physiol Cell Physiol **295,** C1037, 2008.
189. Reed, C., Han, L., Andrady, A., Caballero, M., Jack, M., Collins, J., *et al.* Composite tissue engineering on polycaprolactone nanofiber scaffolds. Ann Plast Surg **62,** 505, 2009.

Address correspondence to:
Elizabeth G. Loboa, Ph.D.
Joint Department of Biomedical Engineering
UNC-Chapel Hill and NC State University
4208B EB3, Campus Box 7115
Raleigh, NC 27695-7115

E-mail: egloboa@ncsu.edu

Received: December 21, 2010
Accepted: February 18, 2011
Online Publication Date: April 1, 2011

CHAPTER 3 Primary Cilia: Control Centers for Stem Cell Lineage Specification and Potential Targets for Cell-Based Therapies

This chapter is in preparation for submission to Physiological Reviews.

3.1 Introduction

The primary cilium is a cell organelle present on most vertebrate cell types. It has emerged as an important sensory organelle, thought to coordinate a multitude of critical cell processes, and it has garnered much research attention over the last decade. Primary cilia were first described by Zimmerman in 1898 in his observations on the lumen of kidney tubules (*4*). However, the structure was largely ignored for the following century, with many researchers deeming it a vestigial organelle. The primary cilium is now known to modulate many cell processes, including cell proliferation, differentiation and cell migration (*4*, *33*, *37*, *42*, *43*). Primary cilia are composed of nine microtubule doublets arranged concentrically in a 9 + 0 configuration, and they are generally considered non-motile, with the exception of specialized nodal cilia (*44*). In contrast, motile cilia structures present in epithelial mucociliary systems such as the airway express a 9 + 2 microtubule configuration, with a central pair of microtubules in the center of the ciliary axoneme. In addition to structural disparities between the two classes of cilia, non-motile primary cilia are typically thought to lack the axonemal dynein motor proteins that facilitate the beating motion of motile cilia

(*45*). In the context of this review, we aim to examine how the structure and function of the primary cilium relates to cell phenotype, particularly focusing on cilium's mechanistic contribution to the development, maintenance and degeneration of specific progenitor and/or stem cell phenotypes.

Primary cilia typically localize to the apical cell surface of epithelial cell types and cells grown in monolayer culture. Their structure is contained within a ciliary membrane contiguous with the cell membrane (*46*). However, they have also been observed within a membrane infolding just below the membrane surface of the cell (*46*). Primary cilia emanate from the mother centriole, anchoring the basal body and docking just below the surface of the cell membrane (*47*). The presence of the primary cilium is intimately associated with the cell cycle, as they are most frequently expressed during the G_0 phase. However, they can be observed any time during interphase and are normally assembled during the G_1 phase (*48*).

In addition to their cell cycle link, many researchers have identified the primary cilium as a chemo- and/or mechanosensory organelle in a variety of cell types, including those derived from bone (*30*, *49*, *50*), cartilage (*51-53*), kidney (*54*, *55*), cardiovascular (*32*, *56*, *57*) and neural tissue (*58*, *59*) . These studies collectively hint at the idea that the primary cilium may be the physical and chemical balance point for cell lineage specification, fulfilling the paradigm that cell proliferation is at odds with cell differentiation; as proliferative activity slows, cells can then differentiate (*60*, *61*).

The function of the primary cilium is not limited to basic cell physiology, and its dysfunction has been implicated in a number of diseases. Clinical presentations of motile or non-motile cilia-associated genetic diseases and disorders have recently been classified as

"ciliopathies" (*62*). Ciliopathies can arise at any time from development through adulthood, and they can affect virtually any tissue in the body. Ciliopathies frequently result in neurosensory or respiratory system disorders or abnormal patterning in bone development. They can also cause tissue degeneration in the liver or kidney due to aberrant cell proliferation and cyst development (*62*).

Research at the convergence of clinical ciliopathies and cilia biology has the potential to uncover the fundamental cell proliferation and differentiation processes that are mediated by the cilium, a once-overlooked vestige of evolution. Investigators estimate that the primary cilium is associated with the activity of over 300 proteins and mediates the signaling processes of many critical signaling pathways (*36*, *63*). This review aims to highlight the major studies elucidating the functions of primary cilia in cell phenotype, with a focus on stem cells and tissue morphogenesis. We will begin with a summary of the methodologies used to direct and define cell phenotype. We will then follow with a brief background on the physiological function of the primary cilium as shown through landmark studies performed in the kidney. Subsequently, we will explore the role of the primary cilium during environmentally-induced changes in cell phenotype, modulating the chemical, mechanical and substrate microenvironment. Each section describes induction factors and processes of cell lineage specification, maintenance of cell lineage and degeneration into a pathological cell phenotype, with primary emphasis on connective and musculoskeletal cell and tissue phenotypes. Finally, we will describe more recent work investigating the role of the primary cilium in regulating adult stem cell fate, particularly for musculoskeletal tissue applications.

3.2 *In Vitro* Approaches to Define Cell Phenotype

In the context of tissue engineering and regenerative medicine, defining cell phenotype has been a critical barrier to the widespread clinical application of stem cell-based tissue replacement therapies. In both stem cell and committed cell types, culture conditions such as chemical factors, mechanical stimulation and substrate microenvironment modulation all affect cell phenotype. A variety of cellular attributes can be examined to determine a committed cell phenotype: cellular morphology, cytoskeletal organization, focal adhesion formation, gene expression profiles, protein expression profiles and end-product expression (*64-67*). Emerging evidence suggests that the primary cilium is another indicator of cell phenotype and is likely linked to phenotypic observations in cytoskeletal reorganization; however, its distinct function in determining/predicting cell phenotype is a relatively new area of study. Further supporting the idea that the primary cilium plays a role in phenotypic determination, loss of cell phenotype and dysregulation of tissue homeostasis is observed in ciliopathies such as autosomal polycystic kidney disease.

3.3 Primary Cilia and Loss of Phenotype - Kidney

The physiological function of the primary cilium was discovered when investigators identified its link with polycystic kidney disease (PKD). That work was the first prominent study to recognize the vertebrate primary cilium as a mechanosensory organelle (Nauli & Zhou 2004). PKD is an autosomal genetic disorder characterized by a loss of primary cilia in the epithelial cells of the kidney distal tubule. Absence of the primary cilia leads to a loss of mechanosensitivity followed by hyperproliferation of the epithelial cells, which eventually form cysts (*6*, *54*). The process of cilia loss is associated with a loss of phenotype or de-

differentiation of the epithelial layer. Frequently in autosomal PKD, the genes PKD1 and PKD2, respectively encoding functional ciliary polycystin-1 (PC1) and polycystin-2 (PC2), are mutated (*6*). The resulting loss of cilia in PKD leads to the deregulation of typical kidney tissue homeostasis, suggesting that PC1 and PC2 serve a functional mechanosensitivity role.

In a study by Nauli *et al.,* murine cells lacking functional PC1 still formed cilia but demonstrated a loss of fluid sensitivity as measured by fluid-induced calcium fluxes (*68*). Other polycystic kidney models have identified KIF3A and IFT88 as critical cilia proteins required for healthy kidney homeostasis, motivating the work behind a large majority of studies on primary cilia in musculoskeletal function (*6*).

3.4 Primary Cilia in the Developing Musculoskeletal System

As the story with primary cilia has unfolded, it appears that the ciliary structure was observed on chondrocytes and osteogenic cell types approximately 30 years prior to their in-depth study in the kidney. However, the cilium structure and its associated proteins are now known to play critical chemo- and mechanosensory roles in osteocytes (*49*, *50*), osteoblasts (*30*), chondrocytes (*46*, *69*), and tenocytes (*70*), amongst other connective tissue cell types (*41*, *71*). Though the expression patterns of these musculoskeletal cell types still remain something of an enigma, they are clearly an important locale for the signaling pathways that modulate musculoskeletal cell lineages, such as Wnt (*72*), Hedgehog (*73*) and TGF-β signaling pathways (*74*).

3.4.1 Cilia in Development - Skeletogenesis

On the heels of the foundational kidney studies, Xiao *et al.* observed primary cilia structures on bone cells in culture and expressed on osteoblasts and osteocytes in extracted bone tissue (*75*). Not only were primary cilia structures present, Xiao *et al.* reported the link between a functional PKD1 gene encoding polycystin-1 and the expression of osteogenic gene markers. Using heterozygous and homozygous *Pkd1*^{m1Bei} mouse models that possessed an inactivating point mutation within the first transmembrane domain of the PC1 protein structure, they demonstrated that this mutation led to osteopenia and skeletal abnormalities in the developing embryo. Additionally, embryonic mice with the homozygous *Pkd1*^{m1Bei} mutation expressed a more severely disrupted skeletal phenotype (*75*). Osteoblasts isolated from these mice exhibited reduced osteogenic *Runx2* expression at both the gene and protein level. Further, they exhibited a reduced capacity for differentiation *ex vivo,* suggesting their osteogenic phenotype was impaired. Xiao *et al.* also showed that an overexpression of PC1 in MC3T3E1 osteoblasts conferred an upregulation of osteoblastic gene markers. Further, in osteoblasts derived from the *Pkd1*^{m1Bei} mice, co-expression of PC1 restored *Runx2* P1 promoter activity and osteogenic gene expression levels (*75*). This study was the first major study to functionally link primary cilia with the osteogenic phenotype.

Following the Xiao *et al.* report, a wide range of *in vivo* and *in vitro* studies implicated primary cilia as a part of the osteogenic and chondrogenic phenotype. Intraflagellar transport is a critical aspect of primary cilia biology because their proteins must be synthesized outside of the ciliary body and subsequently transported into the ciliary pocket or membrane (*43*, *63*). In addition to PKD1 and functional cilia-localized PC1 protein,

a group of kinesin, intraflagellar transport (IFT) and dynein proteins are responsible for antero- and retrograde protein transport through the axoneme of the primary cilium and have been found to modify ciliary structure and function (*30*, *76*).

3.4.2 Cilia in Development - Endochondral Ossification and Subchondral Tissue

3.4.2.1 Mouse Models - Kif3a Knockout

Kif3a is a protein subunit of the Kinesin II Motor complex, which is active in the process of ciliary transport. Kif3a has been of particular interest in the bone and cartilage development of the post-natal growth plate and in the endochondral ossification of developing/growing subchondral tissue. One of the first reports to implicate Kif3a in ciliary activity and skeletogenesis described impaired cilia formation in mouse chondrocytes modified by a Col2a-Cre-mediated Kif3a deletion (*77*). Mice possessing the Kif3a deletion exhibited post-natal dwarfism and premature loss of the endochondral growth plate in long bones. Additionally, this deletion resulted in aberrant chondrocyte rotation; its healthy function is necessary to maintain the columnar organization of the long bone epiphyseal growth plate. This misorientation was concomitant with disruption of the actin cytoskeleton and focal adhesion formation, likely affecting the differentiation activity in the growth plate (*77*).

The role of Kif3a in cartilage was further confirmed in a study by Koyama *et al.,* describing *Kif3a*-deficient mice that by post-natal day 7 lacked ordered zones of proliferative and hypertrophic regions of chondrocytes in the cranial synchondrosis growth plate (*78*). Unusual intramembranous ossification coupled with ectopic cartilage development was also observed. The resulting *Kif3a*-deficient cranial phenotype somewhat coincided with that of

mice deficient in the *Indian Hedgehog* gene (*Ihh)* and led Koyama *et al.* to investigate the distribution of Hedgehog signaling within the Kif3a mutant mice. They reported a differential distribution of topographical Hedgehog signaling activity in the synchondroses of the *Kif3a*-deficient mice relative to the controls. Further, they found that *Ihh*-deficient mice developed abnormal synchondroses. However, the phenotype was distinct from that of the *Kif3a*-deficient mice (*78*), indicating that the cilium uniquely contributes to the localization of Hedgehog signaling in the cranial growth plate.

3.4.2.2 Mouse Models - IFT88 Knockout

The *Tg737*^{orpk} mouse model for autosomal polycystic kidney disease expressed epiphysis and growth plate morphology comparable to the *Kif3a*-deficient mouse (*79*). *Tg737*^{orpk} mice express a global mutation in the *Tg737* gene resulting in a disruption of its encoded protein IFT88, also known as Polaris. Disruption of IFT88/Polaris leads to a lack and/or shortening of cilia expressed in the kidney cells as well as cells of other tissues (*80*). Chondrocytes in the growth plate of *Tg737*^{orpk} mice were reported to express a dearth of ciliary structures and to lack the characteristic cilia orientation in those chondrocytes within the surface layers of the cartilage tissue (*79*). Consistent with the Kif3a epiphyseal growth plate findings, the organization of the actin cytoskeleton was affected by the lack of cilia.

To more closely examine the specific effects of IFT88 on endochondral bone formation, Haycraft *et al.* developed a conditional mutant mouse using a Cre-*lox* system targeting only the mesenchymal tissues, avoiding the lethality of a global IFT88 mutation (*81*). Mice at post-natal day 11 expressing the conditional *prx1cre;Ift88*$^{fl/n}$ mutation exhibited forelimbs stunted along the proximodistal axis with severe polydactylism (*81*). Associated

with the disrupted endochondral bone formation in the mutant mice, Haycraft *et al.* identified irregular Sonic Hedgehog (Shh) signaling in conjunction with abnormal digit patterning and reduced Ihh signaling (*81*). Ectopic deposition of chondrocytes and perichondral organization were abnormal in this mutant model (*81*). These abnormalities were similar to endochondral phenotypes observed in the growth plate irregularities of the Kif3a and Tg737^{orpk} studies (*77*, *79*).

Though IFT88 is a different protein involved in intraflagellar transport within the cilium, like Kif3a it is a critical ciliary protein required for functional cilia expression. This supports the idea that the cilium is required for appropriate cell specification and tissue morphogenesis processes. Taken together, these studies suggest that the primary cilium, and more specifically the intraflagellar transport activity of the cilium, plays an important role in cartilage tissue morphogenesis, with the primary cilium structure likely mediating distinct protein activity in the Hedgehog signaling pathway.

3.4.3 Degeneration – Cilia and Osteoarthritis

Osteoarthritis (OA) is a degenerative joint disease leading to the degradation of articular cartilage and subchondral bone. It can be genetically inherited and/or caused or exacerbated by acute or chronic injury. In OA patients, primary cilia have been observed on localized subpopulations of human chondrocytes undergoing degeneration of fibrillated and non-fibrillated cartilage, both in the superficial and middle zones (*51*). In this early study, cilia were most frequently observed in the middle zone of cartilage from OA patients, while few were observed in the cartilage of non-OA control patients (*51*). A subsequent study published nearly 12 years later quantified the frequency of cilia observed on OA tissue in a

bovine model (*82*). Those authors reported increased cilia expression and length in OA chondrocytes at the degenerating articular surface as compared to healthy cartilage; further, they found an increase in ciliated cells corresponding to the degree of tissue degeneration (*82*). These observations allude to the function of primary cilia in phenotype, corresponding to a change in the degenerating extracellular environment.

Cilia seem to serve an important function in developing endochondral tissue and diseased subchondral tissue of the skeletal system, suggesting that the cilium may indiscriminately coordinate processes of cell differentiation in both tissue homeostasis and tissue degeneration. The primary cilium's multifaceted functionality in directing chondrogenic and osteogenic phenotypes in the subchondral tissue suggests that it may be a potential therapeutic target in treating OA.

3.4.4 Cilia in Development - Chondrogenesis

Primary cilia have not only been observed in the endochondral regions of ossifying bone and in cartilage degeneration in OA; they are also present in mature cartilage and likely serve a mechano-active function in cartilage tissue. In 1997, primary cilia were identified *in situ* on canine articular cartilage of the tibial plateau and femoral condyle (*83*). Cilia were also observed on agarose-cultured canine chondrocytes isolated from the same regions, but the ciliary structure projected out farther from the cytoplasmic surface than the *in situ* cilia, which were observed within a membranous ciliary pocket (*83*). These early reports on cilia in cartilage highlight the differences in cilia structure between chondrocytes *in vivo* and those cultured *in vitro,* pointing to the relationship between the primary cilium and chondrogenic phenotype.

Following the 1997 work, transmission electron microscopy (TEM) and confocal microscopy analyses by Poole *et al.* and Jensen *et al.*, respectively, described the ultrastructure and orientation of the primary cilium in hyaline cartilage derived from the sterna of chick embryos (*84*, *85*). Those studies determined that the chondrocyte primary cilium ranges in length from 1-4 μm, and it was categorically observed by Poole *et al.* to express three patterns of orientation *in situ:* 1) fully extended into the extracellular matrix (ECM), 2) partially extending with bending along the axoneme, 3) folded along the surface of the cytoplasm with minimal matrix contact (*84*). Further, the authors frequently observed the Golgi apparatus to be anchored between the nucleus and the base of the cilium. They hypothesized that the cilium may act as a conduit collecting chemical and/or mechanical cues from the ECM to direct Golgi activity (*84*). These studies demonstrated that the primary cilium structure can be deflected or bent within the cartilage matrix; the mechanical force applied to the tissue is likely transduced to the cilium from the surrounding matrix of collagen fibers and proteoglycans (*84*) (*85*). This idea was supported by TEM images illustrating potential attachment points between collagen fibers and the ciliary membrane. Confocal images also illustrated the differential bending profiles expressed by the chondrocyte primary cilia (*85*).

A recent study published in 2014 explored the relationship between the presence of primary cilia and the mechanical properties of cartilage tissue. It was observed that loss of primary cilia in the *Col2aCre;ift88*$^{fl/fl}$ transgenic mouse model results in upregulation of OA markers. This occurs in conjunction with reduced structural integrity and a thickening of the cartilage tissue (*52*). Somewhat in contrast to the frequency of ciliated cells in typical OA

models, in this model the chondrocytes devoid of cilia were associated with an OA phenotype. However, this study points to the importance of primary cilia in maintaining a healthy chondrogenic phenotype and its role in cartilage homeostasis (*52*).

3.5 Primary Cilia as Chemosensors

Chemical stimulation of cells *in vitro* is known to affect the frequency of expression, length and orientation of primary cilia in culture, demonstrating their sensitivity to the surround chemical environment. Through loss of function animal models, investigators have been able to show the importance of cilia in tissue development in the embryo; however, *in vitro* studies aim to clarify their specific cellular function. Primary cilia have been observed on a variety of cell types under *in vitro* cell culture, including stem and progenitor cells (*3*, *41*, *73*, *86*). The expression patterns of primary cilia on cultured cell types remain an enigma due to the high variation observed across cell types. However, their expression is thought be largely linked to quiescence within the cell cycle (*48*). Under *in vitro* culture conditions, primary cilia exhibit chemosensitivity to their surrounding environment, which can be demonstrated directly through serum starvation to induce cilia expression and elongation (*63*). Their structure and function has been implicated in cell fate determination processes as well as in cellular chemotactic migration (*87*, *88*).

Purportedly, cilia elaboration or resorption modulates Hedgehog and Wnt signaling, and this modulation is likely in response to changes in the chemical environment. Below we describe a number of studies illustrating the chemosensory properties of the cilium and the implications for defining cellular behavior.

3.5.1 Chondrogenic Cell Types

As described above, cilia expression is intimately linked to developing chondrogenic tissue and healthy and degenerating cartilage tissue; however, the specific mechanisms dictating these changes in cartilage cilia expression remain unclear. Changes in chondrocyte cilia expression patterns have been observed in response to the chemical environment, and these changes have been proposed to detect to inflammatory signaling (*69*). IL-1 secretion is a characteristic inflammatory signal present in osteoarthritic tissue (*69*). When stimulated with IL-1β, cultured primary bovine chondrocytes increase both their length and expression frequency, demonstrating chemosensitivity in the chondrogenic phenotype (*69*). Interestingly, the authors also tested this effect against fibroblasts and noted a similar increase in cilia length in response to IL-1β, suggesting that this may be a chemosensing property of cilia across cell types (*69*). To further support that this response was specific to the cilia acting as mediators of IL-1 stimulation, the authors measured nitric oxide (NO) and prostaglandin release in response to pro-inflammatory cytokine IL-1, utilizing chondrocytes derived from IFT88 knockout mice ($Tg737^{ORPK}$). They found that cells devoid of cilia did not characteristically upregulate NO and PGE_2 in response to IL-1 stimulation, whereas wild type cells exhibited the prototypical response described in bovine chondrocytes and fibroblasts (*69*). This study suggests a mechanistic explanation for the typical cilia length increase seen in the inflammatory signaling of osteoarthritic tissue (*82*).

Another study by Rich and Clark described the impact of an osmotic environment on chondrocyte primary cilia (*89*). Interestingly, the authors reported that the primary cilia on explanted, intact femoral condyles derived from mice exhibited changes in the length of the

ciliary axoneme within minutes of exposure to both a hypo- and hyperosmotic environment (200-400mOsm) in the surrounding culture medium (*89*). The authors did note that they did not distinguish between intracellular and extracellular length and therefore did not account for cilia retraction into the ciliary pocket, so length changes were direct measurements of ciliary resorption (*89*). Osteoarthritic (OA) tissue is generally thought to produce a hypo-osmotic environment for chondrocytes with a degenerated cartilage matrix devoid of glycosaminoglycans (GAGs); this study illustrates contrasting results to those described in OA chondrocytes with elongated cilia by McGlashan *et al.* (*82*). These observations taken together with the IL-1 study by Wann *et al.* suggest a differential response in primary cilia chemosensitivity, highlighting its complex function in integrating a variety of chemical signals controlling chondrogenic cell phenotypes.

3.5.2 Osteogenic Cell Types

Primary cilia clearly demonstrate chemosensitivity to soluble factors in the surrounding cell culture environment in a broad range of cell types. This is frequently demonstrated through serum starvation to induce cilia formation and elongation (*42*). Further, changes in cilia expression are observed in response to osteogenic induction factors.

A study by Plaisant *et al.* describes the effect of osteogenic differentiation media on human adipose stem cell (hASC) cilia expression, reporting that 92% of undifferentiated hASCs expressed primary cilia; however, following 5 days of culture in osteogenic media, only 48% of the differentiating hASCs expressed cilia (*73*). The authors also noted that this level of expression was closer to that observed in osteoblastic cell types (*73*). Primary cilia on mesenchymal stem cells (MSCs) have also display a level of chemosensitivity. When cilia

protein IFT88 is knocked down in MSCs, they exhibit a significantly reduced ability to differentiate into osteogenic, adipogenic and chondrogenic cell types, as measured by gene expression markers Runx2, PPARγ, and Sox-9, respectively (*41*). This study suggested that a functional cilium structure was required for chemical induction of lineage specification.

3.6 Primary Cilia Mechanosensitivity in Osteogenic Cell Types

An interesting study by Hoey *et al.* proposed a paracrine signaling function of primary cilia MSCs (*50*). Their findings indicated that when MSCs were cultured in conditioned media from mechanically stimulated osteocytes (MLO-Y4), the MSCs upregulated osteopontin (OPN) and cyclcooxygenase-2 (COX-2) osteogenic gene expression. MSCs cultured in conditioned media derived from osteocytes that were not mechanically stimulated did not upregulate osteogenic genes (*50*). In contrast, conditioned media derived from mechanically stimulated osteoblasts (MC3T3-E1) did not have this effect on MSCs, suggesting unique paracrine signaling activity between mechanically stimulated osteocytes and MSCs.

In osteogenic cell lines, primary cilia exhibit sensitivity to oscillatory fluid flow (OFF), and their frequency of expression is related to osteogenic differentiation (*30*). In MC3T3-E1 osteoblast-like cells and MLO-Y4 cells, both siRNA knockdown of ciliary protein IFT88 and physical abrogation of primary cilia using chloral hydrate resulted in a loss of mechanosensitivity. MC3T3E1 osteoblasts characteristically upregulate osteopontin gene expression and release prostaglandin E2 (PGE2) in response to fluid shear. However, cilia disruption diminished this behavior following exposure to OFF for 1 hour at 1 Hz. Further, in MLO-Y4 osteocytes/osteoclast-like cells, characteristic flow-induced increases in

cyclooxygenase-2 (COX2) gene expression and the ratio of osteprotegerin (OPG) to RANKL gene expression were suppressed under both chloral hydrate exposure and siRNA knockdown. That study also explored the role of primary cilia in the flow-induced release of intracellular calcium, as osteogenic cells tend to exhibit calcium fluxes in response to fluid shear and kidney cells exhibit cilia dependent calcium release via polycystin-2 (PC2), a stretch activated calcium channel. However, they found that the flow-induced release of intracellular calcium occurred independent of primary cilia in osteogenic cell types (*30*).

A subsequent report demonstrated that primary cilia mediated fluid induced osteogenesis in MLO-A5 osteoblasts as measured by calcium accretion following exposure to 2 hours of OFF/day for 12 days, applied with the use of a rocker platform (*90*). Through physical disruption of the primary cilia with chloral hydrate, MLO-A5 cells exhibited a reduced capacity for calcium accretion in response to OFF, suggesting that cilia were required for this process. The authors further reported a reduction in the number of primary cilia in response to OFF stimulation.

Other evidence suggests cilia-specific protein polycystin-1 (PC1) may play an integral role in osteoblastic mechanosensing of the surrounding mechanical environment. When cultured under cyclic tensile strain (2% strain at 0.5 Hz), MC3T3-E1 osteoblasts show PC1-dependent mechanically induced osteogenesis (*91*). PC1 shRNA lentiviral knockdown diminishes characteristically upregulated osteogenic gene markers such as Runx2, osteocalcin, osterix and osteonectin in response to osteogenic induction via chemical or mechanical stimulation. This was observed as early as one hour following mechanical stimulation (*91*). Though this study did not specifically focus on the cilium structure as the

mechanosensor in this case, PC1 localizes to the primary cilium, and its mechanosensitivity likely functions in conjunction with the cilium structure.

3.7 Conclusions

Overall, primary cilia functionally contribute to the chemo- and mechanosensing activities of a variety of cell types both *in vivo* and *in vitro*. They appear to play a crucial role in tissue homeostasis and are the site of critical signaling pathways involved in the phenotypic development of cells and tissues. Within the musculoskeletal system, Kif3a, IFT88 and PC1 emerge as critical cilia proteins required for both their form and function. Clearly, primary cilia are no longer relegated to the vestiges of evolution as they were once considered to be; however, their apparent multifunctional physiological purpose combined with their often elusive expression frequency, has contributed to their broad study in a wide array of cell and tissue types.

CHAPTER 4 Primary Cilia: The Chemical Antenna Regulating Human Adipose-Derived Stem Cell Osteogenesis

This chapter has been published in the journal PLoS One under the following citation:

Bodle JC, Rubenstein CD, Phillips ME, Bernacki SH, Qi J, Banes AJ, Loboa EG. *Primary cilia: the chemical antenna regulating human adipose-derived stem cell osteogenesis.*
PLoS One. 2013 May 17;8(5):e62554. doi: 10.1371/journal.pone.0062554. Print 2013.
PMID: 23690943

4.1 Introduction

The non-motile primary cilium is an organelle composed of tubulin, which projects from the centrosome and is located at the apical cell surface. The cilium axoneme consists of a set of nine peripheral microtubule doublets arranged in a 9 + 0 non-motile primary cilium configuration (Figure 4.1a). This is in contrast to the (9+2) motile cilium configuration, which has a central tubulin pair surrounded by nine tubulin doublets. Discovered over a century ago, non-motile primary cilia were largely considered vestigial organelles, despite their prevalence on a variety of cell types (*4*). More recently, they have been implicated as critically important chemo- and mechanoresponsive cell surface structures, hinting at their role in functional phenotypic maintenance in a variety of mammalian cell types (*28*, *29*). Assembly of the primary cilium is cell cycle dependent and most mammalian cell types express primary cilia at some point during the cell cycle (*29*). The scope of the primary

cilium's function remains largely elusive, though evidence suggests that its function is complex. It acts as an important site for intracellular signaling (*40*) and detects external chemical and mechanical changes in the extracellular environment (*33*). Emerging evidence from our group and others suggests that, in addition to tissue homeostasis, they may also be involved in signaling stem cell lineage commitment in both embryonic as well as in adult stem cells, both *in vivo* and *in vitro* (*33-35*).

Human adipose-derived stem cells (hASC) are a promising autologous cell source for tissue-engineered replacement therapies (*1*, *11*). Due to their relative abundance and multipotent capacity to differentiate into a variety of mesenchymal lineages, hASC have demonstrated potential for a broad range of therapeutic applications (*1-3*, *11*). However, a majority of the mechanisms controlling these differentiation processes have largely remained elusive. We hypothesize the primary cilium and its associated proteins may contribute to these processes.

Primary cilia have been most thoroughly studied in kidney epithelial cells under the autosomal polycystic kidney disease model. Loss of the cilium and its associated proteins polycystin-1 (PC1) and polycystin-2 (PC2) in kidney epithelial cells is associated with the loss of epithelial cell mechanosensitivity, which leads to development of cysts and deregulation of tissue morphogenesis (*6*, *36*). PC1 and PC2 colocalize to the primary cilium (Figure 4.1a) and are thought to have a large component of their functional activity at the site of the cilium (*37*). However, it is important to note both PC1 and PC2 localize to other subcellular compartments as well. PC1 is observed at the apical cell surface and at cell-cell

adhesion junctions in a variety of ductal and epithelial cell types (*92*, *93*). PC2 is found in the plasma membrane and in the endoplasmic reticulum of kidney epithelial cells (*37*).

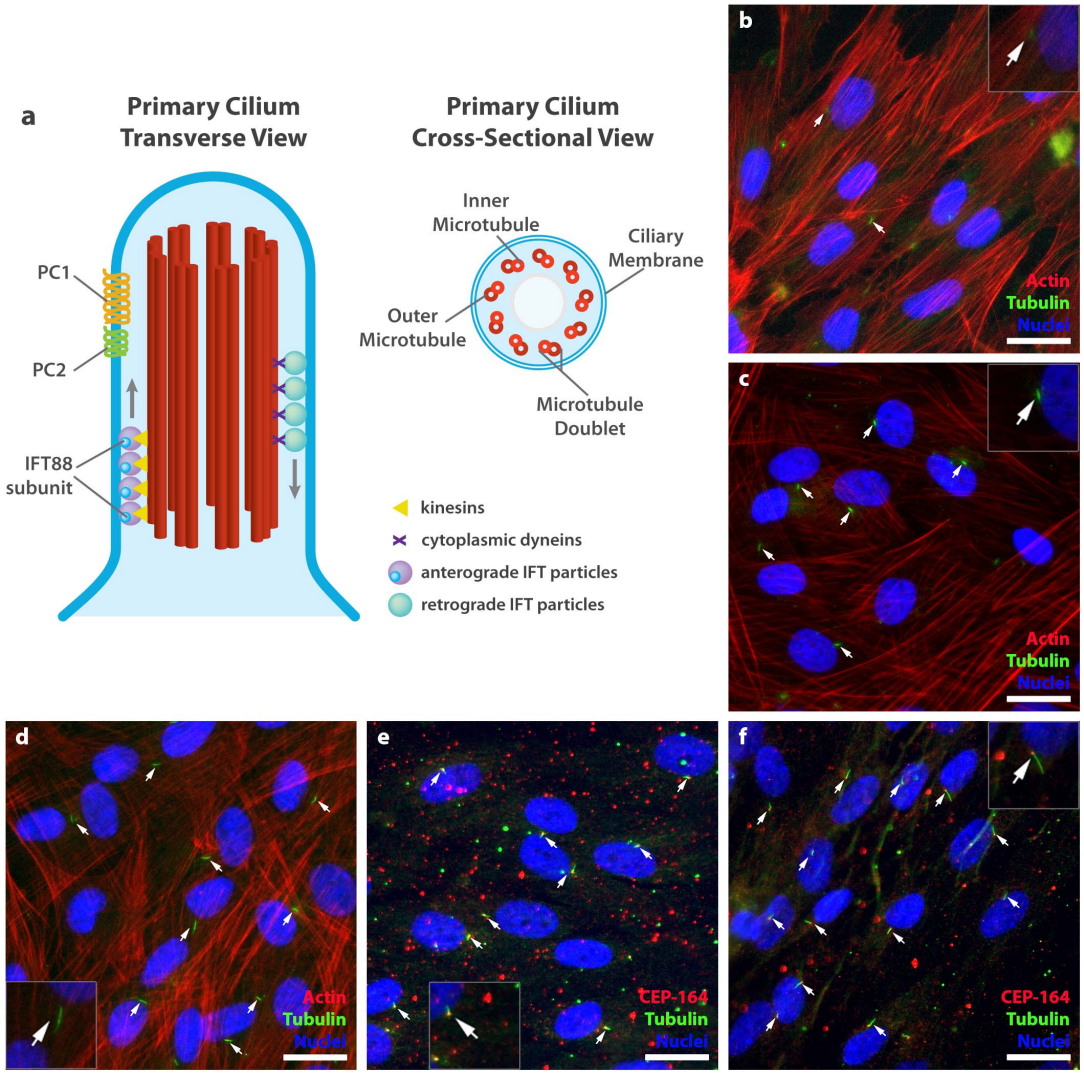

Figure 4.1 Primary cilia on hASC. (a) The non-motile primary cilium axoneme is composed of 9 pairs of peripheral microtubule doublets arranged concentrically in 9+0 configuration, devoid of a central tubulin pair. (b–f) Primary cilia appear as a dense cluster of acetylated tubulin protruding from the apical surface of hASC in confluent culture. (b) Few cilia are observed 24 hours after culture in complete growth expansion media (CGM) in subconfluent culture. They are observed at day 3 (c) undifferentiated in CGM, (d) differentiated in osteogenic differentiation medium (ODM) and at day 12 in (e) undifferentiated in CGM and (f) differentiated in ODM. Cilia are identified with anti-acetylated tubulin (green) or in combination with CEP164 (red), actin identified with phalloidin (red) and nuclei are identified with DAPI staining (blue). Scale bar = 25 μm.

In addition to PC1 and PC2, intraflagellar transport protein-88 (IFT88), also known as polaris, is another critical cilia-associated protein required for proper cilia structure and function (Figure 4.1a). Disease models incorporating IFT88 knockout result in a cystic kidney phenotype similar to that observed in autosomal polycystic kidney disease (*94*). This is likely due to the fact that IFT88 is responsible for transporting proteins into the cilium axoneme, building the cilium microtubule structure, and transporting functional cilia proteins into the cilium. Due to this critical activity, disrupted IFT88 expression results in a shortened ciliary axoneme (*94*).

IFT88 activity in primary cilia has been of particular interest in bone cell cilia-mediated mechanosensing. Transient knockdown of IFT88 has been reported to reduce the frequency of primary cilia observed on osteoblastic cell lines. Further, IFT88 knockdown leads to reduced expression of osteogenic gene markers known to be upregulated with fluid shear stimulation, indicating a suppression of functional osteogenic phenotype (*95*).

In this study, we investigate the role of the primary cilium in hASC differentiation. Human ASC are excellent cell source candidates for musculoskeletal tissue engineering and regenerative medicine applications; however, characterizing the mechanisms of hASC differentiation is a barrier to implementing their clinical use. We hypothesize that primary cilia are present on hASC and that their associated proteins PC1, PC2 and IFT88 dynamically control hASC differentiation potential. Based on previous work by our group, as well as others, hASC are known to readily differentiate into an osteogenic cell phenotype. They upregulate osteogenic gene markers, and proteins, as well as accreting calcium and exhibiting changes in alkaline phosphatase activity, in response to a variety of osteogenic induction

factors (*2*, *15*, *96*, *97*). The aim of this study is to elucidate the primary cilia-mediated mechanisms of the hASC differentiation process, specifically exploring the action of PC1, PC2 and IFT88.

4.2 Materials and Methods

4.2.1 Cell Isolation and Propagation

Human adipose-derived stem cells (hASC) are obtained from waste adipose tissue derived from anonymous patients undergoing elective abdominoplasty surgeries (IRB exemption protocol #10-0201), at University of North Carolina hospitals (Chapel Hill, NC). All data were analyzed anonymously and the only patient information obtained included age, sex and ethnicity. The Office of Human Research at UNC hospitals deemed that this study does not constitute human research, "as defined under federal regulations [45 CFR 46.102 (d or f) and 21 CFR 56.102(c)(e)(l)] and does not require IRB approval." Isolation of hASC was performed according to previously established protocols from our lab (*7*), adapted from methods initially reported by Zuk et al. (*2*). Once isolated, hASC obtained from approximately 50g of tissue were allowed to propagate in culture in complete growth medium (CGM) until ~80% confluency (or up to two weeks). CGM contained Eagle's Minimum Essential Medium, alpha-modified supplemented with 10% fetal bovine serum, 2 mM L-glutamine, 100 units/ml penicillin and 100 μg/ml streptomycin. The hASC were then trypsinized and frozen down at passage 0 (p0). All hASC used in these experiments were passage 4 or lower, and were derived from three female donors (ages 47 – 55 years).

4.2.2 Osteogenic and Adipogenic Differentiation

To characterize the growth and differentiation potential of each cell line isolated per donor, p0 cells were grown in complete growth medium (CGM), adipogenic differentiation medium (ADM) and osteogenic differentiation medium (ODM). ADM contained the aforementioned CGM supplemented with 1 μM dexamethasone, 5 μg/ml insulin, 100 μM indomethacin and 500 μM isobutylmethylxanthine. ODM contained complete growth medium with the addition of 50 μM ascorbic acid, 0.1 μM dexamethasone, and 10 mM β - glycerolphosphate.

To confirm multipotency, p0 hASC were grown in each medium condition for 14 days to evaluate adipogenic and osteogenic differentiation potential. Cells were seeded in 6-well plates (5 x 10^4 cells/well) and 12-well plates (2 x 10^4 cells/well) and were grown to 90-100% confluency in CGM (1-3 days), then transferred to ODM or ADM (14 days) for osteogenic or adipogenic differentiation induction, respectively. Evidence of differentiation was visualized using Alizarin Red S for calcium accumulation in osteogenesis and Oil Red O for lipid droplet accumulation in adipogenesis.

4.2.3 siRNA Knockdown

hASC at ~ 60% confluency were transfected with Lipofectamine 2000® (Invitrogen, Carlsbad, CA) using siRNA knockdown for PC1, PC2 and IFT88. A ratio of 24 pmol siRNA to 1.2 μL lipofectamine 2000® per sample in a 12-well plate were prepared according to manufacturer's protocol. hASC were transfected for 4-5 hours exposure to siRNA-lipofectamine solution in serum-free Opti-MEM-I transfection media. Cells were placed in complete growth media following initial transfection and subsequently placed in treatment

media (CGM, ODM, ADM) 24 hours later. Serial knockdown was applied at Day 0 and 7 for experiments lasting longer than 7 days.

To assess initial knockdown efficiency to optimize knockdown protocol, RNA was collected from duplicate samples of hASC transfected with either PC1 siRNA or Scramble-A control siRNA at 24, 48 and 72 hours after transfection. Real-time PCR using Taqman® was used to evaluate the relative mRNA expression levels between time-dependent controls and polycystin-1 knockdown samples. Following optimization with PC1, qRT-PCR was used to further evaluate mRNA expression of PC1, PC2 and IFT88 following knockdown.

4.2.4 Immunostaining

hASC were fixed in 10% formalin for 15 minutes. Following fixation, cells were blocked with a 0.2% Triton X-100/5.0% BSA stock solution for 40 minutes in 12-well plates on a shaker table. Following blocking, the coverslips were incubated in the primary antibody solution in humidified chambers. Primary antibody solutions contained mouse monoclonal acetylated α-tubulin antibody (diluted 1:100) (Sigma), CEP164 (1:50) (Santa Cruz) rabbit PC1 (diluted 1:50) (Santa Cruz), rabbit PC2 (diluted 1:50) (SantaCruz) or goat IFT88 primary antibody (1:50) (Abcam), with 0.2% Triton X-100, and 0.5% BSA in PBS. The cells were then incubated in the chambers overnight at 4^{o}C.

Samples were rinsed three times in PBS for five minutes each on a shaker table and then incubated in the secondary antibody (1:250), phalloidin 594 (Molecular Probes) (1:500) and DAPI (1:500) stain solutions. A chicken anti-mouse Alexa Fluor 488 (Molecular Probes) secondary (Molecular Probes) was used against the mouse acetylated α-tubulin primary, donkey anti-goat Alexa Fluor 594 secondary (Molecular Probes) was used against the goat

IFT88 and CEP164 primaries and goat anti-rabbit Alexa Fluor 594 secondary (Molecular Probes) was used against PC1 and PC1 primaries. The samples were incubated for three hours at room temperature. Following the secondary incubation, the samples were placed in PBS for the final three rinses and excess liquid was blotted on a kimwipe in preparation for mounting. Prolong Gold Mounting Media (Molecular Probes) was used to mount the samples and slides were allowed to dry in the dark for 24 hours prior to imaging.

4.2.5 Phase Contrast and Fluorescence Microscopy

Phase contrast microscopy was used to monitor hASC viability and to visualize cell morphology throughout the duration of differentiation. Fluorescence microscopy was used in conjunction with immunohistochemistry to visualize cytoskeletal organization, cell surface markers, primary cilia conformation, PC1, PC2 and IFT88 localization, cell-cell junctions and matrix deposition.

Samples were imaged on a Leica DM5500B Fluorescent Microscope using the compatible LAS-AF software. Three images were taken for each section: DAPI (blue), Alexa 488 (green), and Alexa 594 (red). They were used for nuclei visualization, cilia visualization, and actin/CEP164/PC1/PC2/IFT88 visualization respectively. Optimized exposure, gain, and intensity experiment settings were determined by using the quick LUT function of the LAS-AF program. Images were taken at 40x magnification, 500-1000ms exposure time (depending on filter), and a lamp intensity of 4.

4.2.6 Cellular Proliferation

To measure proliferative activity, DNA content was measured at days 0, 3, 5, 7 and 10. Cell lysates were digested overnight at 60°C in 2.5 units/mL papain from papaya latex in PBS with 5mM ethylenediaminetetra-acetic acid and 5mM cysteine hydrochloride. Hoechst 33258 (Molecular Probes), a DNA-binding fluorescent dye, was applied to samples at 0.1μg/mL in a black 96-well microplate. Fluorescence was measured at an excitation wavelength of 352 nm and an emission wavelength of 461 nm on a microplate reader (TECAN GENios, Männedorf, Switzerland). A DNA standard curve was generated using DNA derived from calf thymus (Sigma) and DNA concentration was calculated as a function of fluorescence.

4.2.7 RNA Extraction and Gene Expression Analysis

Quantitative RT-PCR analysis was used to determine relative mRNA expression levels of lineage specific gene markers for osteogenic gene markers. RNA cell lysate samples collected at days 0, 3, 10 and 14 were run through a Qiashredder column (Qiagen, Valencia, CA) at 15,000g for 2 minutes to homogenize samples. Total RNA was extracted using the RNeasy Mini Kit (Qiagen, Valencia, CA). RNA concentrations were measured using a NanoDrop spectrophotometer (Thermo Scientific, Wilmington, DE). To synthesize first strand cDNA, 110 – 600 ng of RNA in a 21μL reverse transcriptase (RT) reaction was used with the Superscript III RT with oligo(dT) primers kit (Invitrogen, Carlsbad, CA). Taqman Gene expression assays with pre-determined primer-probe sets were used to amplify diluted (1:1) cDNA (Assays-on-Demand, Applied Biosystems, Foster City, CA). All gene expression

profiles were normalized to Glyceraldehyde-3-phosphate dehydrogenase (GAPDH) (Assay HS99999905_M1) in an ABI Prism 7000 system.

4.2.8 Histological Staining

After 14 days of culture in osteogenic differentiation medium, or complete growth medium, hASC were fixed in 10% formalin for 15 minutes and rinsed 2 times with deionized water. They were stained with a 2% (w/v) Alizarin Red S solution to characterize calcium accretion and degree of hASC osteogenic differentiation. After exposure to stain for 3 minutes, wells were rinsed 4 times and stains were qualitatively evaluated and visualized using a dissecting microscope (Leica Microsystems, Buffalo Grove, IL).

4.2.9 Calcium Accretion

Total calcium concentration was quantified on day 14 using an absorbance assay. Briefly, cells were rinsed with PBS, and digested in 0.5 N HCl overnight. Samples were centrifuged at 1000g for 2 minutes and supernatant was assayed using the Calcium Liquicolor kit (Stanbio Laboratory, Boerne, TX). $CaCl_2$ included in the kit was used to generate a standard curve. The standard curve was used to determine sample calcium concentration based on absorbance values read at 550nm. Calcium data was normalized to either total protein quantified using the BCA absorbance assay, or to total DNA using the DNA Hoechst fluorescence assay. To visualize calcium accretion, calcium deposits were stained using Alizarin Red S applied directly to the well following a 30-minute fixation in 10% formalin. Images were captured with a Leica (Wetzlar, Germany) EZ 4D Digital Dissecting Scope.

4.2.10 Endogenous Alkaline Phosphatase

Endogenous alkaline phosphatase (ALP) activity was evaluated at days 10 and 14 of osteogenic differentiation. Alkaline phosphatase enzymatic activity was quantified with the Alkaline Phosphatase Liquicolor® Test (Stanbio Laboratory, Boerne, TX), using the P-nitrophenylphosphate methodology. Briefly, hASC were scraped in RIPA protein lysis buffer and were frozen for storage at -30^{o} C. Samples were then thawed, vortexed and centrifuged (1000g for 2 min). Supernatant was assayed using absorbance (405nm) in a kinetic fashion, measuring change in absorbance at 5 minute intervals. Quantified alkaline phosphatase activity was normalized to total protein content using the BCA absorbance assay (570 nm).

4.2.11 Statistical Analysis

Statistical differences between experimental groups in hASC proliferation, mRNA gene expression, and calcium accretion were analyzed using an unpaired Student's t-test compared to control conditions as denoted on presented graphs. To ensure comprehensive statistical analysis, a one-way, non-repeated measures ANOVA test with a Newman-Keuls multiple comparison test was also used to analyze gene expression and calcium quantification data. A one-way repeated measures ANOVA with a Newman-Keuls post-test was used to analyze alkaline phosphatase kinetic activity data. Statistical significance is indicated as follows: *$p < .05$, **$p < .01$, ***$p < .001$. Data are presented as mean ± standard error of the mean (SEM).

4.2.12 Controls

hASC transfected for primary cilia protein abrogation were measured against hASC

transfected with a non-targeting scramble siRNA knockdown control, and a no knockdown control group of hASC. Cellular controls were cultured under identical conditions in all assays.

4.3 Results

4.3.1 Identification of Primary Cilia

To initially test our hypothesis, it was necessary to confirm the presence of primary cilia on our hASC populations. Using immunofluorescence to visualize the cilia, a mouse α-acetylated tubulin antibody was used to stain the microtubule cilia structure. Primary cilia were most frequently identified as a dense clustering of acetylated tubulin projecting from the apical surface of the cell membrane (Figure 4.1b-f). Cilia were observed in a variety of conformations within the undifferentiated hASC population after 24 hours (Figure 4.1b), 3

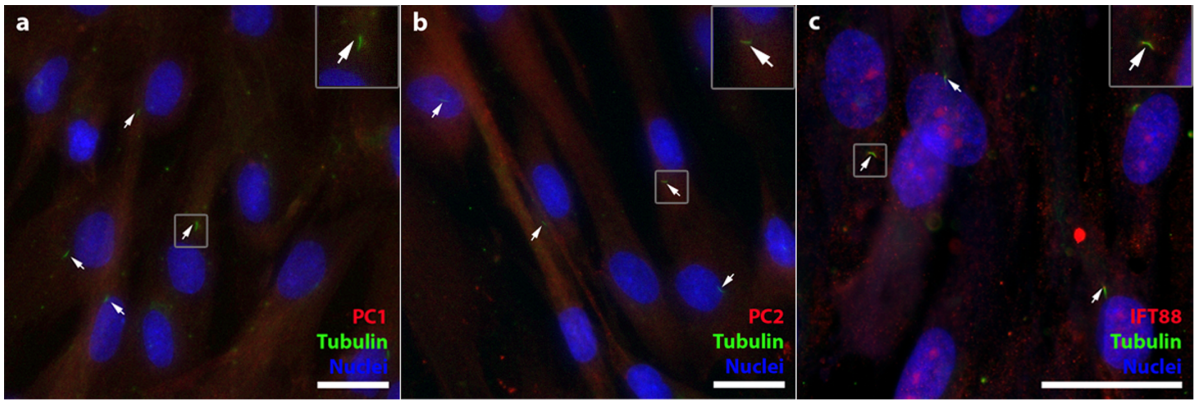

Figure 4.2 hASC expression of polycystin-1 (PC1), polycystin-2 (PC2) and intraflagellar transport protein-88 (IFT88). (a) PC1 and (b) PC2 are observed as a diffuse signal on the cell body and at the base of the cilium. (c) IFT-88 is localized at the base and tip of the primary cilium. Cilia are identified with anti-acetylated tubulin (green), PC1, PC2 and IFT88 (red), and nuclei are identified with DAPI staining (blue). Scale Bar = 25 μm.

days (Figure 4.1c) and 12 days (Figure 4.1e) of culture in complete growth medium (CGM), and within the osteogenically differentiated population after 3 days (Figure 4.1d) and 12 days (Figure 4.1f) of culture in osteogenic differentiation medium (ODM). Cilia length tended to vary with phenotype: cells grown in hASC growth media tended to express shorter cilia (Figure 4.1b,c,e), while osteogenically stimulated hASC expressed more extended cilia (Figure 4.1c,f) as they committed to the osteogenic lineage, with the day 12 osteogenically differentiated hASC expressing the longest cilia (Figure 4.1f). A portion of the hASC population consistently expressed primary cilia, however, since their expression is linked to the cell-cycle, primary cilia were observed on approximately 30% of the undifferentiated hASC in sub-confluent culture and up to 60% of hASC in confluent culture (data not shown). Incidence and length of primary cilia on hASC were found to be directly related to the chemical culture environment and cell phenotype.

4.3.2 siRNA Knockdown of Cilia-Associated Proteins IFT88, PC1, and PC2

hASC expression of polycystin-1 (PC1) (Figure 4.2a), polycystin-1 (PC2) (Figure 4.2b) and intraflagellar protein-88 (IFT88) (Figure 4.2c) was determined by immunostaining. To assess cilia co-localization, hASC were also co-immunostained for acetylated α-tubulin. IFT88 colocalized to the base and tip of the ciliary axoneme, as denoted by the arrows (Figure 4. 2c). PC1 and PC2 exhibited diffuse expression throughout the hASC cell membrane as well as localization at the base of the cilium (Figure 4.2a,b).

To elucidate the function of primary cilia-associated proteins in hASC osteogenesis, we systematically abrogated expression of each of the three cilia-associated proteins of interest. To do this, we used serial transient siRNA transfections to allow for sustained mRNA knockdown of PC1, PC2, and IFT88. The serial siRNA knockdown method was used to eliminate any off-target effects associated with other stable knockdown techniques, which can result in a possible alteration in hASC multipotency. This serial siRNA approach yielded a minimum of 50% knockdown efficiency. Transfection with siRNA was performed on day 0 and day 7 of the standard osteogenic differentiation procedure to ensure cilia-associated knockdown for the duration of chemically stimulated osteogenic differentiation. Diminished mRNA expression of PC1, PC2 and IFT88 was confirmed with real-time RT-PCR for up to 15 days of

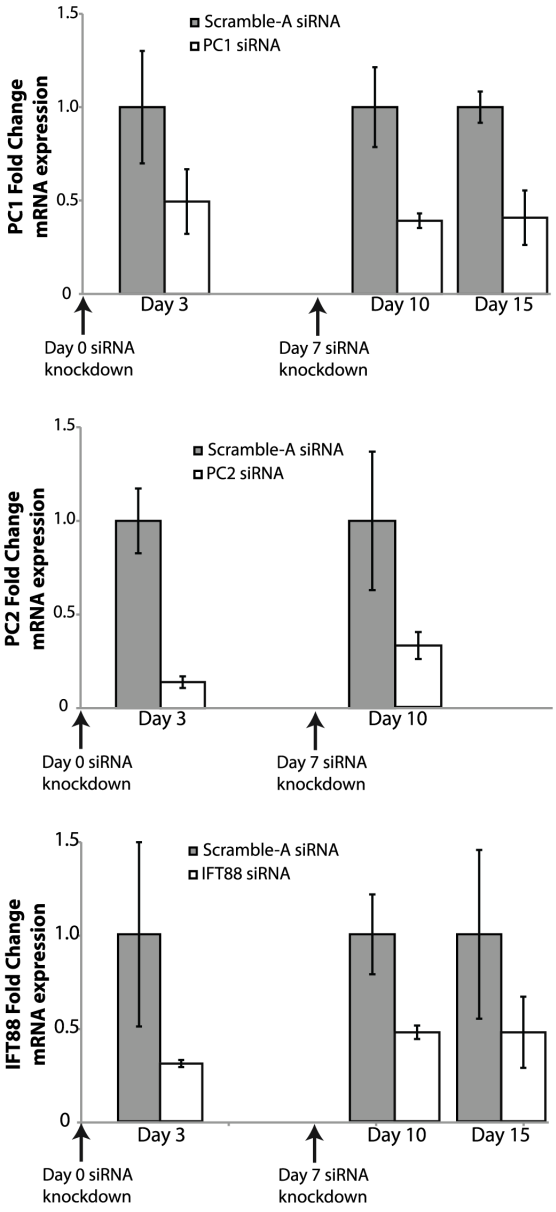

Figure 4.3 PC1, PC2 and IFT88 gene expression up to 15 days in ODM culture. siRNA knockdown applied at days 0 and 7, confers at least a 50% reduction in mRNA expression of each cilia-associate protein (n = 3, Error bars = SEM).

osteogenic differentiation (Figure 4.3).

As PC1, PC2 and IFT88 are cilia associated proteins, it is expected that their

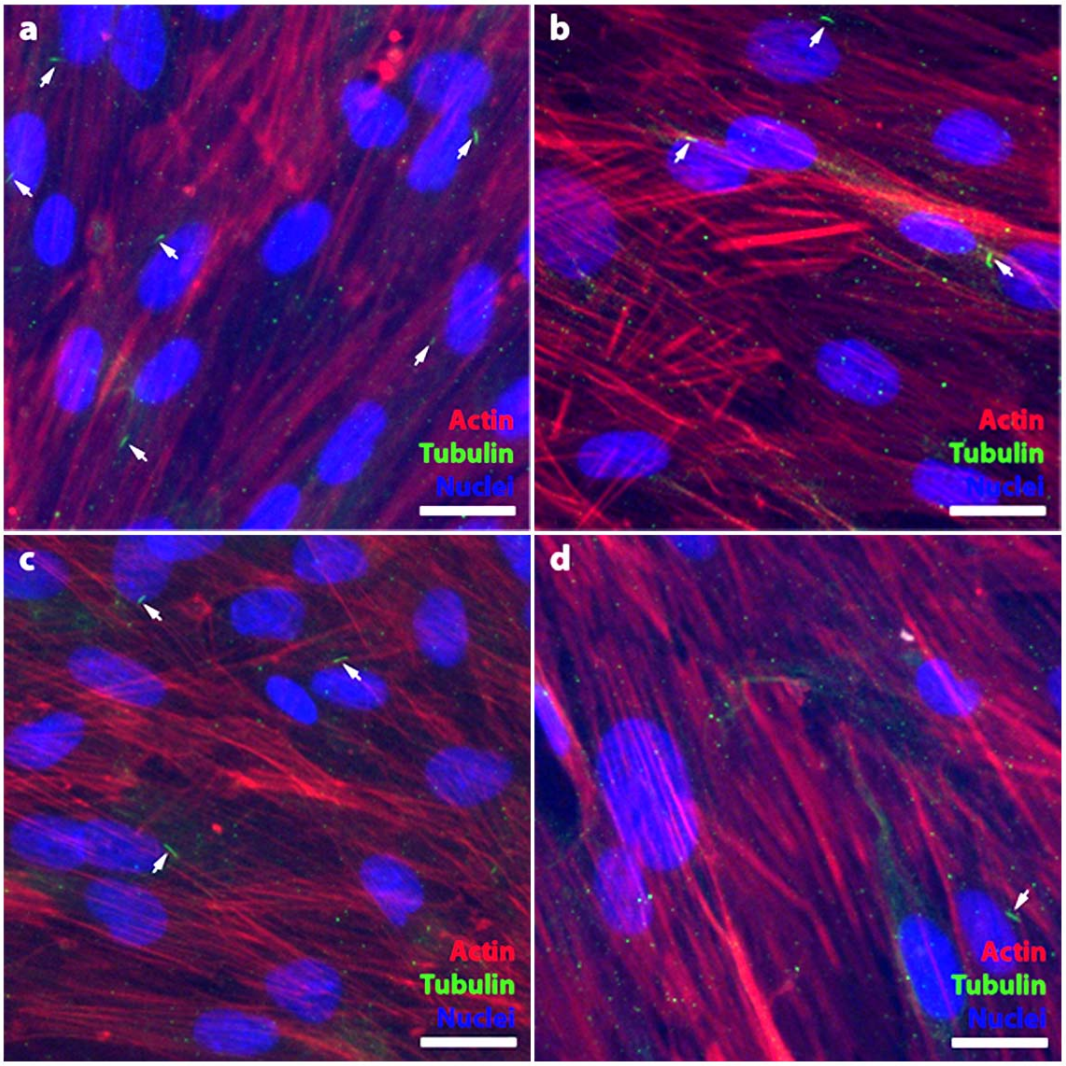

Figure 4.4 The effects of PC1, PC2 and IFT88 siRNA knockdown on hASC primary cilia. hASC were cultured in expansion media (CGM) for 72 hours. Cilia expression on hASC: (a) Non-targeting scramble siRNA baseline cilia expression on approximately 50% of the hASC population (b) PC1 and (c) PC2 knockdown conditions express more cilia observed in a curved conformation and a minimal decrease in cilia population frequency, (d) IFT88 knockdown confers a reduction in cilia frequency on the hASC population. Cilia are identified with anti-acetylated tubulin (green), actin identified with phalloidin 594 (red) and nuclei are identified with DAPI staining (blue). Scale Bar = 25 µm.

knockdown would have an effect on cilia structure. hASC were cultured for 72 hours and cilia-associated proteins were assessed via immunostaining (Figure 4.4).

We found that IFT88 knockdown had the greatest impact on the frequency of cilia expression observed on the hASC population (Figure 4.4d) as compared to the non-targeting scramble siRNA control (Figure 4.4a). Further, we observed that PC1 (Figure 4.4b) and PC2 (Figure 4.4c) knockdown had a moderate impact on the primary cilia structure with hASC expressing cilia that tended to be expressed in a more curved conformation than cilia in control conditions. PC1 and PC2 knockdown had no noticeable effect on the frequency of cilia observed on the hASC population.

4.3.3 Cilia-Associated Protein Knockdown Affects hASC Proliferation

The presence of the primary cilium structure is intimately associated with the cell cycle and thus it was necessary to establish the baseline effects of PC1, PC2, and IFT88 knockdown on the basal hASC phenotype. To assess hASC proliferation activity under siRNA knockdown, the Hoechst DNA Assay was used to measure DNA content incrementally over a 10 day

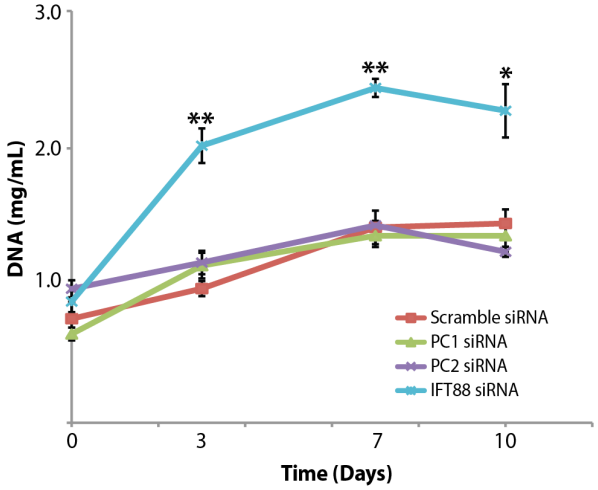

Figure 4.5 The effect of knockdown on hASC proliferation in expansion media (CGM). DNA was collected at days 0, 3, 7 and 10 to measure proliferative activity with siRNA knockdown of PC1, PC2 and IFT88 in as compared to the non-targeting scramble control siRNA. Knockdown of IFT88 significantly increases hASC proliferation as compared to control (n = 3, error bars = SEM, Student's t-test comparing each treatment to control, * p,0.05, ** p,0.01).

culture in expansion media (CGM) (Figure 4.5). hASC were transfected at day 0 and subsequently cultured in expansion media (CGM) for up to 10 days. We collected DNA at days 0, 3, 7 and 10 and used a fluorimetric assay to measure DNA concentration at each time-point. Interestingly, we found that IFT88 knockdown conferred a significant increase in hASC proliferative activity, whereas PC1 and PC2 knockdown did not alter hASC proliferation as compared to the siRNA non-targeting control (Figure 4.5). The IFT88 knockdown significantly increased hASC proliferative activity as compared to the control. However, PC1 and PC2 exhibited a comparable level of proliferation activity to the control, non-targeting siRNA (Figure 4.5).

hASC are density-dependent; and once they reach confluency, they slow down their proliferative activity and quickly become quiescent. Under phase contrast microscopy, control hASC, PC1- and PC2-knockdown hASC expressed similar cell morphology in confluent culture. In contrast, IFT88 knockdown hASC exhibited a loss of this characteristic hASC density-dependent behavior and rather exhibited crowding and much denser hASC monolayer coverage, as observed by phase contrast microscopy (data not shown).

4.3.4 Knockdown of Cilia-Associated Proteins Downregulates hASC Osteogenic Gene Marker Expression

To evaluate how PC1, PC2 and IFT88 function during the hASC osteogenic differentiation process, real-time RT-PCR was used to analyze mRNA expression for early markers of hASC osteogenesis at days 3,10 and 15 of osteogenic differentiation in ODM. We probed for gene expression of runt-related transcription factor (Runx2) (Figure 4.6a) at day 3, gene expression of alkaline phosphatase (ALP) (Figure 4.6b) and bone morphogenetic

protein-2 (BMP-2) (Figure 4.6c) at day 10, and osteocalcin at day 15 (Figure 4.6d), all hallmarks for development of an osteogenic phenotype. After siRNA knockdown and 3 days of culture in osteogenic differentiation medium, IFT88 knockdown resulted in significant downregulation of Runx2 expression, suggesting suppressed osteogenesis (Figure 4.6a). This indicated that the function of IFT88 may be important in the early signals of osteogenic lineage specification in hASC. After siRNA knockdown and 10 days of osteogenic

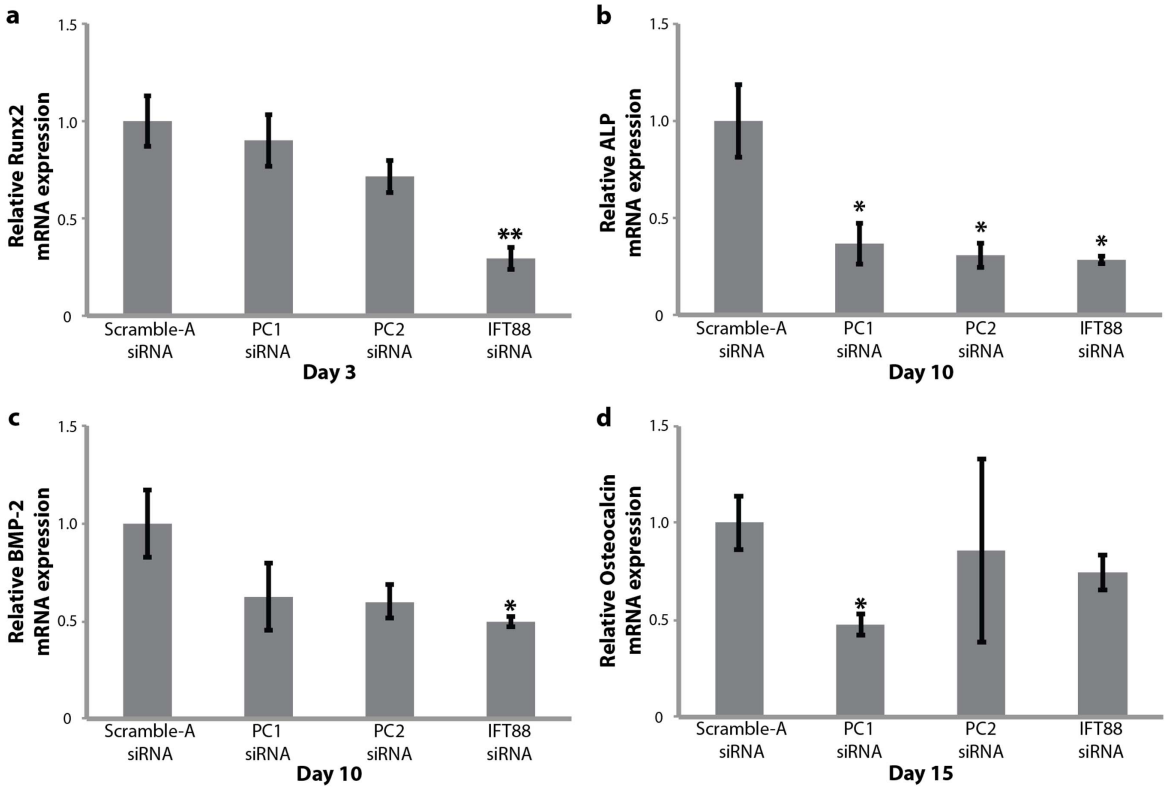

Figure 4.6 Osteogenic gene marker expression in hASC. IFT88 knockdown confers a reduction in (a) Runx2 gene expression after 3 day and (c) BMP-2 gene expression after 10 day culture in osteogenic differentiation medium (ODM). (b) PC1, PC2 and IFT88 knockdown confer a reduction in alkaline phosphatase (ALP) gene expression after 10 days of culture in ODM. (d) PC1 knockdown confers downregulation of osteocalcin after 15 days of culture in osteogenic differentiation. Knockdown treatments applied at day 0 and day 7 of differentiation, (n = 3, error bars = SEM, Student's t-test comparing each treatment to control, * $p<0.05$, ** $p<0.01$).

differentiation, we observed that IFT88 knockdown resulted in a significant downregulation of BMP-2 gene expression (Figure 4.6c) and PC1, PC2 and IFT88 knockdown resulted in significant downregulation of ALP gene expression (Figure 4.6b). At day 15 of osteogenic differentiation, PC1 knockdown resulted in a significant decrease in osteocalcin expression (Figure 4.6d). Evaluation of osteopontin gene expression was also assessed at day 15 of osteogenic differentiation; however there was no significant change in osteopontin expression with knockdown (data not shown). These results suggest that PC1 and PC2 may function in intermediate signaling processes related to hASC osteogenesis, IFT88 function is necessary at the early-to-intermediary duration of the osteogenic differentiation process, and PC1 in particular is critical in later steps of the osteogenic differentiation process.

4.3.5 Cell-Mediated Calcium Accretion of Osteogenically Differentiated hASC

Calcium accretion and endogenous alkaline phosphatase activity are canonical hallmarks of functional osteogenesis and development of bone-like calcified tissue. To extend our study further, we looked at the effects of PC1, PC2, and IFT88 knockdown on hASC mediated mineralization after 14 days of osteogenic differentiation to determine if the activity of these proteins was involved in the development of functional osteogenic tissue. Alizarin Red results indicated that PC1 and PC2 knockdown led to a diminished level of calcium accretion after 14 days of osteogenic differentiation with culture in ODM (Figure 4.7a). Quantification of calcium accretion using a colorimetric absorbance calcium assay further corroborated this qualitative data. Evaluating calcium concentration as normalized to DNA content, we observed a diminished calcium concentration (Figure 4.7b). This data suggested that PC1 and PC2 were critical in the ability of hASC to functionally differentiate

into an osteogenic mineralized phenotype. Taken together with the gene expression data (Figure 4.6), these findings support the idea that PC1 plays a particular role in the later signaling pathways of hASC osteogenesis.

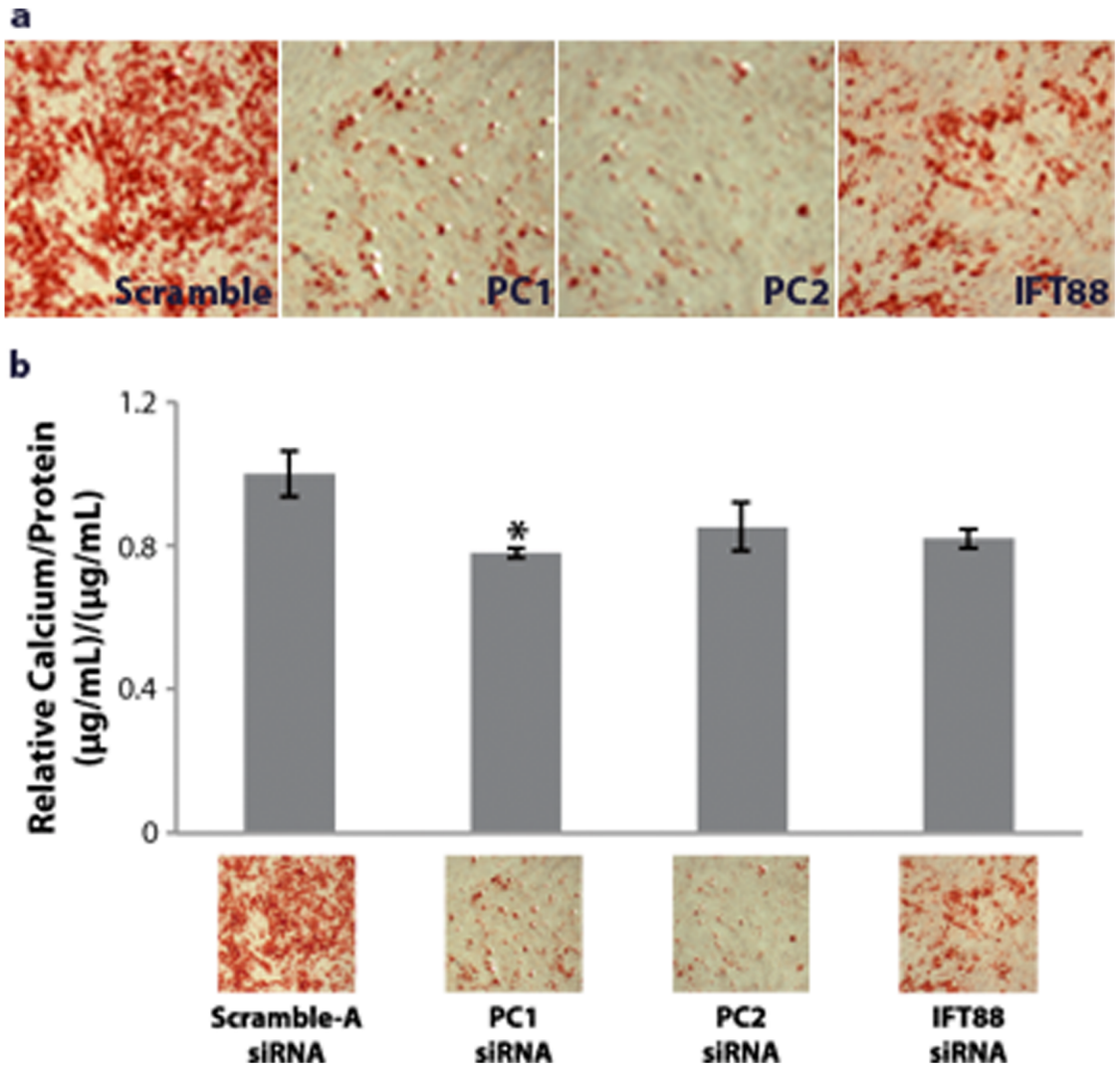

Figure 4.7 Calcium accretion is affected by cilia-associated protein knockdown. (a) Alizarin Red staining indicating degree of mineralization after 14 days ODM with knockdown. (b) Quantified calcium accretion normalized to DNA content. PC1 and PC2 knockdown leads to diminished calcium accretion, (n = 3, error bars = SEM, Student's t-test comparing each treatment to control, * p,0.05).

4.3.6 PC1, PC2 and IFT88 Affect ALP Enzymatic Activity

End product expression of ALP and its enzymatic activity level is another important hallmark of development of a true osteogenic phenotype. To further understand how PC1, PC2 and IFT88 knockdown suppresses development of a functional osteogenic phenotype in hASC, we evaluated ALP enzymatic activity. At 14 days of culture in ODM, we analyzed

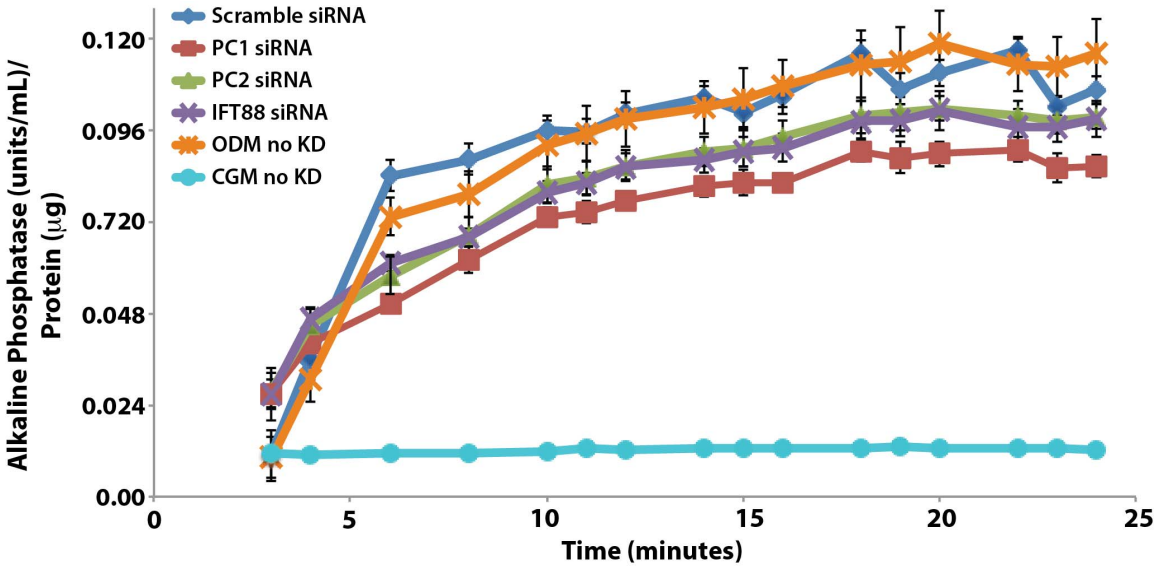

Figure 4.8 Endogenous alkaline phosphatase (ALP) activity of hASC after 14 days of culture. hASC were cultured in osteogenic differentiation medium (ODM) and transfected with non-targeting scramble, PC1, PC2 and IFT88 siRNA. ODM and complete growth medium (CGM) hASC without knockdown (no KD) were also measured for comparison of baseline activity. Alkaline phosphatase activity is suppressed with cilia- associated protein knockdown. Knockdown of PC1 (*** p,0.01), PC2 (* p,0.05) and IFT88 (* p,0.05) all led to a significant decrease in ALP enzymatic activity compared to the non-targeting scramble siRNA knockdown control (n = 3, error bars = SEM, One-way repeated measures ANOVA, with Newman-Keuls post-hoc test).

ALP activity using a kinetic colorimetric absorbance assay (Stanbio, Boerne, TX) over the course of 25 minutes. Our results indicated that knockdown of PC1, PC2 and IFT88 led to significantly decreased ALP enzymatic activity suggesting diminished development of an

osteogenic phenotype (Figure 4.8). This data supports the idea that all three proteins are necessary to induce a hASC osteogenic response, with the greatest suppression of ALP activity observed in the PC1 knockdown (Figure 4.8), consistent with the calcium accretion data (Figure 4.7).

4.4 Discussion

This study has demonstrated that primary cilia are prevalent on hASC and that cilia proteins appear to play a critical role in mediating the osteogenic differentiation of hASC. Additionally, we have determined that the presence of the primary cilium and functional IFT88 is likely linked to early lineage commitment signals and may be important in appropriate hASC proliferation. This proliferative behavior suggests that IFT88 may either play a role in maintenance of a normal baseline hASC progenitor cell phenotype, or it may conversely suggest that IFT88 is necessary to prevent aberrant, over-proliferative activity. A further study analyzing stemness and cell cycle gene markers in IFT88 knockdown hASC will be required to elucidate IFT88 function in progenitor cell types. hASC do not express typical stemness cell markers such as Oct-4, Sox2, and Nanog found in pluripotent stem cells; however they do generally express a panel of consensus cell surface markers distinctive to their multipotent population (*11*). Future comparative work characterizing immunophenotypes of wild type hASC and IFT88 knockdown hASC will be critical and interesting mechanistic work in understanding IFT88's role in stemness phenotype. Our findings showed that IFT88 knockdown led to a significant increase in hASC proliferative activity, suggesting the ciliary activity of IFT88 is likely acting in the process of cell cycle progression (Figure 4.5).

Interestingly, IFT88 knockdown of osteogenically differentiated hASC also conferred significant downregulation of Runx2 and BMP-2 gene expression, which are early and intermediary markers for osteogenesis (Figure 4.6a,c). The Runx2 result was consistent with previous work in MSC demonstrating IFT88 knockdown disrupted MSC osteogenesis as indicated by diminished Runx2 expression (*41*). BMP-2 gene expression is important in the process of wound healing and tissue remodeling in bone and interacts with Hedgehog, Wnt and TGF-β signaling - pathways that localize processes in the primary cilium (*29*, *98*, *99*). It follows that IFT88 knockdown disrupts gene expression of BMP-2 as the cilium structure is likely involved in BMP-2 signaling processes, which in turn affect hASC osteogenesis. Taken together these data indicate IFT88 may be an early modulatory switch dictating hASC to operate in either a proliferation signaling modality or the contrasting differentiation signaling modality. These findings hint that the function of IFT88 may be more dynamic than just regulating protein transport in the primary cilium, suggesting instead that it may also participate in the early stages of hASC fate determination. These findings are consistent with IFT88 studies in immortalized cell lines (*100*).

While IFT88 knockdown confers early effects on hASC differentiation, disrupting early signals modulating osteogenic lineage commitment, PC1 and PC2 knockdown resulted in disruption of later markers of osteogenesis. Both PC1 and PC2 knockdown conferred a downregulation of alkaline phosphatase gene expression (Figure 4.6b) and end-product expression conferring a decrease in the endogenous alkaline phosphatase enzymatic activity (Figure 4.8). siRNA knockdown of cilia-specific PC1 and PC2 resulted in reduced calcium accretion (Figure 4.7), which is somewhat intuitive as PC1 and PC2 are thought to couple

together forming a calcium channel (*37*). However, the PC1-PC2 complex is generally thought to be a stretch activated calcium channel, though the mechanistic function of the PC1-PC2 complex is a matter of debate (*37*, *101*).

In our static culture system, we have observed significant diminished cell-mediated calcium accretion with knockdown of PC1 (Figure 4.7b) and downregulation of osteocalcin gene expression at day 15 of differentiation (Figure 4.6d), which suggests that there is also a non-mechanical signaling component in the function of PC1. This finding is consistent with mouse model work showing heterozygous PC1 knockout mice embryos exhibit reduced bone mineralization (*102*). Osteocalcin is an osteogenic bone marker molecule, and its gene expression is typically upregulated in osteoblastic cell types (*103*). Secreted osteocalcin is known to closely associate with mineralized bone matrix, which supports the critical activity of PC1 in formation of an appropriate bone matrix as evidenced by calcium accretion and osteocalcin gene expression. Our data supports a similar global effect of PC1 knockdown within the static *in vitro* system. Taken together with other recent evidence, our findings suggest that PC1 may have multiple functions in the osteogenic differentiation process and, further, that its function is likely critical to the development of properly mineralized bone.

In general, there was a greater qualitative difference in the alizarin red staining data than the quantitative data for calcium accretion, which may be attributed to variations in cell number, and/or differences in the assays (Figure 4.7). Though IFT88 knockdown did not significantly reduce the amount of calcium accreted, the quantitative trend followed with the staining, showing that knockdown of all three proteins may have an effect (Figure 4.7). This smaller quantitative change may also be attributed to siRNA knockdown efficiency. In a

stable knockdown model with complete abrogation of ciliary protein mRNA expression, we would potentially expect a more exaggerated difference between treatments.

Our results diverge somewhat from what is reported in IFT88 knockdown by Pazour *et al.* showing a more severe cilium phenotype in Chlamydomonas and mice than our hASC using transient siRNA techniques (*94*). Their study used different model organisms and reported that Chlamydomonas IFT88 mutants did not exhibit an increase in proliferative activity, which is not consistent with the results in our model. Though cilia formation is disrupted in our IFT88 knockdown, it is by no means completely abrogated and this likely contributes to the differences between our findings and those of the Pazour *et al.* study.

Increased endogenous alkaline phosphatase activity is a characteristic marker indicating development of a functional osteogenic phenotype. Knockdown of PC1, PC2 and IFT88 all conferred downregulated alkaline phosphatase gene expression after 10 day exposure to ODM, chemical osteogenic induction (Figure 4.6b). This data was further corroborated with the enzymatic activity of alkaline phosphatase, showing reduced activity in all three knockdown conditions (Figure 4.8). These findings support consistent observations in hASC osteogenesis *in vitro* and evidence of disrupted skeletogenesis in heterozygous mouse embryo knockouts (*102*).

To summarize our findings, we established the relative temporal activities of PC1, PC2 and IFT88. We generalized that IFT88 activity was critical in earlier stages of hASC lineage specification processes (Figure 4.5, Figure 4.6), whereas PC1 and PC2 activity affected later stages of hASC osteogenic phenotypic development. Osteogenic transcription factor Runx2 and Hedgehog related osteogenic signaling molecule BMP-2 gene expression

were sensitive to IFT88 knockdown. PC1 and PC2 activity specifically affects intermediary and later gene expression markers of hASC osteogenesis (Figure 4.6). In particular, PC1 appeared to be critical for later functional hallmarks of the osteogenic phenotype, affecting osteocalcin gene expression (Figure 4.6d) and conferring effects at the level of end product expression – calcium accretion and alkaline phosphatase activity (Figure 4.7, Figure 4.8). These data suggest that IFT88 may be a mediator between a proliferative signaling modality (Figure 4.5) and a differentiation signaling modality (Figure 4.6b,c), as its significant effects seem to occur at the early stages of differentiation. Further, PC1 is critical in the appropriate expression of end-product expression and the functional activity of osteogenic cells derived from hASC.

This study temporally assayed a subset of typical hallmark osteogenic measures: endogenous alkaline phosphatase activity, upregulation of gene markers, morphological changes, and calcium accretion, but the techniques used in this study were by no means exhaustive. As seen from the mRNA data, each of these specific ciliary protein knockdowns temporally effects alterations in the osteogenic process. The calcium data, taken together with gene expression and alkaline phosphatase activity data suggest that PC1 is more critically involved in the later stages of osteogenesis, which provides a compelling explanation for its effect on calcium accretion. IFT88 is critical in the formation of the ciliary structure and significantly affects early lineage commitment signals. However, the cilium structure is by no means the only mediator of this process. Taken together our data imply that cilia-associated proteins are involved in the osteogenic process, and temporally IFT88 is a

mediator of early differentiation signals, while PC1 mediates later lineage commitment signals.

Our results shed light on primary cilia-mediated aspects of hASC osteogenesis. We have established the presence of primary cilia on hASC cell populations and have uncovered primary cilia and its key associated proteins are linked to determining hASC phenotype. Additionally, we have demonstrated that primary cilia play a role in controlling hASC proliferation and thus may also be involved in regulating cell proliferation/cell cycling activity of this cell population. We have established that primary cilia-associated proteins PC1, PC2 and IFT88 all have a chemosensitive role in mediating hASC differentiation and propose that they are critically active proteins in this process, despite their unchanged level of gene expression.

To mechanistically understand PC1, PC2 and IFT88's mode of action, an extensive protein study tracking protein localization, pathway activity and post-translational modifications throughout hASC differentiation should be pursued. While exploring mechanistic cilium mediated signaling is important and interesting, the focus and scope of this study was to initially identify whether the cilium was affecting hASC osteogenesis, and to investigate how ciliary proteins affect typical hallmarks of differentiation in the context of regenerative medicine applications. As the primary cilium is emerging as a critical organelle that modulates a number of signaling and tissue homeostasis properties, we aimed to understand if they were players in hASC osteogenesis. Our ongoing and future work will explore the more intimate mechanisms of cilia modulated hASC differentiation, by means of investigating pathways such as PDGF, Hh and Wnt signaling, known to be important in

processes of lineage commitment and localized to the primary cilium. Additionally, a further extension of this work will include incorporation of mechanical stimulation to enhance osteogenesis as all three of these cilia proteins also exhibit mechanosensitivity as chemosensitivity is only part of the story (*38*, *95*, *101*).

This work is the first step to understanding the intricacies of primary cilia function in hASC differentiation in order to better harness hASC potential for creating bone tissue replacements. This is the first study to demonstrate that primary cilia play an important role in chemically mediated osteogenic differentiation of hASC.

4.5 Conclusion

We have conclusively demonstrated that primary cilia are present on hASC and that three of their key structural/functional proteins are critical in hASC osteogenic lineage specification. Primary cilium morphology changes with respect to chemically induced changes in cell phenotype. Specifically, we have shown that osteogenically differentiated hASC exhibit longer cilia than hASC cultured in basal growth media. Our study is the first to show that IFT88 is likely an early mediator controlling the switch between a proliferative stem cell phenotype and a committed osteogenic phenotype in hASC. We have also demonstrated that PC1 plays a particularly important role in osteogenic end product expression and is critical in developing truly functional osteogenic-like tissue. Taken together, the results from this study indicate that the structure of the primary cilium is intimately associated with the process of hASC osteogenic differentiation and that its associated proteins are critical players in this process. Elucidating the dynamic role of the primary cilium and its associated proteins will help advance the application of hASC in

generating autologous tissue engineered therapies for the potential treatment of critical defect bone injuries.

4.6 Summary

Adipose-derived stem cells (ASC) are multipotent stem cells that show great potential as a cell source for osteogenic tissue replacements and it is critical to understand the underlying mechanisms of lineage specification. Here we explore the role of primary cilia in human ASC (hASC) differentiation. This study focuses on the chemosensitivity of the primary cilium and the action of its associated proteins: polycystin-1 (PC1), polycystin-2 (PC2) and intraflagellar transport protein-88 (IFT88), in hASC osteogenesis. To elucidate cilia-mediated mechanisms of hASC differentiation, siRNA knockdown of PC1, PC2 and IFT88 was performed to disrupt cilia-associated protein function. Immunostaining of the primary cilium structure indicated phenotypic-dependent changes in cilia morphology. hASC cultured in osteogenic differentiation media yielded cilia of a more elongated conformation than those cultured in expansion media, indicating cilia-sensitivity to the chemical environment and a relationship between the cilium structure and phenotypic determination. Abrogation of PC1, PC2 and IFT88 effected changes in both hASC proliferation and differentiation activity, as measured through proliferative activity, expression of osteogenic gene markers, calcium accretion and endogenous alkaline phosphatase activity. Results indicated that IFT88 may be an early mediator of the hASC differentiation process with its knockdown increasing hASC proliferation and decreasing Runx2, alkaline phosphatase and BMP-2 mRNA expression. PC1 and PC2 knockdown affected later osteogenic gene and end-product expression. PC1 knockdown resulted in downregulation of alkaline phosphatase and osteocalcin gene

expression, diminished calcium accretion and reduced alkaline phosphatase enzymatic activity. Taken together our results indicate that the structure of the primary cilium is intimately associated with the process of hASC osteogenic differentiation and that its associated proteins are critical players in this process. Elucidating the dynamic role of the primary cilium and its associated proteins will help advance the application of hASC in generating autologous tissue engineered therapies in critical defect bone injuries.

CHAPTER 5 Examining the Phenotypic-dependent Effects of Cyclic Tensile Strain on Primary Cilia in Adipose-derived Stem Cells.

This chapter is in preparation for submission to the Journal of Cell Science.

5.1 Introduction

Human adipose-derived stem cells (hASC) are a multipotent stem cell type that can be easily isolated from excess fat tissue. Due to their ability to differentiate along a variety of mesenchymal lineages, they are being actively explored for their potential use in a wide range of tissue engineering and regenerative medicine therapeutics (*1*, *2*, *104*). However, many of the underlying mechanisms of hASC lineage specification have yet to be elucidated.

hASC are capable of differentiating into adipogenic, osteogenic, chondrogenic, vasculogenic and myogenic lineages (*1*, *2*, *11*, *105*). Specific combinations of chemical, mechanical and environmental factors are known to induce hASC differentiation towards these various cell phenotypes (*1-3*). Previous work from our group and others has shown that physiologically relevant mechanical stimulation can enhance hASC lineage specification (*15*, *97*, *105-107*); this phenomenon is particularly observed when directing hASCs towards musculoskeletal cell phenotypes, which have a largely mechanical function *in vivo.* More specifically, we have shown that hASCs exhibit enhanced osteogenic differentiation when

cultured under 10% cyclic tensile strain and osteogenic differentiation media (ODM), as compared to hASCs cultured in ODM in static culture (*108*). Other groups have reported an enhanced osteogenic phenotype in hASC when cultured under fluid flow conditions (*97*). Further, this mechanically controlled phenotypic development has also been observed in hASC-derived chondrogenic (*106*) and myogenic lineages (*105*).

The mechanisms behind mechanical sensing and signal transduction have been investigated, and these studies have largely implicated the cytoskeleton along with cell-cell and cell-matrix interactions as sensors and effectors of mechanical stimuli (*109*). We propose that the primary cilium may be another important cell structure involved in this process. Primary cilia are known to act as mechanosensors in bone and kidney epithelial cells when exposed to fluid shear (*54*), and are also known to change their length in response to their mechanical environment in tendon explants (*70*).

Primary cilia are non-motile cilia, and they can be observed on nearly every mammalian cell type at some point during the cell cycle. The primary cilium emanates from the basal body, formed by the centriole, and it is composed of nine microtubule doublets arranged in a 9+0 configuration, with nine concentric tubulin doublets forming the axoneme of the cilium. Primary cilia are structurally distinct from motile cilia (9+2), which are present in the mucosal epithelial layers of tissues such as the lung and intestinal tract and have a 9+2 microtubule configuration with a pair of microtubules in the center of the axoneme. Previous work from our group has shown that hASC express primary cilia on anywhere from 20 to 65% of their cell population, depending on confluency (*71*). Further, we have shown that the expression of cilia-associated proteins PC1 and IFT88 plays an important role in the

osteogenic differentiation capacity of hASC (*71*). Under chemically-induced osteogenic differentiation, knockdown of PC1 and IFT88 conferred a reduction in hASC osteogenic differentiation. These data implicate primary cilia as chemosensitive cell organelles.

During the process of cell lineage specification, cells change and reorganize their cytoskeleton, thus changing their cell morphology to be characteristic of a particular phenotype (*110*). In *in vitro* model systems, physically controlling cell morphology also modulates phenotypic specification in human mesenchymal stem cells (hMSC) and adipose-derived stem cells (hASC) (*66*, *111*). Moreover, applying mechanical stimulation to stem cells effects changes in lineage commitment signals, often enhancing chemically induced phenotypes (*14*, *97*, *112*). The primary cilium is somewhat contiguous with the cytoskeleton via the docking of the centrosome at the apical surface of the cell (*33*), so it follows that the cilium structure itself may be sensitive to morphological changes effected by cytoskeletal reorganization in response to mechanical cues. Conversely, the cilium structure is known to be a mechanosensing organelle in many tissues, and in the case of stem cell differentiation, it may play a role in facilitating the mechanically-induced cytoskeletal reorganization.

Based on our previous work, we have established that primary cilia-associated proteins are involved in hASC osteogenic differentiation (*71*) and that tensile strain enhances hASC osteogenesis (*15*, *113*). We hypothesize that the mechano-active primary cilium may be a critical structure in this process. We postulate that the cilium structure is intimately involved in lineage specification processes and that it dynamically modulates and/or is modulated by chemically- and mechanically-induced hASC differentiation.

5.2 Materials and Methods

5.2.1 Cell Isolation and Expansion

Human adipose-derived stem cells (hASC) were obtained from waste adipose tissue derived from anonymous patients undergoing elective abdominoplasty surgeries (IRB exemption protocol #10-0201), at University of North Carolina hospitals (Chapel Hill, NC). All data were analyzed anonymously and the only patient information obtained included age, sex and ethnicity. The Office of Human Research at UNC hospitals deemed that this study does not constitute human research, "as defined under federal regulations [45 CFR 46.102 (d or f) and 21 CFR 56.102(c)(e)(l)] and does not require IRB approval." Isolation of hASC was performed according to previously established protocols from our lab (*7*), adapted from methods initially reported by Zuk et al. (*2*). Once isolated, hASC obtained from approximately 50 g of tissue were allowed to propagate in culture in complete growth medium (CGM) until they reached ~80% confluency (or up to two weeks). CGM contained Eagle's Minimum Essential Medium, alpha-modified, supplemented with 10% fetal bovine serum, 2 mM L-glutamine, 100 units/ml penicillin and 100 μg/ml streptomycin. The hASC were then trypsinized and frozen down at passage 0 (p0). All hASC used in these experiments were passage 4 or lower and were derived from three female donors (ages 47 – 55 years).

5.2.2 Culture and Differentiation Under Cyclic Tensile Strain.

hASC were cultured in Bioflex plates (Flexcell International, Hillsborough, NC) that contained a culture surface composed of collagen I-coated silicone membranes. The hASC

were cultured under both static and dynamic growth conditions. hASC cultured under mechanical stimulation were exposed to 10% cyclic tensile strain at 1Hz, for 4 hours/day. In addition to the mechanical stimulation, they were cultured in three different media: complete growth media (CGM), osteogenic differentiation media (ODM) and adipogenic differentiation media (ADM). ODM contained complete growth medium with the addition of 50 μM ascorbic acid, 0.1 μM dexamethasone, and 10 mM β -glycerolphosphate. ADM contained the aforementioned CGM supplemented with 1 μM dexamethasone, 5 μg/ml insulin, 100 μM indomethacin and 500 μM isobutylmethylxanthine. hASC were cultured in all media formulations both with and without tensile strain as indicated in the schematic (Figure 5.1).

5.2.3 Visualization of hASC - Phase Contrast Microscopy

hASC cultures were monitored using phase contrast microscopy throughout the duration of the culture/differentiation period for up to three weeks. Images were collected at day 14 of culture to record morphological changes in cell phenotype based on media formulation and culture environment. Phase contrast microscopy allowed for detection of cell morphology, orientation, deposition of extracellular calcium crystals and formation of lipid vacuoles.

5.2.4 RNA Extraction and Gene Expression Analysis

Quantitative RT-PCR analysis was used to determine the relative mRNA expression levels of lineage specific gene markers for osteogenesis (Runx2, BMP-2, Alk Phos) and adipogenesis (ppar-γ and LPL). RNA cell lysate samples were collected following 24 and 72

hours in culture. Lysates were run through a Qiashredder column (Qiagen, Valencia, CA) at 15,000g for 2 minutes to homogenize samples. Total RNA was extracted using the RNeasy Mini Kit (Qiagen, Valencia, CA). RNA concentrations were measured using a NanoDrop spectrophotometer (Thermo Scientific, Wilmington, DE). To synthesize first strand cDNA, 110 – 600 ng of RNA in a 21 μL reverse transcriptase (RT) reaction was used with the Superscript III RT with oligo(dT) primers kit (Invitrogen, Carlsbad, CA). Taqman Gene expression assays with pre-determined primer-probe sets were used to amplify diluted (1:1) cDNA (Assays-on-Demand, Applied Biosystems, Foster City, CA). All gene expression profiles were normalized to hypoxanthine-guanine phosphoribosyltransferase (HPRT) (Assay Hs02800695_m1) in an ABI Prism 7000 system (Life Technologies, Grand Island, NY).

5.2.5 Immunostaining

hASC were fixed in 10% formalin for 15 minutes. Following fixation, cells were blocked with a 0.2% Triton X-100/5.0% BSA stock solution for 40 minutes in the twelve well plates on a shaker table. Following blocking, the coverslips were incubated in humidified chambers with the primary antibody solution, containing primary mouse monoclonal acetylated α-tubulin antibody (diluted 1:100) (Sigma) or rabbit polyclonal Runx2 primary antibody (1:50) (Abcam), 0.2% Triton X-100, and 0.5% BSA. The cells were then incubated in the humidified chambers overnight at 4°C.

Samples were rinsed 3 times in PBS for five minutes each on a shaker table and then incubated in the secondary antibody (1:500), phalloidin 594 (Molecular Probes) (1:500) and DAPI (1:500) stain solutions. A chicken anti-mouse secondary was used against the mouse

acetylated α-tubulin primary, and goat anti-rabbit secondary was used against the rabbit primary. The samples were incubated for 3 hours at room temperature. Following the secondary incubation, the samples were rinsed three final times, and the PBS and excess liquid was blotted using a kimwipe in preparation for mounting. Prolong Gold Mounting Media (Molecular Probes) was used to mount the samples and slides were allowed to dry in the dark for 24 hours prior to imaging.

5.2.6 Categorical Analysis of Cilia Conformation and Cell Morphology

ImageJ software (National Institutes of Health, Bethesda, MD) was used to quantitatively analyze variations in frequency of cilia expression, cilia conformation, cilia length, cilia orientation, cell aspect ratio and cell orientation in static and actively strained hASC in 2D culture. Relative fluorescence was correlated with quantified cell and cilia morphological changes to determine the relationship between morphology and level of marker expression. Additionally, we adapted a method described by Gardner *et al.* to categorically analyze cilia conformation and parse out changes in cilia structure following culture in various differentiation media (*70*). For each condition n > 300 cells.

5.2.7 End-Product Expression

Alkaline phosphatase activity and lipid accumulation were used to analyze end-product expression for evidence of osteogenesis and adipogenesis, respectively. After 14-16 days of culture in osteogenic differentiation media and/or 10% cyclic tensile strain (1 Hz, 4 hours/day), the ELF® 97 phosphatase substrate assay (Life Technologies, Grand Island, NY) was used to visualize localized alkaline phosphatase activity, following 10% formalin

fixation and permeabilization in 5% bovine serum albumin (BSA), with 0.2% Triton-X-100. Analysis of alkaline phosphatase activity was done using an ELF filter cube on an epifluorescent microscope (Leica Microsystems, Buffalo Grove, IL). Lipid accumulation was measured using a colorimetric adipogenesis absorbance assay (Biovision, Milpitas, CA) quantifying triglyceride content. Following culture in adipogenic differentiation media for 14-16 days, cells were scraped in 200 µL lipid extraction buffer (Biovision, Milpitas, CA), collected into microfuge tubes, incubated at 90-100°C for 30 minutes on a heat block, and then stored at -30°C. The lysate was then thawed and spun down at 1000 rcf for 2 minutes, and the supernatant was transferred to a new tube to eliminate debris that could interfere with absorbance readings. The sample was then diluted 1:1 with adipogenesis assay buffer (Biovision, Milpitas, CA) and 50 µL of each lysate was prepared according to the manufacturer's protocol. Briefly, the 50 µL sample was combined with 46 µL adipogenesis assay buffer, 2 µL Adipogenesis Probe (Biovision, Milpitas, CA), and 2 µL Adipogenesis Enzyme Mixture (Biovision, Milpitas, CA). Absorbance was read using a 96 well plate on a Tecan Microplate Reader (Tecan Group Ltd, Switzerland) using Magellan™ Data Analysis Software (Tecan Group Ltd, Switzerland) at a wavelength of 570 nm. Adipogenesis measurements were normalized to protein content using a colorimetric bicinchoninic acid (BCA) absorbance assay (Thermo Scientific Pierce, Rockford, IL). Remaining adipogenesis samples were processed according manufacturer's protocol for the BCA assay and samples were read at a wavelength of 560 nm.

5.3 Results

When cultured in complete growth media (CGM), osteogenic differentiation media (ODM) and adipogenic differentiation media (ADM) over the course of 14 days, hASC begin to alter their cell morphology as they assume a committed cell phenotype (Figure 5.1). In CGM, expansion media devoid of additional chemical inducers of differentiation, hASC orient randomly in a multitude of directions as they grow; however, with the addition of mechanical stimulation in the form of 10% cyclic tensile strain (1 Hz, 4 hours/day) hASCs

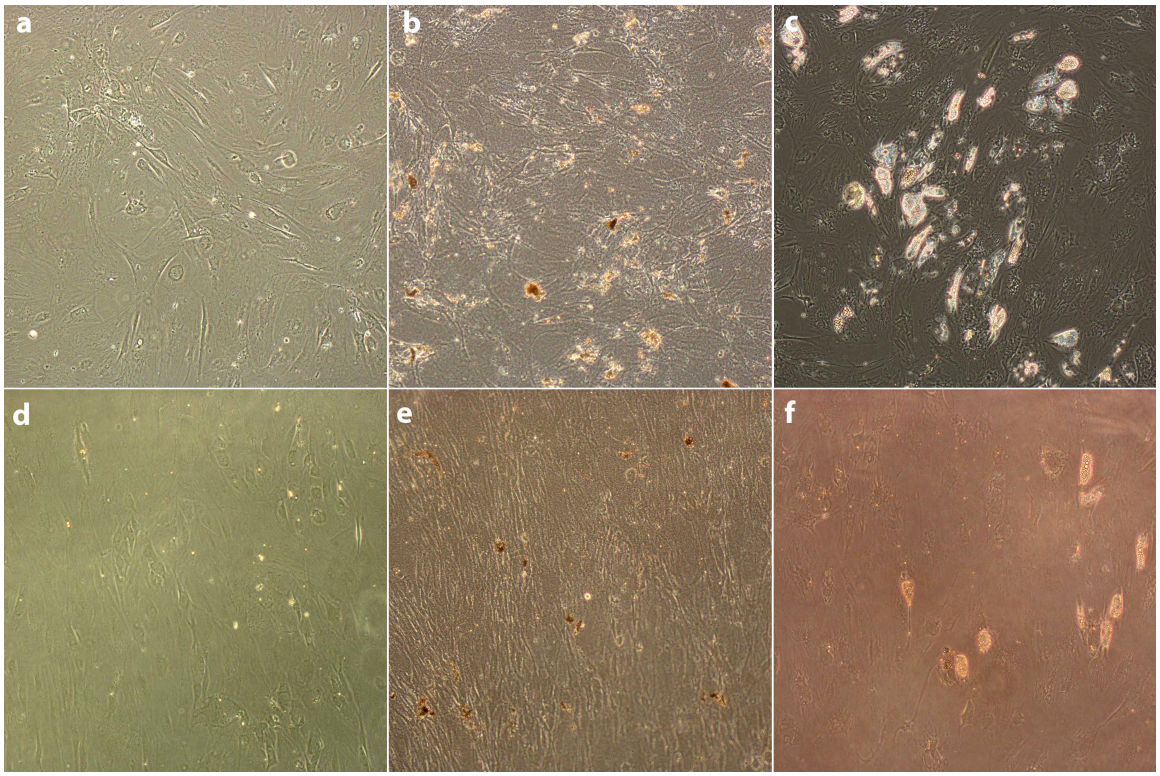

Figure 5.1 hASCs exhibit different cellular morphology in response to both chemical and mechanical stimulation. hASCs cultured under CGM (a,d), ODM (b,e) and ADM (c,f) for 14 days either in static culture (a-c) or under 10% cyclic tensile strain (4 hours/day, 1Hz) (d-f). Accumulation of calcium deposits indicates osteogenic differentiation in both static and strain osteogenic hASCs (b,e). Lipid droplets indicate adipogenesis in both static and strained adipogenic hASCs (c,f). No demarcated evidence of differentiation is observed in CGM, however all hASC exposed to strain tend to align perpendicular to the axis of strain (d-f).

tend to align roughly perpendicular to the axis of strain (Figure 5.1). This cell orientation was consistent with cells cultured in ODM and ADM under strain, with all cell types demonstrating a proclivity to orient perpendicular to the axis of strain. Under static culture conditions osteogenic hASC show evidence of calcium accretion, as visualized by deposited calcium over the monolayer cell surface (Figure 5.1). When osteogenic hASCs are cultured under cyclic tensile strain, they appear highly oriented perpendicular to the axis of strain and the cells assume a very elongated morphology compared to undifferentiated hASCs and hASCs cultured in ODM without strain. Osteogenic hASCs exposed to strain also exhibit calcium deposition; however, the crystal formations tended to be smaller and more dispersed

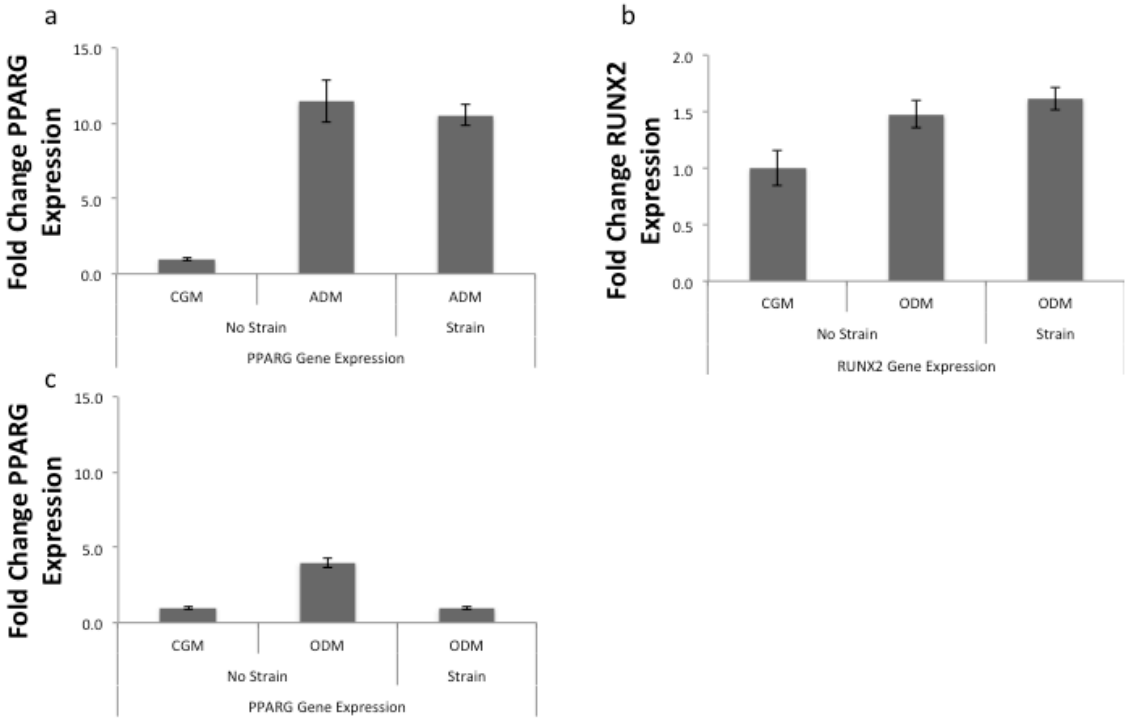

Figure 5.2 Expression of osteogenic and adipogenic gene markers PPARG and RUNX2 following 3 days of culture in CGM, ODM and ADM with and without mechanical stimulation of cyclic tensile strain. At day 3 strain moderately downregulates PPARG in adipogenic hASCs (a) and moderately upregulates RUNX2 expression in osteogenic hASC (b). It also downregulates baseline PPARG expression levels in osteogenic hASCs (c). n=3, Error bars represent SEM.

(Figure 5.1). Adipogenic hASCs tend to assume a more rounded cell phenotype, indicative of osteogenic differentiation, and show evidence of adipogenesis via the accumulation of lipid vacuoles within the cells. Interestingly, strain tended to encourage a slightly more elongated cell morphology than in adipogenic cells cultured in static culture; strain resulted in fewer

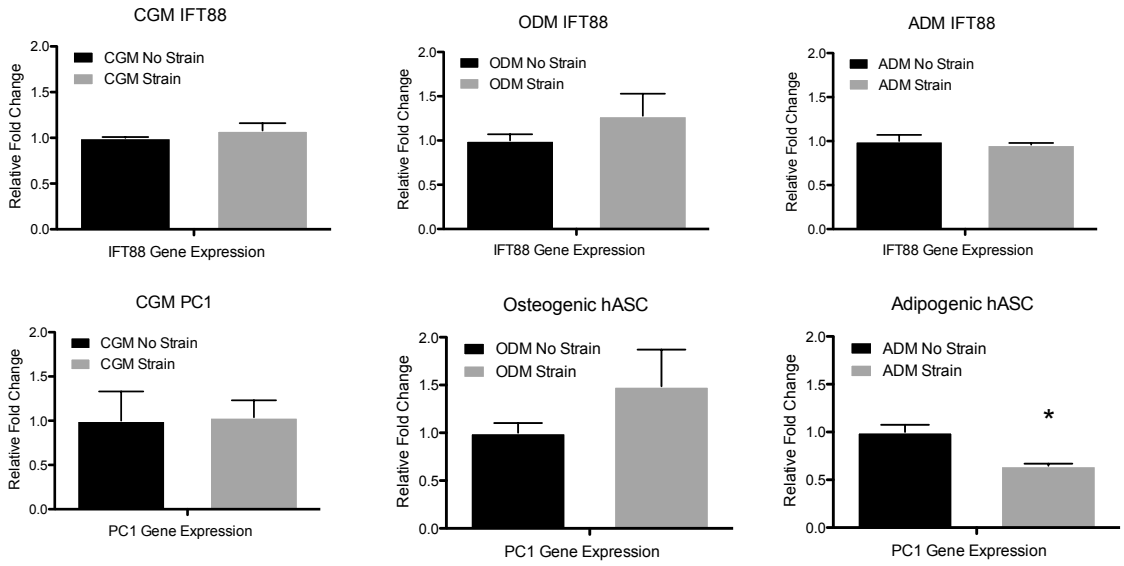

Figure 5.3 Gene expression of cilia-associated genes IFT88 (top row) and PC1 (bottom) following 3 days of culture. Strain upregulates cilia-associated gene expression in undifferentiated hASCs and osteogenic hASCs, but downregulates cilia-associated gene expression in adipogenic hASCs. n=3, Error bars represent SEM, * $p < 0.05$.

cells expressing lipid vacuoles (Figure 5.1).

In light of these general observations, we then examined peroxisome proliferator-activated receptor gamma (PPAR-γ) and runt-related transcription factor-2 (RUNX2), early gene expression markers upregulated in osteogenesis and adipogenesis, respectively. As expected, expression of PPAR-γ and RUNX2 genes were upregulated under ADM and

ODM, respectively (Figure 5.2a-b). hASCs cultured under cyclic tensile strain conferred a slight downregulation of PPAR-γ in ADM and a slight upregulation of RUNX2 gene expression however the change was not significant after only 3 days of exposure to strain.

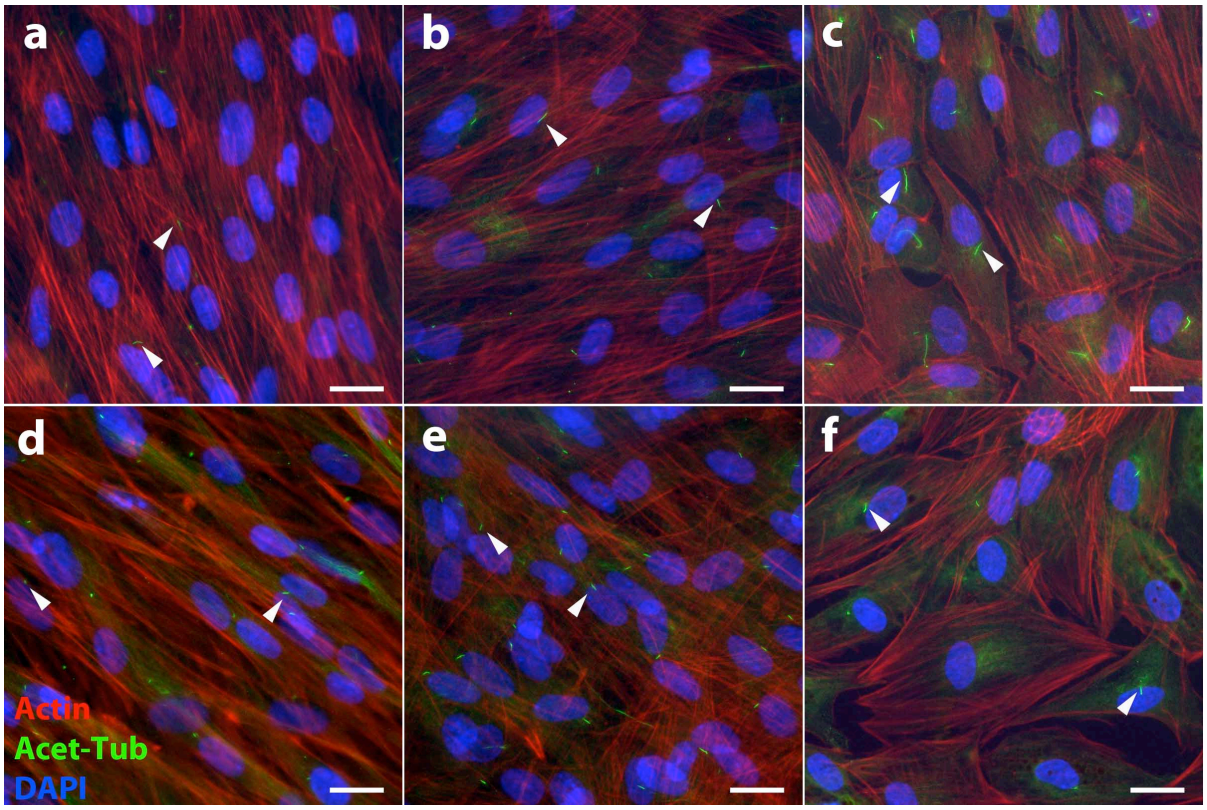

Figure 5.4 Primary cilia expression in differentiating hASCs at day 3 (a-c) and day 14 (d-f) of culture. Primary cilia exhibit variation in their expression frequency, length and conformation temporally throughout the differentiation process amongst different lineages. hASC cultured in CGM (a,d), hASC cultured in ODM (b,e), hASCs cultured in ADM (c,f). Scale bar = 25 μm.

Intriguingly, PPAR-γ expression in osteogenically differentiated cells was significantly downregulated in response to strain, restoring expression to the levels of non-stimulated hASCs (Figure 5.2c).

To determine whether cilia function varied under exposure to cyclic tensile strain under differing types of chemical induction media, we analyzed the gene expression of cilia-associated proteins IFT88 and PC1, known mediators of hASC osteogenesis. We found that after 3 days of culture, PC1 and IFT88 were upregulated with exposure to strain in cells cultured in both CGM and ODM. In contrast, the opposite was true for cells cultured in ADM, with strain conferring a reduction in IFT88 and PC1 gene expression (Figure 5.3). Taken together, this suggests that primary cilia exhibit a differential response to their surrounding mechanical environment depending on cell phenotype.

To explore this concept further, we examined changes in cell morphology and primary cilia expression following 3 days and 14 days of culture under differing conditions (Figure 5.4). We observed qualitatively that morphological changes in response to chemically-induced differentiation were concomitant with changes in cilia expression. Fewer cilia appeared to be expressed in hASC cultured in expansion media; however, there was an increase in cilia expression with increasing osteogenic

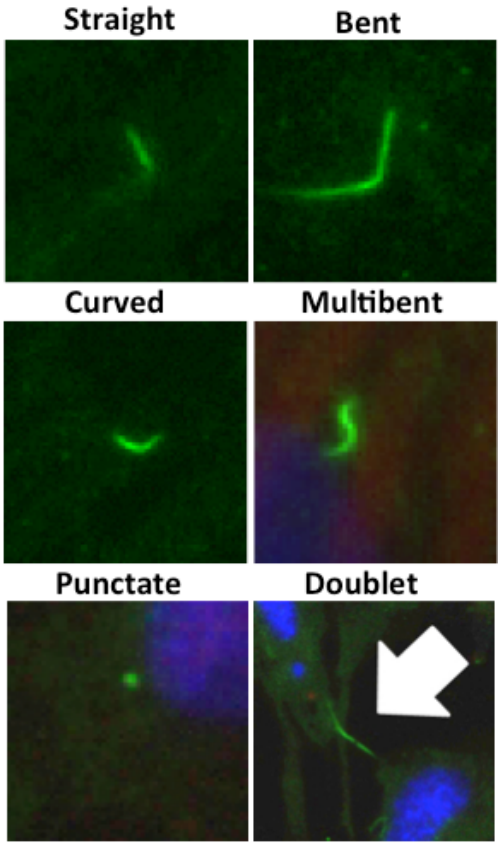

Figure 5.5 Categorical analysis of primary cilia. Examples of cilia conformation frequently observed under immunofluorescence. Doublets stained with acetylated tubulin are quantified, but excluded from cilia frequency analysis as they are generally thought to be cytokinetic bundles, not cilia.

differentiation, and assumption of an osteogenic cell morphology. Further, adipogenic cells appeared to express elongated cilia at day 3 of culture in ADM, with shorter and potentially fewer cilia as the cells progressed towards a more committed adipogenic phenotype after 14 days of culture (Figure 5.4).

Following our qualitative analysis of primary cilia in hASC cultured under different media conditions, we adapted from Gardner *et al.* a semi-quantitative categorical analysis approach to analyze changes in cilia conformation (*70*). We used this analysis to visualize the distribution of cilia conformations present in each culture condition (Figure 5.5). When quantifying cilia conformation following three days under expansion, adipogenic or osteogenic differentiation media, we found distinct differences in the cilia expressed on each hASC phenotype (Figure 5.6). Interestingly, adipogenic media resulted in the most variety in the distribution of cilia shapes, though this may be due to the elongated cilia structure being more prone to bending (Table 5.1). When considering the mechanosensitive

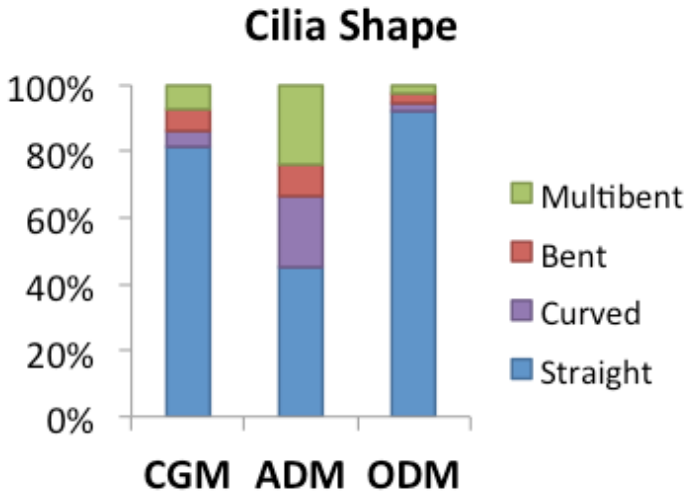

Figure 5.6 Analysis of the cilia conformation following 3 days of culture under expansion medium (CGM), adipogenic differentiation medium (ADM) and osteogenic differentiation medium (ODM). Distribution of cilia conformation varies based on chemical stimulation and may be phenotype-specific. n>300 cells.

properties of the primary cilium, it is important to consider the length and shape of the mechanosensor because that effectively changes the forces experienced by the structure.

Table 5.1 A summary of apparent ciliary length as measured on immunofluorescent images. n>300 cells.

Media	Average Cilia Length (μm)	Standard Deviation
CGM	1.43	±0.45
ADM	3.14	±1.56
ODM	1.38	±0.49

We next aimed to determine whether the effect of mechanical stimulation observed in cilia-associated gene expression reflected the overall level of cilia expression. In fact, we found that cilia expression increased with strain in hASC in CGM, but fewer cilia were observed in hASC cultured in ODM (Figure 5.7a-g). In the adipogenic condition, cilia remained elongated both in static culture and under cyclic tensile strain, but we observed that ciliated cells in ADM appeared less adipogenic than non-ciliated cells. Further, it appeared that strain allowed for cilia expression to persist (Figure 5.7c,f).

A more in-depth analysis of hASC conformation revealed an inverse relationship between cell spreading and cilia length in the static culture environment (Figure 5.8a,b). Interestingly, cilia appear to align closer to the long axis of the cell when osteogenic and adipogenic hASC were cultured under strain; however, the opposite was the case for hASC grown in expansion media (Figure 5.8c). In support of the gene expression data, we found that nuclear Runx2 protein expression qualitatively appeared upregulated with culture in ODM under cyclic tensile strain (Figure 5.9a,b).

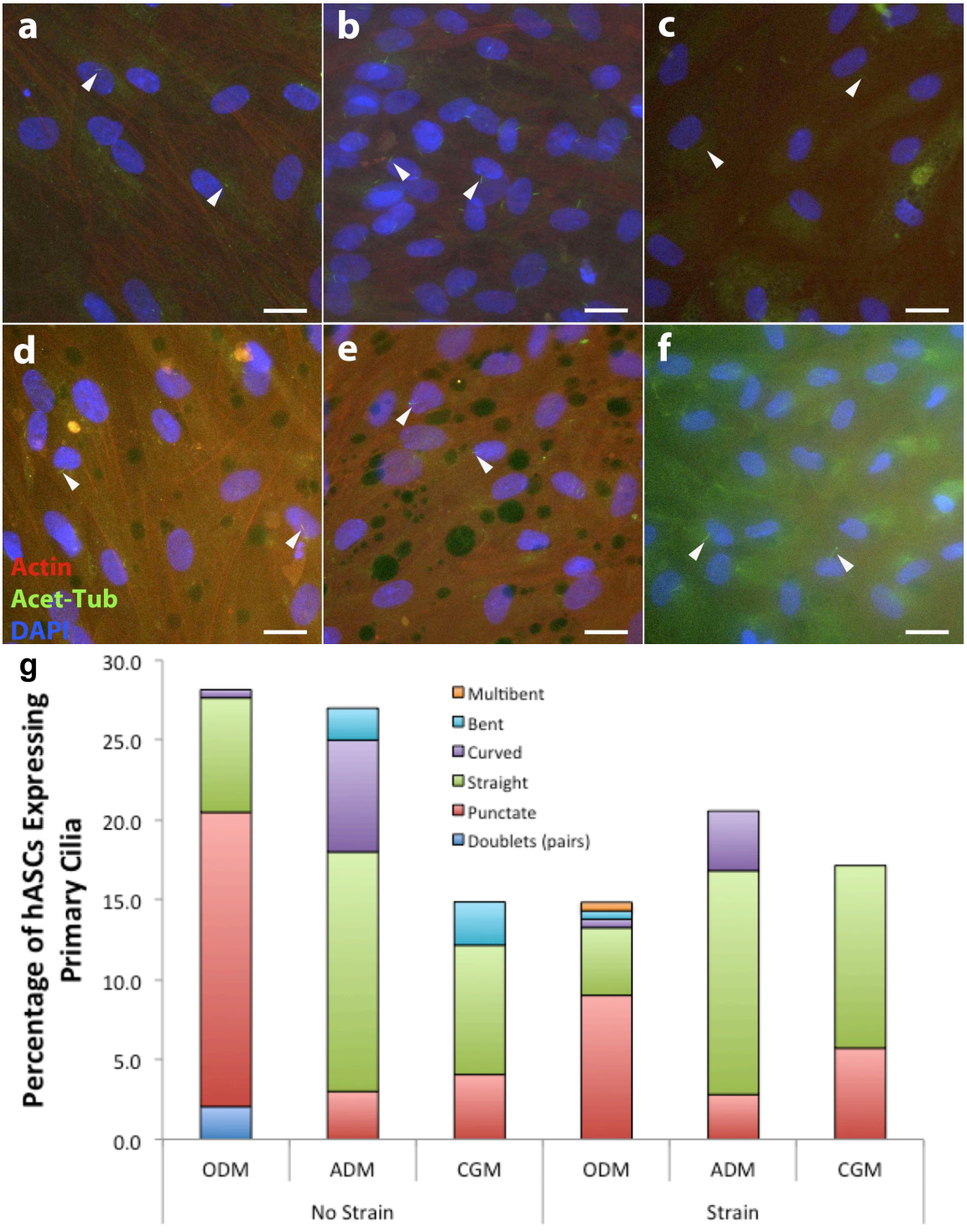

Figure 5.7 Primary cilia expression following 3 days of culture under CGM (a,d), ODM (b,e) and ADM (c,f) on hASCs exposed to static culture (a-c) or mechanical stimulation in the form of 10% cyclic tensile strain (4hours/day, 1 Hz) (d-f). Scale bar = 25 μm. Cilia frequency of expression and distribution of conformations in culture were analyze semi-quantitatively using the aforementioned categorical shape analysis (g).

Additionally, adipogenesis is suppressed with exposure to cyclic tensile strain following 14 days of culture in adipogenic media (Figure 5.9c).

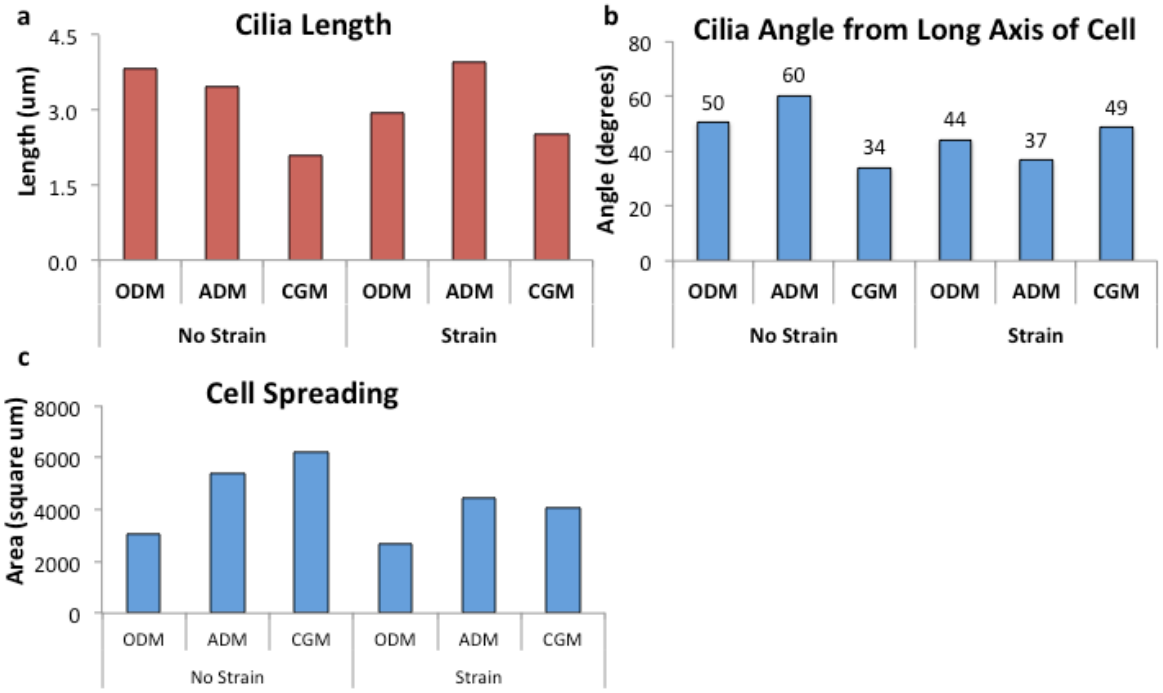

Figure 5.8 Semi-quantitative analysis of cilia and cell morphology under different chemical and mechanical culture conditions. Average cilia length was calculated for each media type, with and without strain (a). Angle of the primary cilia compared to the long axis of the cell body was measured to determine ciliary alignment (b). Cell adhesion and spreading were quantified by measuring cell area (c).

5.4 Discussion

Within mesenchymal and adipogenic stem cell types, adipogenesis is generally thought to be at odds with osteogenesis because each lineage results in cell types with very different physiologies. This theory of stem cell differentiation is somewhat supported by the signaling pathways involved in phenotypic differentiation, suggesting that adipogenic cell

types are mutually exclusive with osteogenic cell types when undergoing these lineage commitment processes (*114*).We hypothesized that strain may contribute to separating the

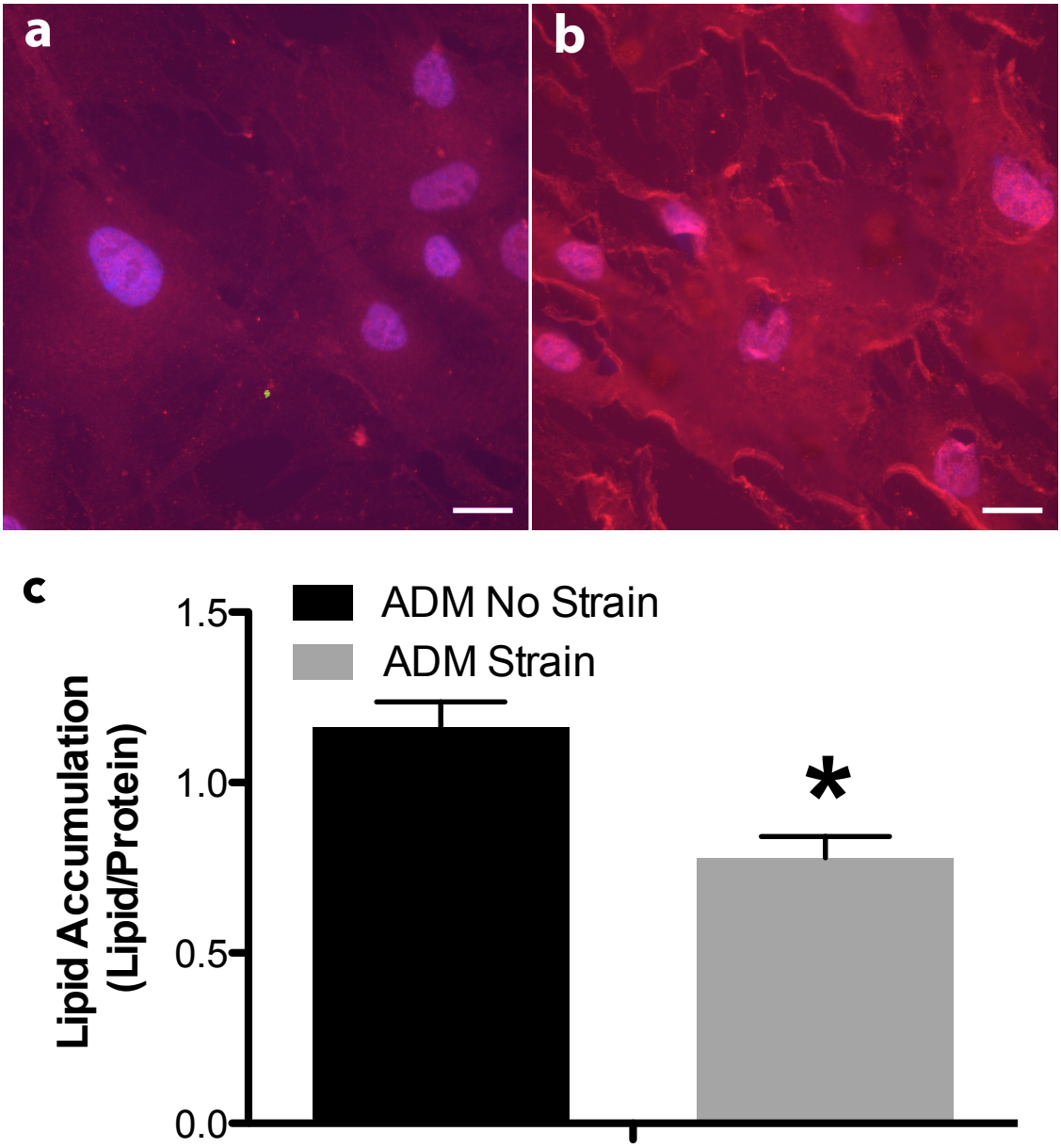

Figure 5.9 Osteogenic factors are upregulated under exposure to cyclic tensile strain and adipogenic factors are suppressed under exposure to strain. Runx2 nuclear expression in hASCs in ODM (a,b) under static culture (a) and dynamic culture under cyclic tensile strain (b) at 3 days. Lipid accumulation is suppressed in hASCs cultured under adipogenic media and cyclic tensile strain for 14 days (c). Scale bar = 25 μm. n=3, Error Bars represent SEM, * $p < 0.05$.

two lineages further; that is to say that strain not only enhances osteogenesis of hASCs (*15*), but also may suppress inherent adipogenic signals. Studies in *in vivo* and cell models other than hASCs suggest that mechanical stimulation likely suppresses adipogenesis (*115-117*), but it is unclear whether a specific stimulation modality and/or magnitude optimally inhibits adipogenesis.

Through our baseline analysis of hASC differentiation in CGM, ODM and ADM with and without strain, we observed stark differences between cell morphology in hASCs cultured in a static environment and those cultured under 10% cyclic tensile strain (1 Hz, 4 hours/day) (Figure 5.1). There was evidence of osteogenic and adipogenic differentiation in both the static and strained cultures after 14 days; however, the hASC tended to orient perpendicular to the axis of strain, whereas non-mechanically stimulated cells exhibited a more random organization pattern (Figure 5.1). This result is consistent with other studies on fibroblasts and cyclic tensile strain (*118*), suggesting that a realignment of the actin cytoskeleton perpendicular to the axis of strain prevents disruption of the internal tension within the cytoskeleton (*119*). Further, in the strained, adipogenically differentiated cells, fewer cells appeared to accumulate lipid vacuoles than did adipogenically differentiated hASCs in static culture. This qualitative observation was the first sign that cyclic tensile strain may have an inhibitory effect on hASC adipogenesis, separate from our previous findings in hASC and hMSC osteogenesis (*14*, *15*, *112*).

To determine the temporal effect of strain, we analyzed early gene markers for osteogenesis and adipogenesis at day 3 (Figure 5.2a). PPAR-γ, a gene marker for adipogenesis, was very moderately downregulated in adipogenic hASCs under tensile strain,

consistent with trends observed in adipogenic hASCs at day 14 in culture. Likewise, expression of the osteogenic gene marker RUNX2 exhibited a moderate increase in expression in osteogenic hASCs under strain, consistent with the trends in Figure 1 and our previously published work on strain mediated osteogenesis (Figure 5.2b). Unexpectedly, PPAR-γ expression in osteogenically differentiated hASCs was significantly downregulated following 3 days of culture under 10% cyclic tensile strain (1 Hz, 4 hours/day) (Figure 5.2c). This finding suggests that mechanical stimulation via tensile strain may not simply enhance osteogenic signals but rather may be inhibiting the baseline adipogenic signals present, allowing for the osteogenic signals to have a greater effect on determination of hASC phenotype.

Our previous work in hASC strain-mediated osteogenesis(*15*) and the role of the primary cilia in osteogenesis (*71*) provided the impetus to explore the role of the primary cilium as a potential mechanosensor. Following daily exposure to cyclic tensile strain and 3 days of stimulation in differentiation medium, we analyzed the gene expression of cilia-associated proteins IFT88 and PC1, which are known to be involved in hASC osteogenesis (Figure 5.3). We found that both PC1 and IFT88 were upregulated under strain in undifferentiated hASCs and osteogenically differentiated hASCs, while adipogenically differentiated hASCs exhibited the opposite affect (Figure 5.3). These inversely-related cilia gene expression findings suggest that the primary cilia may differentially sense the surrounding mechanical environment based on cell phenotype, in part validating their phenotype-specific function (Figure 5.3).

To analyze further the primary cilium structure in differentiated hASCs, we used immunostaining to characterize the level of cilia expression and length of cilia elongation for each media type after 3 and 14 days of culture (Figure 5.4). Our immunofluorescent results illustrated stark differences in cilia expression amongst committed cell types concomitant with changes in overall cell morphology over time in culture (Figure 5.4). Very few studies have explored changes in cilia with phenotype, however a study by Nathwani *et al.* observed changes in cilia length and presumed reductions in cilia rigidity in human induced pluripotent stem cells (iPSCs) derived from fibroblasts (*120*), thus indicating that changes in cilia structure can change with phenotype. Further, another study on Bardet-Biedl syndrome proteins revealed that pre-adipocytes transiently express primary cilia during the adipogenesis process, yet they lose their cilia upon terminal differentiation (*31*). The findings of that study were consistent with our observations of cilia on hASCs undergoing adipogenic differentiation (Figure 5.4).

In our observations of cilia expression lengths varying with changes in cell phenotype, we noted that cilia tended to present in a variety of shapes. We adapted a semi-quantitative categorical analysis approach from a report by Lavagnino *et al.* to analyze differences in cilia shapes among differing cell populations (Figure 5.5) (*121*). In quantifying the cilia conformations observed on hASCs cultured in expansion media, adipogenic differentiation media and osteogenic differentiation media for 3 days, we found that each phenotypic population had a distinctly different distribution of cilia conformations (Figure 5.6). Adipogenic hASCs had a stark change in the distribution of cilia shapes within the cell population, exhibiting a relatively higher percentage of cells in curved or bent conformations

(Figure 5.6). This is likely related to the increase in average length of adipogenic hASC cilia (3.14 μm ±1.56) as compared to cilia observed in hASCs cultured in CGM (1.43 μm ±0.45) or ODM (1.38 μm ±0.49) (Table 5.1), as the longer cilia may be more susceptible to bending. This may also be due to changing mechanical integrity of the cilia and a reduction in cilia rigidity, as proposed in an iPSC study categorizing changes in cilia morphology with fibroblast reprogramming (*120*).

Extending this analysis further, we examined cilia expression and conformation in hASCs cultured on the collagen I-coated silicone membranes of Bioflex plates, comparing the effects of strain on each hASC phenotype (Figure 5.7). Strain appeared to not only affect the morphology of each specified cell type but also affect the level of cilia expression. In hASC cultured in CGM for 3 days, strain appeared to increase the number of cells expressing cilia, though it is unclear why this is the case. It may be related to strain itself signaling the hASC to assume a more committed phenotype, so that as the proliferative signaling is quieted, the cilia simply elongate due to a level of quiescence. Osteogenically differentiated hASCs expressed the highest percentage of cilia in static culture, though a smaller proportion of osteogenic hASCs expressed cilia under strain (Figure 5.7b, e, g). This finding is consistent with observations in tendon explants and supports the idea of the "stress deprivation paradigm," which states that in the absence of mechanical stimulation, cilia lengthen, and in the presence of strain, the ciliary axoneme is shortened or resorbed (*70*).

In adipogenically differentiated hASC, there was a moderate decrease in the percentage of cells expressing primary cilia following exposure to strain; however, the effect was much more muted than that observed in the osteogenic phenotype (Figure 5.7). Further,

it appeared that elongated cilia persisted in strained hASCs in ADM more so than in those in ODM. This resulted taken together with the idea that differentiating hASCs transiently express elongated cilia in the pre-adipocyte stage (*31*), suggests that strain may be delaying the temporal stages of adipogenesis. This question could be further addressed by analyzing the effects of strain on hASCs cultured in ADM at a later time point than 3 days to determine whether cilia persist for a longer amount of time than those in static adipogenic culture.

A more in-depth morphometric analysis revealed interesting lineage-specific trends in cilia conformation as well as global trends in cilia expression (Figure 5.8a). In general, we found that hASC grown in CGM on Bioflex plates tended to have the shortest average cilia length but showed a slight increase in average length with exposure to cyclic tensile strain. Adipogenic cells exhibited a similar trend with a slightly higher average cilium length under cyclic tensile strain. We hypothesize that this may occur because strain prolongs the ciliated pre-adipocytic phenotype, delaying progression into the lipid-filled adipocyte. However, this contrasts the frequency of cilia expression results in Figure 5.7, which shows a slight reduction in the percentage of ciliated adipogenic hASC. This disparity may be explained by the heterogeneous cell population which comprises hASCs. A subset of the population may be more mechanosensitive, and thus these remaining hASCs persistently express elongated cilia under strain. Future studies focused on enriching specific hASC subtypes may help tease out these differences; however, our cilia data (Figure 5.7-5.8) still support the notion of lineage-specific mechanosensitivity.

Osteogenic hASCs were the longest cilia in static culture but exhibited axonemal shortening under cyclic tensile strain, consistent with the aforementioned stress deprivation

paradigm (Figure 5.8a). This paradigm is based on the principle that presumably a more extended cilium may detect smaller magnitude changes in the surrounding mechanical environment, and when larger magnitude mechanical forces are present, the cilium no longer requires such a large "lever arm" to sense mechanical signals (*70*). This explanation follows for mechanically sensitive tissue such as bone. However, these changes can also be explained through a cell physiology model, suggesting that strain confers changes in the ciliary signaling pathways such as hedgehog and therefore that the cell modulates cilia length to adjust hedgehog signaling activity (*73*). It is likely that both models are accurate and there may be both a mechanical and biochemical component to the lineage dependent response of cilia to their mechanical surroundings.

In addition to length changes in the cilia, strain also tended to reduce the angle between the cilium and the long axis of the cell in hASCs cultured in ODM and ADM, suggesting the cilium was more apt to conform with cytoskeletal alignment in the presence of mechanical stimulation (Figure 5.8c). Cyclic tensile strain conferred the largest magnitude effect on ciliary alignment, reducing the average angle of cilia from the long access of the cell body from 60° to 37°. Osteogenic hASCs exhibited a modest 6° reduction in angle between the ciliary axoneme and the long axis of the cell, while osteogenic hASC cilia generally tended to align more closely with the axis of the cell. The alignment of undifferentiated hASCs exhibited an opposite effect in response to strain, with the angle between the ciliary axoneme and the long axis of the cell increasing by 17°. This trend is consistent with the increasing length of the cilium in hASCs grown in CGM exposed to strain, but it is difficult to speculate on the cause of this decrease in ciliary alignment. It is

possible that the mechanical rigidity of the cilium is changing along with phenotype, as predicted by both chemical and mechanical induction, and thus it is more susceptible to the bending influence of the tensile strain (*120*). Additionally, cytoskeletal and nucleoskeletal rigidity are both affected by lineage commitment (*122*, *123*), though manipulating the mechanics of these structures can effectively change the mechanical properties of a cell and thus phenotype (*111*, *124*). Because the basal body of the cilium is docked at the cell membrane, the cilium is contiguous with the cytoskeleton, and thus it follows that the rigidity of the cilium likely also changes with cytoskeletal tension. In the static culture condition, a clear inverse relationship between cell spreading and cilia length further supports the relationship between cytoskeletal tension and cilia expression, with cells with the lowest surface area expressing the longest cilia and vice versa (Figure 5.8a,c). This result is consistent with a study in retinal epithelial cells (RPE1 cells) showing that RPE1 cells cultured on harder substrates with larger surface areas expressed shorter and fewer cilia (*125*). Similarly, MSCs cultured on grooved substrates also expressed a higher average cilia length as compared to MSCs cultured on flat substrates. The grooved substrates confer a less-spread conformation onto the cell and, thus, our observations are also consistent with the morphological findings of this study (*126*).

Our results clearly indicated that both cyclic tensile strain and lineage specific chemical induction media can modify cilia expression along with lineage changes. Evidence from this study and previous work in our lab has established that cyclic tensile strain enhances osteogenesis, further supported by upregulation of Runx2 protein expression (Figure 5.9a-b). An analysis of lipid accumulation following 14 days of culture in adipogenic

induction medium with exposure to strain further confirms not only that osteogenesis is enhanced by cyclic tensile strain but also that adipogenesis is suppressed by strain (Figure 5.9). hASCs are a multipotent lineage with a general proclivity to become either cell phenotype; however, adipogenesis and osteogenesis are considered to be orthogonal processes of differentiation. Based on this theoretical principle (*114*), it may be the case that cyclic tensile strain diminishes baseline adipogenic signals as much as it enhances osteogenic signals. This finding is in line with work done in pre-adipocytes, illustrating the impact of exposure to a compressive force for 12 hours on diminishing adipogenic differentiation (*117*). Our observations were also consistent with an *in vivo* mouse model study showing that MSCs in mice were less adipogenic when exposed to high frequency, low magnitude mechanical stimulation (*115*). It is important to note a contrasting study which reported an enhancement of adipogenesis under exposure to strain. However, the parameters of their strain system were quite different, as their 3T3-L1 cells were exposed to a static application of strain (*127*). From our work, it is clear that strain reduces adipogenic differentiation and enhances osteogenic differentiation; these phenotypic changes also affect the primary cilium structure, a known mediator of cell differentiation.

In this body of work, we have clearly demonstrated that hASC primary cilia exhibit a lineage-specific response to mechanical stimulation in the form of cyclic tensile strain, but it is important to acknowledge the limitations of this study. Primary cilia are notoriously difficult to study under *in vitro* culture due to their variability in expression level depending on the cell cycle phase (*37*, *48*). Further, their expression can additionally be modulated through cell plating density and serum starvation (*48*), and their frequency of expression is

not always predictable in a given cell population. These challenges are why investigators tend to look at general relative trends within cilia expression as opposed to absolute quantification. Additionally, hASCs are a somewhat heterogeneous cell population (*128*), and the variation in cilia expression may be attributed to cell population subtypes, further complicating how the data is interpreted. Future work in this area may include enriching hASC population subtypes for a more in-depth analysis of cilia behavior.

Another caveat for consideration in this study is the notion of donor-to-donor variability in hASCs (*129-131*). In this study we selected three relatively age-matched female donors whose cells were known to exhibit an acceptable proclivity for both osteogenic and adipogenic differentiation. These donor hASC lines were already screened for multipotency and as such were preselected based on their ability to differentiate. Therefore, the results of this study are most relevant to hASCs which exhibit similar characteristics and may have a limited relevance to hASC lacking the ability to osteogenically or adipogenically differentiate. Further research is required to better understand the physiological differences amongst hASC donor lines.

5.5 Conclusions

Cumulatively, the results of this study elucidate the global effects of mechanical stimulation in the form of 10% cyclic tensile strain (4 hours/day, 1 Hz) on hASC differentiation. We compared and contrasted the differential effects of strain on both osteogenic and adipogenic phenotypes as well as strain's effect on the primary cilium organelle and its associated proteins. We established that cilia are indisputably affected by strain, as measured by increases in cilia-associated gene expression and length and changes

in cilium structure morphology across cell populations cultured under different types of chemical and mechanical stimulation. Cilia expression is intimately associated with hASC phenotype and, as such, their response to the strain environment seems in part dictated by their lineage specificity. We confirmed that strain enhances osteogenesis via the upregulation of osteogenic gene markers, and morphological changes corresponding to an osteogenic cell morphology. Through a similar analysis, we also found that adipogenesis was downregulated under cyclic tensile strain, as measured by delayed adipogenic morphological changes in hASCs, a reduction in lipid accumulation, and a downregulation of adipogenic gene expression. Overall, we also found that under our strain parameters of 10% cyclic tensile strain at 1 Hz for 1 hour per day, cells tended to align roughly perpendicular to the axis of strain, which is consistent with the behavior of many fibroblastic cell types cultured under cyclic tensile strain in 2D culture and likely relates to the development of the hASC phenotype. In spite of our efforts to elucidate cilia function in this study, we suggest further research into primary cilia as biomarkers within hASC populations is needed. We hypothesize that their expression patterns are likely somewhat indicative of the level of stemness of particular hASC sub-populations and/or may help tease out some of the physiological differences between hASC donor lines; however, this type of population sorting study was outside the scope of this work. This is the first study to demonstrate that hASC primary cilia are mechanosensitive to uniaxial cyclic tensile strain and that their primary cilia exhibit a differential response to mechanical stimulation upon chemically induced differentiation. Further, we also showed that adipogenic signals were quelled by culture under strain both in adipogenically differentiated cells and in the baseline expression

levels of osteogenically differentiating hASCs. Taking these results together, we have highlighted the importance of the primary cilium structure in mechanosensing and lineage specification, and we suggest that further work may identify this structure as a novel target in manipulating hASC for developing tissue engineering applications.

5.6 Summary

Non-motile primary cilia have been implicated as dynamic sensory structures in a variety of mammalian cell types, including adipose-derived stem cells (hASC). Previous work in our group has identified primary cilia on hASC, and we have demonstrated that siRNA knockdown of cilia-associated proteins affects their capacity for chemically induced osteogenic differentiation. Further, we have described the mechanosensitivity of hASC and have shown that when exposed to 10% cyclic tensile strain, hASC exhibit enhanced osteogenic differentiation. We hypothesize that primary cilia play a dynamic role in transducing chemical and mechanical cues, effecting global changes in hASC lineage commitment. In this study, we established that adipogenesis is suppressed in hASC exposed to 10% cyclic tensile strain (1 Hz, 4 hours/day) as measured through adipogenic markers of gene expression and end-product expression as determined by lipid accumulation. Interestingly, we found that the primary cilia-associated genes intraflagellar transport protein-88 (IFT88) and polycystin-1 (PC1) were upregulated in response to strain in hASC grown in expansion and osteogenic induction media; however, their expression is downregulated in hASC cultured under adipogenic induction media. hASC morphology, alignment, cilia length and conformation vary in response to chemical stimulation with complete growth media (CGM), adipogenic differentiation media (ADM) and osteogenic

differentiation media (ODM), with the longest cilia expressed in adipogenically differentiating cells. Mechanical stimulation effectively led to a marked reduction in cilia length for osteogenically differentiated cells and a modest reduction for adipogenically differentiated cells, but it led to an increase in the cilia length of hASC grown in expansion media. Additionally, when exposed to 10% cyclic tensile strain, hASC tended to orient perpendicular to the axis of strain regardless of the type of chemical induction media, while cilia tended to align along the long axis of strain in osteogenic and adipogenic committed cell types. With this study, we have identified the differential mechanosensitive nature of primary cilia in hASC undergoing lineage commitment processes and observed concomitant morphological changes associated with phenotypic specification. This study is the first to analyze changes in ciliary gene expression, conformation and frequency of expression in differentiating hASCs, and it will likely contribute to elucidating the fundamental mechanisms of hASC differentiation to better harness the potential applications of hASC in tissue engineering.

CHAPTER 6 Age-Related Effects on the Potency of Human Adipose Derived Stem Cells: Creation and Evaluation of Superlots and Implications for Musculoskeletal Tissue Engineering Applications

This chapter has been published in the journal under the following citation:

Bodle JC, Teeter SD, Hluck BH, Hardin JW, Bernacki SH, Loboa EG.
Age-Related Effects on the Potency of Human Adipose-Derived Stem Cells: Creation and Evaluation of Superlots and Implications for Musculoskeletal Tissue Engineering Applications.
Tissue Eng Part C Methods. 2014 May 1. [Epub ahead of print]
PMID: 24628423

6.1 Introduction

The study of human adipose-derived stem cells (hASC) has been a rapidly expanding area of research due to the potential implementation of hASC in a wide range of clinical applications. Both *in vitro* and *in vivo* studies have demonstrated the ability of these cells to differentiate into a variety of mesodermal lineages such as adipogenic, osteogenic, chondrogenic, myogenic and vasculogenic cell types (*1*, *2*, *11*, *12*, *132*). Despite their multilineage differentiation potential, hASC exhibit a high level of donor-to-donor variability (*131*, *133*) (*134*, *135*). This particular characteristic presents a challenge for studying and manipulating hASC on the bench top, as well as employing their widespread use in regenerative medicine applications in the clinic.

With this high level of donor variability, it is necessary to consider the possible sources of donor-specific hASC differentiation capacity when selecting appropriate experimental donor cell lines. To obtain data representing the consensus behavior of differentiating hASC, it is critical to incorporate both experimental technical replicates within each donor cell line and use the statistically appropriate number of donors. Generating this data can become quite experimentally expensive and may not yield reports of consensus data, as accessible patient history is often limited to gender and age. Further, this experimental challenge translates into a larger clinical barrier to understanding how to appropriately utilize hASC in a regenerative medicine capacity.

To circumvent the need to run multiple replicates for various cell lines derived from individual donors, some labs and companies now generate pooled cell lines derived from a number of donors – termed "superlots," in their studies (*136*, *137*). The rationale for superlots, or pooled donor cell lines, is that the number of samples necessary to generate consensus data on hASC differentiation behavior can be minimized. However, this method of pooling cell lines has not been thoroughly investigated. It is well established that age affects stem cell activity *in vivo* and *in vitro*, however characterizing potency changes in aging stem cells is a complex process (*135*, *138*-*141*). A number of investigators have reported conflicting data on whether adipose and/or mesenchymal stem cell potency varies with age (*135*, *138*, *142*, *143*). This may be due to variations in donor health, isolation, and culture procedures, but may also depend on the assays used for characterization. Further complicating the consensus data in the application of hASC for musculoskeletal tissue engineering, investigators have reported that mesenchymal and adipose-derived stem cells

isolated from patients or animal models of osteoarthritis have full capacity to differentiate into osteogenic, chondrogenic and adipogenic tissues (*144*, *145*). Additionally, there is evidence that rabbit ASC derived from osteoporotic rabbits have a comparable capacity for *in vitro* osteogenic differentiation as compared to healthy rabbits, suggesting that a disease such as osteoporosis does not preclude the use of ASC in autologous therapies (*146*). However, what a majority of investigators do agree upon is that high donor-to-donor variability is a barrier to understanding the consensus behaviors of hASC differentiation and moreover a barrier to their widespread clinical use.

In this study, we present a method by which we generate hASC superlots derived from 4-5 individual donors per superlot group, with each group delineated by age, with the goal of further understanding and potentially streamlining research approaches in studying hASC for tissue engineering applications. The donor lines were clustered based on the estimated average age of menopause in Western societies being 51 years old (*147*). As all donors were female, they were generally categorized into three age groups based on the availability of cells in a specific donor range in our cell bank: pre-menopausal (24-36 years), peri-menopausal (48-55 years) and post-menopausal (60-81 years). It is important to note that the ages and number of donor cell lines incorporated in this study were based on the availability of donor cell lines within our lab bank of cells. Due to isolating and maintaining our own cell bank, number of contributing donor cell lines and the range of ages incorporated is a limitation of this study. Our overall objective was to present a method for generating hASC superlots, and to validate the approach of generating age-matched pooled samples to obtain consensus data on age-matched hASC.

6.2 Materials and Methods

6.2.1 hASC Isolation and Propagation

Human adipose-derived stem cells (hASC) were isolated from excess adipose tissue derived from anonymous patients undergoing elective surgery (Office of Human Research at UNC, IRB exemption protocol #10-0201), at University of North Carolina hospitals (Chapel Hill, NC). Anonymous patient data obtained included age, gender, ethnicity and procedure from which the tissue was collected. Isolation of hASC was performed according to previously established protocols from our lab (*7*), adapted from methods initially reported by Zuk et al. (*2*). Once hASC were extracted from approximately 50g of tissue, they were allowed to propagate in culture in complete growth medium (CGM) until ~80% confluency (or up to two weeks). Cells were expanded in CGM containing Eagle's Minimum Essential Medium, alpha-modified supplemented with 10% fetal bovine serum, 2 mM L-glutamine, 100 units/ml penicillin and 100 μg/ml streptomycin. The hASC were then trypsinized and frozen down at passage 0 (p0). All hASC used in these experiments were derived from female donors (ages 24 - 81 years).

6.2.2 Potency Characterization: Osteogenic, Adipogenic and Chondrogenic Differentiation

At the time of each individual donor hASC isolation, the cell isolates were characterized based on their growth and differentiation potential. Each donor cell line was characterized at p0 cells and cultured in complete growth medium (CGM), adipogenic

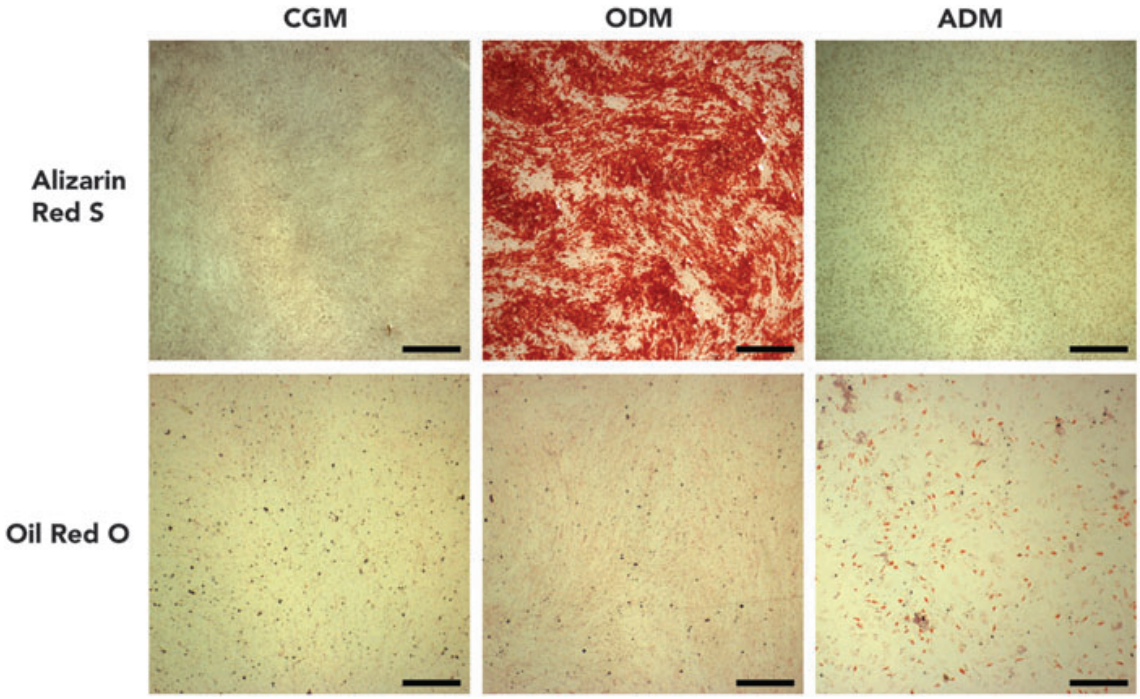

Figure 6.1 Characterization and validation procedure used to evaluate freshly isolated human adipose-derived stem cells (hASC) lines. hASC seeded in a six-well plate are grown in the complete growth medium (CGM), osteogenic differentiation medium (ODM), and adipogenic differentiation medium (ADM), two wells per medium treatment, in columns. Following 14 days of culture, the hASC are then fixed and stained with Alizarin Red S indicating cell-mediated calcium accretion or Oil Red O indicating formation of lipid droplets, hallmarks of osteogenesis and adipogenesis, respectively. CGM wells provide a benchmark control to evaluate hASC responses to differentiation media and to ensure hASC are not undergoing random differentiation in the absence of induction factors. To further confirm the hASC are undergoing appropriate differentiation, cross staining of Alizarin Red S to ADM-cultured hASC and Oil Red O to ODM-cultured hASC was used to check for aberrant staining. Scale bar = 500 μm. hASC, human adipose-derived stem cells.

differentiation medium (ADM) and osteogenic differentiation medium (ODM). Differentiation media contained inductive supplements to the aforementioned CGM. ADM was composed of CGM combined with 1 μM dexamethasone, 5 μg/ml h-insulin, 100 μM indomethacin and 500 μM isobutylmethylxanthine. ODM was composed of CGM with the addition of 50 μM ascorbic acid, 0.1 μM dexamethasone, and 10 mM β -glycerolphosphate.

To assess multipotency, p0 hASC were grown in each medium condition for 14 days. Staining and monitoring of morphological changes via microscopy were used to evaluate adipogenic and osteogenic differentiation potential. Cells were seeded in 6-well plates (5 x 10^4 cells/well) and were grown to 90-100% confluency in CGM (1-3 days). Upon confluency, hASC were cultured in their treatment media, ODM or ADM (14 days) for osteogenic or adipogenic differentiation induction, respectively as well as CGM for a baseline comparison. Evidence of differentiation was visualized with phase contrast microscopy and using Alizarin Red S for calcium accumulation (osteogenesis) and Oil Red O for lipid droplet accumulation (adipogenesis) as visualized on a dissecting microscope (Leica Microsystems, Illinois). Cross staining of Alizarin Red S in ADM and CGM treated wells and Oil Red O staining in ODM and CGM treated wells, was performed to ensure hASC yielded an appropriate differentiation response (Figure 6.1). Any cell lines that exhibited aberrant staining such as lipid accumulation under culture with osteogenic induction medium or calcium accretion under culture with adipogenic induction medium were excluded.

For an expanded study of multipotency, we also characterized our hASC lines for their chondrogenic differentiation potential. To induce chondrogenesis, hASC are cultured in chondrogenic induction media (Dulbecco's Modified Eagle's media, high glucose without

glutamine, supplemented with 1% FBS, 100 units/mL Penicillin, 100 µg/mL Streptomycin, 4 mM L-glutamine, 6.25 µg /mL h-Insulin, 10 ng/mL Transforming growth factor-β3, 50 nM Ascorbate-2-phosphate) for 3 – 4 weeks and are fixed, embedded in paraffin and sectioned for analysis. Sections of the pellets are typically stained with Safranin O or Alcian Blue to characterize levels of hASC chondrogenesis (data not shown).

6.2.3 Age-Matched Approach to hASC Superlots

It is well known that bone density changes with age. Further, during and after menopause a decrease in bone density is frequently observed. Additionally, the development of osteoporosis is often associated with the occurrence of menopause (*148*). Therefore, in an attempt to take this information into consideration, we generated pooled donor hASC superlots. We categorized donor groups by the average reported ages of pre-, peri-, and post-menopausal women (*147*). The pre-menopausal superlot was composed of cells derived from donors of age 24-36 years, the peri-menopausal superlot derived from donors of age 48-55 years and the post-menopausal superlot was derived from donors of age 60-81 years. It should however be noted that these groupings were based on average reported data and the availability of donor cells within each age group, and were not selected based on the reported menopausal phase of the specific donor as that information was not, and is not typically, reported with the anonymous patient data.

6.2.4 Generating hASC Superlots

The goal of creating an hASC superlot is to increase the throughput of experimental data, to acquire true consensus hASC growth and differentiation characteristics to best harness their potential for clinical applications, and to streamline the bench-to-bedside

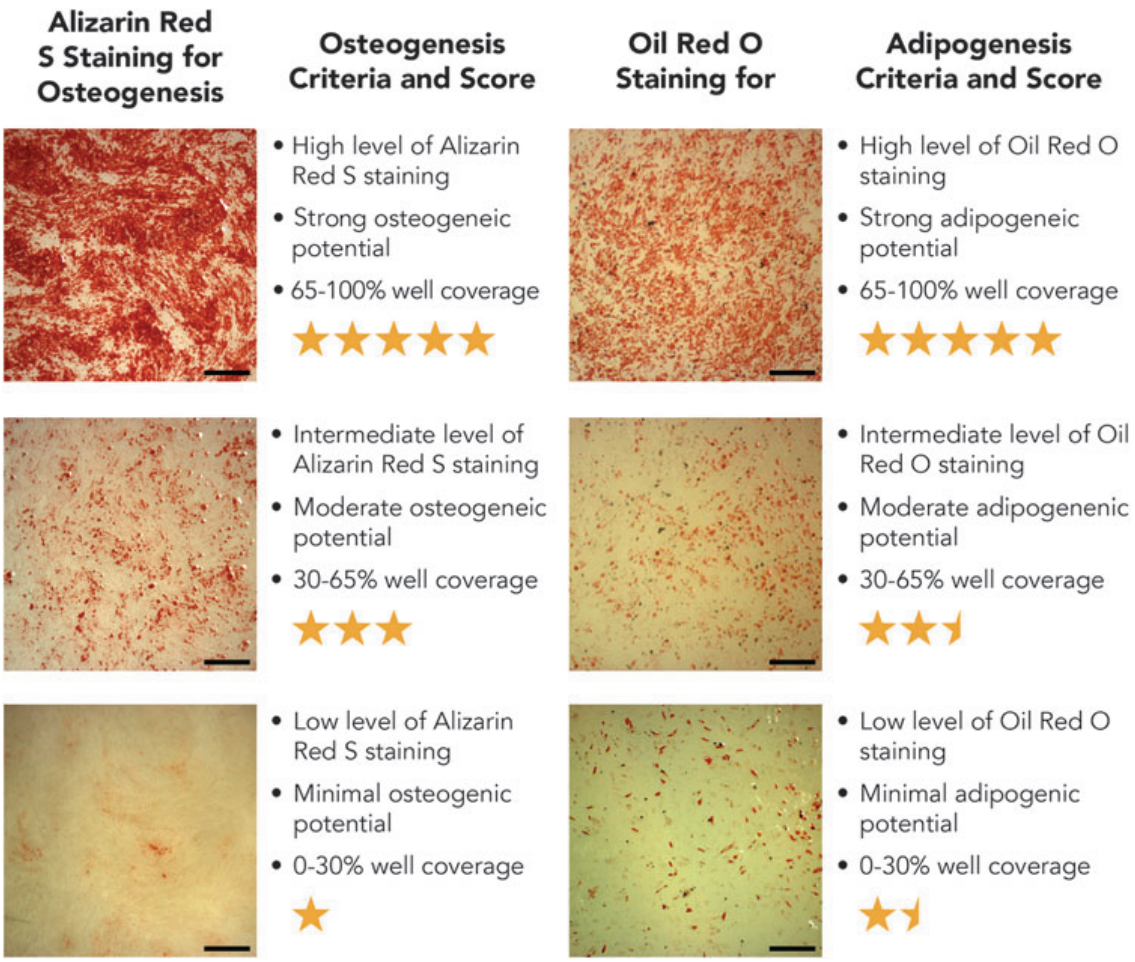

Figure 6.2 Qualitative potency characterization system. Once a freshly isolated donor hASC line has been validated, its differentiation potential is qualitatively ranked on a scale from one to five stars. Chart shows examples of high-, intermediate-, and low-level differentiators, from top to bottom, and their relative osteogenic (left) and adipogenic (right) potency ranking. Scale bar = 500 µm.

process to produce hASC-derived therapeutics that behave in a predictable regenerative capacity *in vivo.* In general, high donor-to-donor variability exists among hASC donor cell

lines. In a lab setting it is simple enough to select lines that generally express a high level of potency towards osteo- and/or adipogenic lineages. In contrast, when considering autologous replacement therapies in a clinical setting, one does not have the luxury of selecting for potency. It is therefore important to evaluate hASC with both high and low differentiation potential for osteogenic, adipogenic and/or other lineages of interest.

Four to five donor cell lines were chosen as contributing cell populations to each superlot. Prior to selecting the specific donor hASC lines, candidate cells were qualitatively

Table 6.1 Age and gender information was supplied for all hASC lines used in this study. Characterization of all 14 donor lines, as described in Figure 1, was used to validate hASC lines. Donor hASC differentiation potential was ranked on a scale from 1 to 5 as represented in Figure 2. Information on patient ethnicity and the surgical procedure from which the hASC were derived from were included in the chart, where available. hASC, human adipose-derived stem cells.

Table 1. Donor Patient Profile and hASC Characterization Following Isolation

Donor ID	*Age (years)*	*Gender*	*Ethnicity*	*Tissue origin and procedure—if reported*	*Initial osteogenic differentiation (scale 1–5)*	*Initial adipogenic differentiation (scale 1–5)*
Premenopausal						
1	36	F	Other	Adipose	1.5	3.5
2	36	F	Caucasian	Adipose	3.5	3
3	24	F	Caucasian	Adipose (liposuction)	1.5	4
4	29	F	Native American	Adipose	2	2.5
5	34	F	Caucasian	Adipose	1.5	3
Perimenopausal						
6	48	F	Caucasian	Adipose (liposuction)	1	1.5
7	50	F	Caucasian	Adipose	2	2
8	55	F	Unreported	Adipose	2	1
9	49	F	Caucasian	Adipose	3	2
Postmenopausal						
10	60	F	Caucasian	Adipose (surgical removal)	3	3
11	60	F	African American	Adipose (panniculectomy)	1	2
12	70	F	Unreported	Adipose (abdominoplasty)	1.5	3.5
13	81	F	Caucasian	Adipose	3.5	2
14	61	F	Caucasian	Adipose (abdominoplasty)	3	1

rated as strong, moderate, or poor differentiators as designated by their characteristic staining

for osteogenic differentiation or adipogenic differentiation with Alizarin Red S or Oil Red O, respectively (Figure 6.2).

Following this qualitative ranking, a combination of strong, moderate and poor

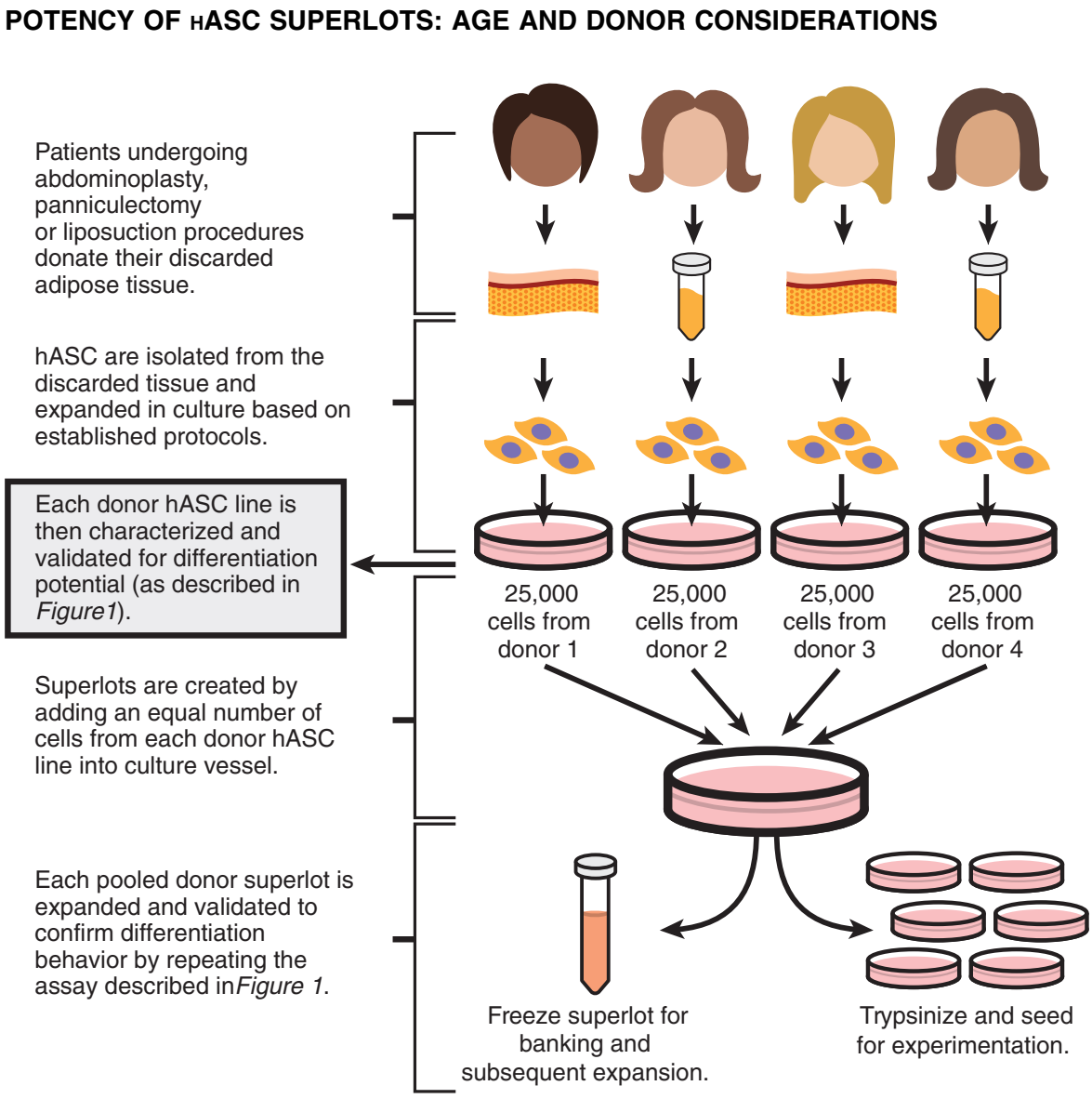

Figure 6.3 Schematic describing isolation procedure of individual hASC donor cell lines, their characterization, and subsequent generation of age-matched superlots.

differentiator hASC lines were selected to compose each age-grouped superlot with the goal of generating a cell population that would represent the average hASC differentiation potential of a particular age group, i.e. pre- peri- and post-menopausal (Table 6.1, Figure 6.3).

To create each superlot, each individual donor cell line was expanded to 80% confluency in complete growth medium (CGM) with medium changes every three to four days. Once each cell line reached 80% confluency, cells were trypsinized, counted and combined in equal proportions into a mixed superlot cell population. For one single 75 cm^2 flask, 1 x 10^5 total hASC were seeded per flask, therefore 2 x 10^4 cells from each hASC donor cell line were added to create a 5-donor cell line superlot for each the pre-, peri-, and post-menopausal superlots (Figure 6.3). For 4-donor superlots, the proportions were adjusted accordingly with 2.5x 10^4 cells per line to total 1 x 10^5 cells in one 75 cm^2 flask.

6.2.5 Validating Superlots

The differentiation potential and proliferative activity of each individual donor and superlot cell line were then evaluated to validate the representative behavior of the pooled-donor superlots. Proliferative activity was evaluated using the alamarBlue® assay (AbD Serotech, UK). Differentiation potential was measured qualitatively using Alizarin Red S to stain calcium deposits indicating osteogenesis, and Oil Red O to stain lipid droplets, indicating adipogenesis, following 14 days of differentiation and fixation in a 10% buffered formalin solution. Differentiation images were captured using a Leica EZ4 D Digital Stereomicroscope (Leica Microsystems Inc., Buffalo Grove, IL). Additionally, colorimetric absorbance assays were used to quantitatively measure osteogenesis and adipogenesis on a

Tecan Microplate Reader (Tecan Group Ltd, Switzerland) using Magellan™ Data Analysis Software (Tecan Group Ltd, Switzerland). To measure osteogenesis, cell lysates were collected in 0.5 N HCl and calcium was extracted via mild agitation, overnight at 4°C. To measure adipogenesis, lipid extraction buffer was used to extract lipid from accumulated lipid vacuoles in adipogenically differentiated hASC. A Calcium LiquiColor ® Assay (StanBio, Boerne, TX) was used to analyze osteogenesis via calcium accretion and a colorimetric adipogenesis assay (BioVision, Milpitas, CA) was used to measure lipid accumulation. The levels of calcium accretion and lipid accumulation of the individual cell lines were compared to those of the superlots to investigate the behavior of the pooled samples relative to hASC from each individual donor.

6.2.6 Measuring DNA and Protein Content

Total DNA and protein content were measured to analyze total cell number and physiological changes in osteogenically differentiated hASC in relation to both age and culture within a superlot. To measure DNA content, osteogenically differentiated hASC were lysed in a papain digest DNA lysis buffer (5mM EDTA, 5mM cysteine HCl, 2.5 units papain/mL in PBS). DNA content was measured under fluorescence on a Tecan Microplate Reader (Tecan Group Ltd, Switzerland) using 0.2 μg/mL Hoechst 33258 dye (Molecular Probes®). To measure protein content, cells were collected in 0.5 N HCl and the protein content of hASC lysates was measured using a colorimetric BCA absorbance assay (Thermo Scientific Pierce).

6.2.7 Statistical Analysis

Statistical analysis was performed using Prism 5 for Mac OS X, Version 5.0a (GraphPad Software, Inc, La Jolla, CA). A one-way ANOVA with a Newman-Keuls multiple comparison post-hoc test was used to analyze statistical difference and to identify statistical significance amongst sample conditions. For each individual donor condition n=3 replicates. Pre- and post-menopausal groups had n = 5 individual donors and peri-menopausal had n=4 individual donors. Statistical significance is indicated as follows: * $p < 0.05$, ** $p < 0.01$ and *** $p < 0.001$.

6.3 Results

To ensure all cell lines were propagating in the pooled superlot cultures, we analyzed the proliferation profiles of individual cell lines in addition to the profiles of the superlots. We analyzed the pre-, peri- and post-menopausal age groups to see if there were any notable differences in the proliferation rates as measured by alamarBlue, indicative of metabolic activity (Figure 6.4). In general, the proliferation profile of the superlots fell roughly within the range of all the individual cells lines for the pre-, peri- and post-menopausal clusters (Figure 6.4). There was no noticeable difference in the proliferation rate between the two age groups, however there were differences amongst specific donor cell lines in pre-, peri and post-menopausal groups, suggesting hASC proliferation is donor-specific as opposed to age-related.

High donor-to-donor variability generally existed in both osteogenic and adipogenic differentiation levels amongst all of the three age groupings (Figures 6.5, 6.6). Osteogenic levels for individual donors ranged from 0.0179 – 11.63calcium/DNA for pre-menopausal cell lines, from 0.548 – 2.489 calcium/DNA for peri-menopausal cell lines and from 0.548 – 16.030 calcium/DNA for post-menopausal cell lines (Figure 6.5). Adipogenic values for individual donor cells lines ranged from 0.8 – 5.0 pmol lipids/µg protein for pre-menopausal cell lines, 0.7 – 2.9 pmol lipids/µg protein for peri-menopausal cell lines and 0.0 – 0.6 pmol lipids/µg protein for post-menopausal cell lines (Figure 6.6). Individual cell lines did not consistently demonstrate multipotency, but rather,

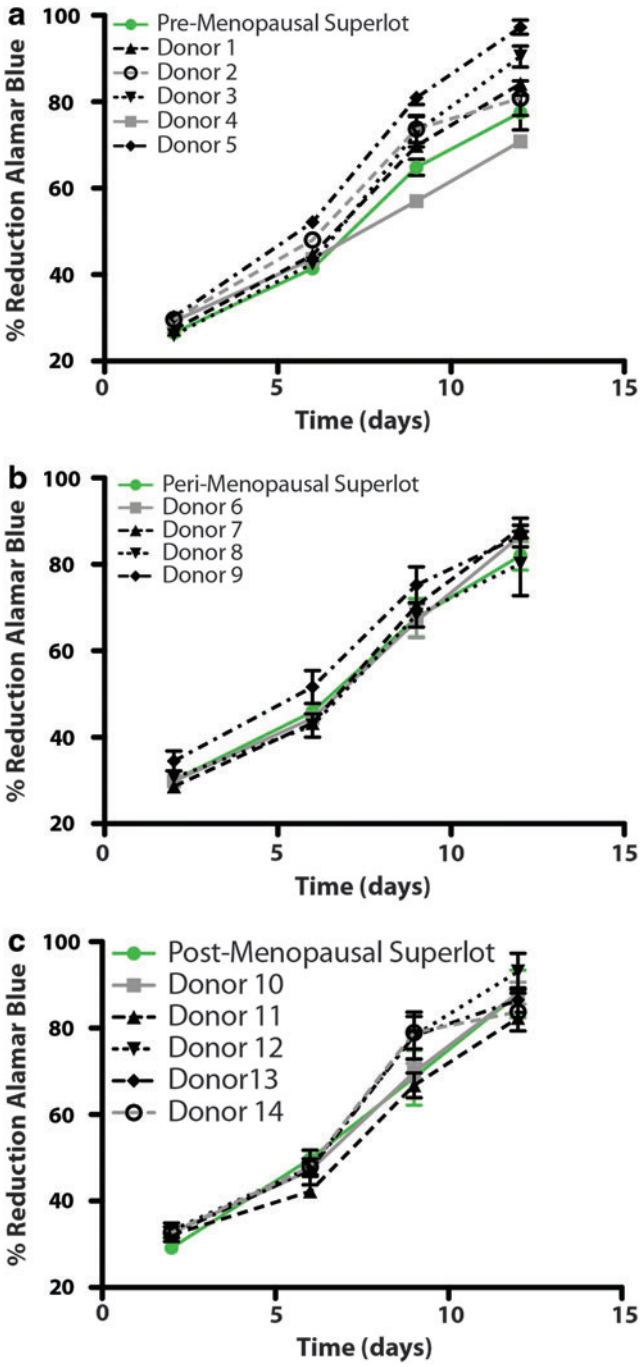

Figure 6.4 Proliferation profiles of pre- (a), peri- (b), and postmenopausal (c) donor and superlot cell lines for up to 12 days in an expansion medium (CGM). The proliferation activity is measured by percent reduction of alamarBlue, indicative of metabolic activity and increased proliferation. n=3 replicates, error bars represent SEM. SEM, standard error of the mean.

particular lines exhibited a proclivity for differentiating towards a particular lineage.

Calcium accretion (Figure 6.5) and lipid accumulation levels (Figure 6.6) of each of the age-grouped superlots fell within the range of differentiation levels of each individual donor cell line contributing to the superlot. This result was generally observed for all age groups in osteogenesis and adipogenesis, roughly validating the principle of pooled donor cell lines exhibiting the average differentiation behavior of the combined donor cells. In general, the superlots roughly approximated the combined average adipogenesis levels of the individual donor lines. This also followed for the osteogenesis of the peri-menopausal superlot, however, the pre- and post-menopausal superlot osteogenic levels were the exception to this trend with the combined donor averages (4.035 calcium/DNA and 6.11 calcium/DNA, respectively)

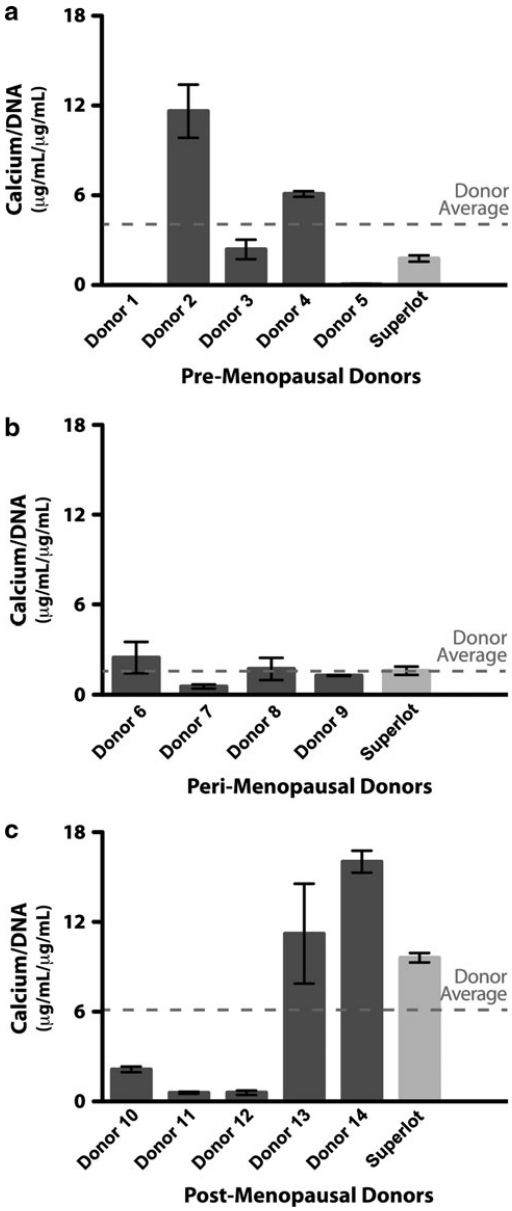

Figure 6.5 Osteogenic differentiation of pre- (a), peri- (b), and postmenopausal (c) donor lines and superlots following 14 days of culture in ODM. Calcium accretion is normalized to DNA content for individual donor lines contributing to each age-matched superlot. Red line indicates the combined average calcium/DNA value of the contributing donor lines, which represents the theoretical reference value for the calcium/DNA superlot value. High donor-to-donor variation is observed across age groups. n = 3 replicates per donor or superlot, error bars represent standard error (SEM).

predicting a value twice the superlot calcium accretion levels of the pre-menopausal superlot and two-thirds that of the post-menopusal superlot (1.7822 calcium/DNA and 9.605 calcium/DNA, respectively) (Figure 6.5a,c).

Though the high level of donor variability was observed across all age groups, some general differentiation trends were observed amongst age groups. Surprisingly, the post-menopausal group exhibited higher osteogenic calcium accretion levels as compared to the pre- ($p < 0.001$) and peri-menopausal superlots ($p<0.001$) (Figure 6.7a,c-e). Conversely, the peri-menopausal group had approximately half the adipogenic lipid accumulation levels of the pre-menopausal superlot ($p<0.01$) and the post-menopausal superlot had nearly half of the peri-

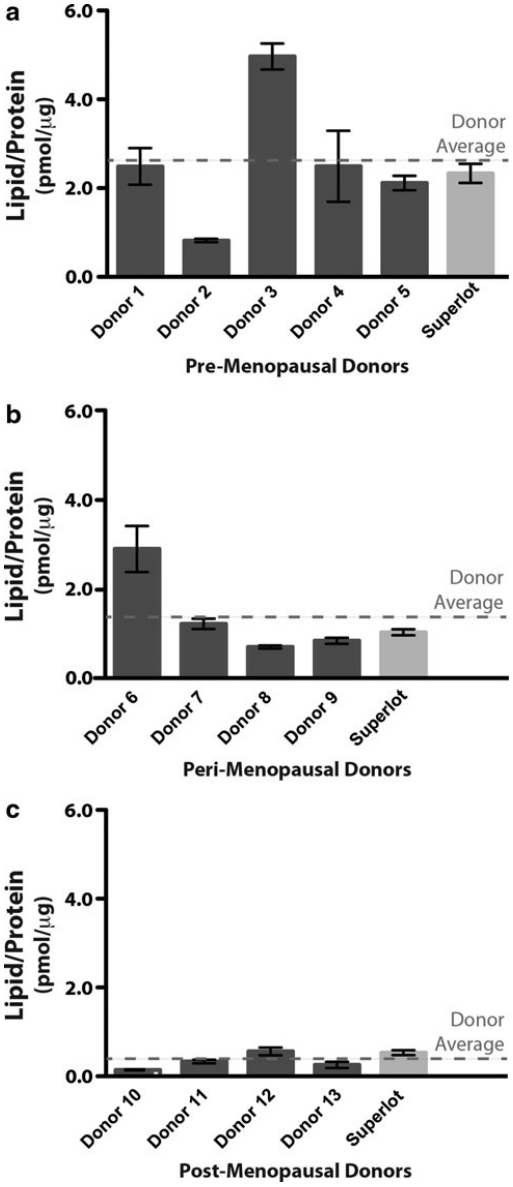

Figure 6.6 Adipogenic differentiation of pre- (a), peri- (b), and postmenopausal (c) donor lines and superlots following 14 days of culture in ADM. Lipid accumulation levels normalized to protein for individual donor lines contributing to each age-matched superlot. Red line indicates the com- bined average lipid/protein value of the contributing donor lines, representing the theoretical value for the lipid/protein superlot value. High donor-to-donor variation is observed within age groups. Generally, donor hASC derived from older patients expressed reduced potential for adipogenic differentiation, particularly, the postmenopausal group. n = 3 replicates per donor or superlot, error bars represent standard error (SEM).

menopausal lipid accumulation levels (Figure 6.7b, f-h).

As hASC undergo osteogenic differentiation, continued proliferation persists as a part

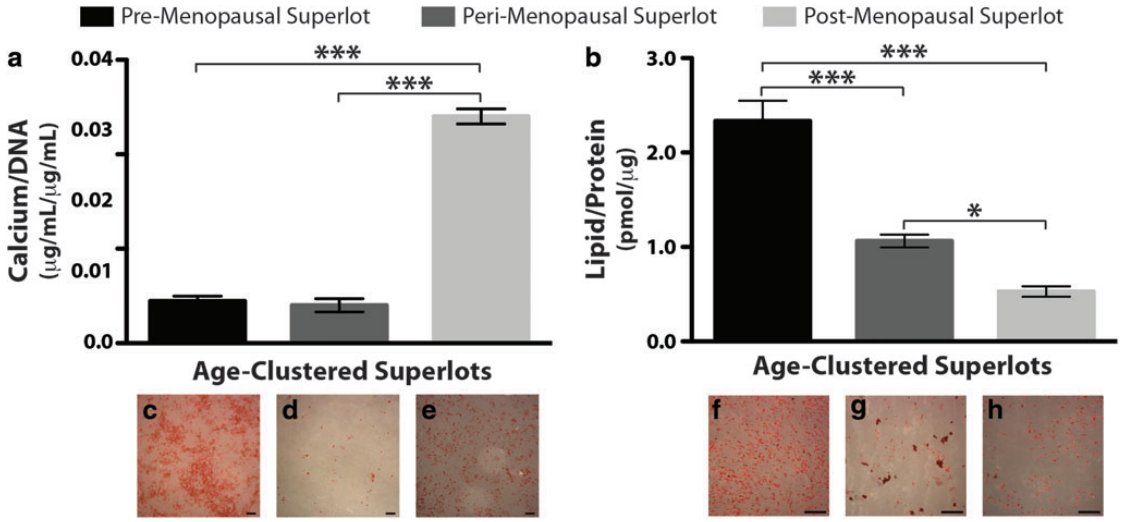

Figure 6.7 Summary of pre-, peri-, and postmenopausal superlot potency. Osteogenic differentiation as measured quantitatively by Calcium Liquicolor Assay (a) and adipogenic differentiation as measured by lipid accumulation assay (b), following 14 days of culture in ODM and ADM, respectively. Alizarin Red S staining to visualize superlot osteogenesis through calcium accretion of pre- (c), peri- (d), and postmenopausal (e) superlots. Oil Red O staining to visualize superlot adipogenesis through lipid droplet staining of pre- (f), peri- (g), and postmenopausal (h) superlots. n=3 replicates per superlot, error bars represent SEM. Scale bar=500μm. *$p<0.05$; ***$p<0.001$.

of the osteogenic phenotype. Further, as osteogenesis proceeds hASC begin to deposit extracellular matrix proteins. To evaluate this, we measured total DNA and protein content following 14 days of osteogenic differentiation. We found total DNA yield decreased with age (Figure 6.8a,c), however total protein yield following osteogenic differentiation increased with age (Figure 6.8b, d). This trend was observed both in the combined donor averages and superlots (Figure 6.8). The consistent trends between superlot and average

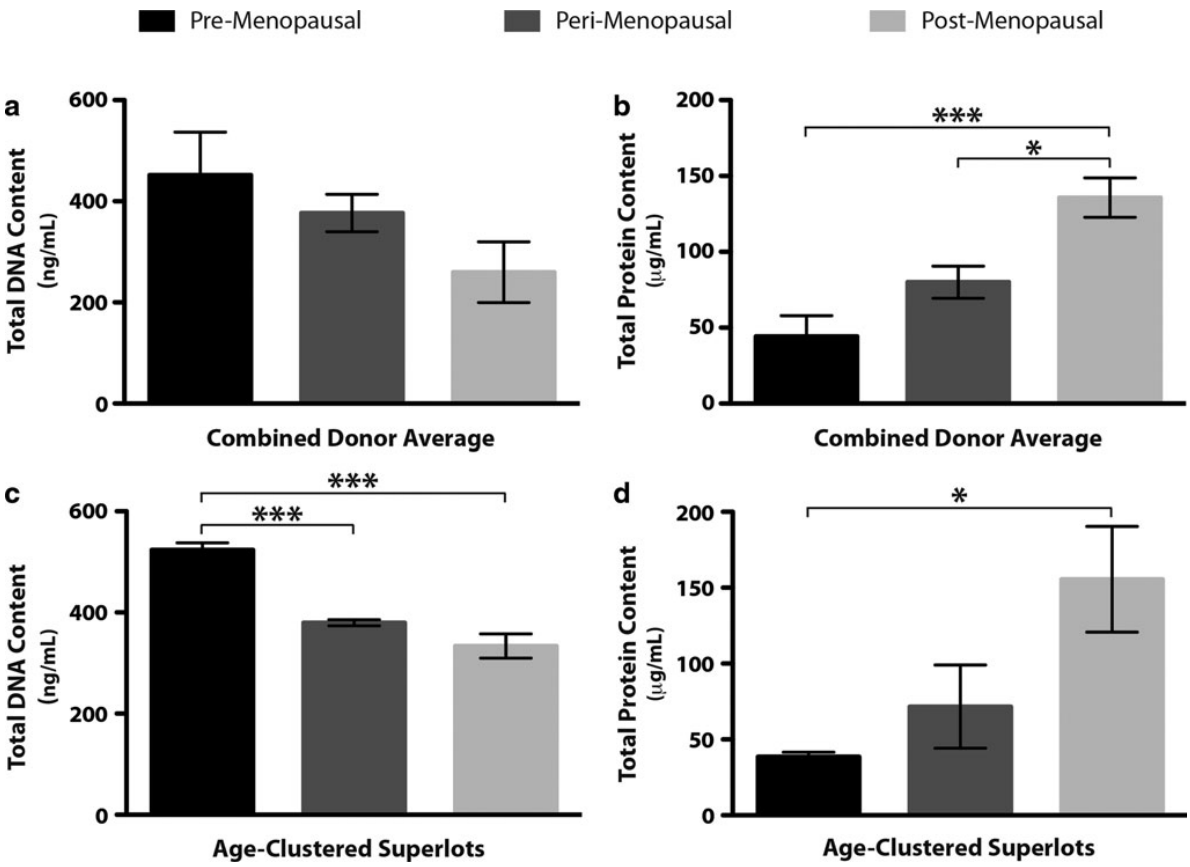

Figure 6.8 Total DNA and protein content levels in age-clustered groups. Following 14 days of osteogenic differentiation, total DNA (a, c) and protein (b, d) content were measured for each individual donor cell line and superlots. Top row graphs represent the average DNA (a) and protein (b) content of individual cell lines (n = 5 donors for pre- and postmenopausal, n = 4 donors for perimenopausal). Bottom row graphs represent DNA (c) and protein (d) content of each superlot (n = 3 replicates for each superlot). Error bars represent SEM.

donor data further validate the use of superlots to represent the average behavior of individual donors. They also provide a useful tool in highlighting age-related differences in the physiology of hASC undergoing osteogenic differentiation (Figure 6.8).

6.4 Discussion

The goal of this paper was to evaluate and present a method to more efficiently execute studies using hASC to facilitate their eventual use in clinical applications. More specifically, we presented an approach to globally understand hASC as a cell type, to more effectively evaluate their potential as an autologous cell source in tissue replacement therapies. A majority of studies reporting data on hASC use pre-selected donor cell lines known to be "good differentiators" and often hASC characterized as "poor differentiators" are excluded from experimental cell sources (*3*, *149*). More recently, some investigators have been utilizing commercially available hASC superlots or have been preparing them in-house; however, there is a dearth of data characterizing the effects of propagating these mixed donor cell populations. Clearly, studying pooled cell populations will significantly increase throughput, but validating their differentiation potential in a mixed donor population is critical to drawing results from more sophisticated hASC superlot studies.

To effectively understand the physiological behavior of hASC for clinical applications, it is necessary to study the range of their differentiation capacities. To address this issue, we have used the approach of generating superlots, containing 4 – 5 age-clustered pooled cell populations. In our superlots, we pre-selected cell lines that were characterized to include low, medium and high level differentiators (Figure 6.2, Table 6.1), to determine whether they would accurately exhibit a differentiation pattern characteristic of the combined average of the individual cell lines. When compared to the osteogenic and adipogenic differentiation levels of each individual donor, the superlot differentiation levels generally approximated the average value of all the individual donors, with the exception of calcium

accretion of the pre- and peri-menopausal superlots (Figures 6.5, 6.6). For the most part, we confirmed our expected result, suggesting that there is likely minimal reactivity between cells from different donors. Moreover, this also suggests that the proportion of each donor cell population remains roughly equal following propagation and differentiation. This is further supported by only nominal differences in the proliferation profiles amongst hASC donors across age groups and the fact that the superlot proliferation profiles fit within the range of donor profiles (Figure 6.4).

The caveat to utilizing the superlots can be observed in the case of the pre- and post-menopausal superlots expressing calcium accretion levels notably below or above the predicted combined average, respectively. The pre-menopausal superlot underperformed, while the post-menopausal over performed in representing the consensus osteogenic differentiation level of the group, with the pre-menopausal expressing approximately half the expected level average calcium accretion (Figure 6.5a) and the post-menopausal superlot expressing an approximately 30% increase compared to the predicted average (Figure 6.5c). We speculate that the large difference between the expected average combined donor value and the superlot value of calcium may be skewed due to specific donor lines accreting little to no calcium over the course of a 14-day differentiation. This particularly comes into play when normalizing to the DNA content, which is proportional to the number of cells in culture. Human ASC growing in culture, expressing minimal calcium have the potential to significantly reduce the calcium/DNA ratio. Moreover, the general cell lineage specification paradigm proposes that proliferation and differentiation are somewhat opposing processes (*150*). Once a cell population begins to undergo differentiation, its proliferation activity is

impeded. However, it may be possible that the proliferative activity remains higher through day 14 for donor hASC that show little to no evidence of osteogenic differentiation, skewing the calcium/DNA data. These results are corroborated by the high level of DNA content in pre-menopausal donors, and a relatively low level of DNA in postmenopausal donors, following 14 days of differentiation (Figure 6.8a,c). Interestingly, this issue did not affect donor lines undergoing adipogenic differentiation, but this may also be due to the lowered metabolic activity of the adipogenic phenotype and the media formulation. We have observed that hASC cultured under ODM tend to persist in a proliferative capacity slightly longer than hASC cultured under ADM. This could also be related to lineage-specific metabolic and physiologic processes resulting in hASC quiescence/senescence under induction of lineage commitment (*138*, *140*). The skewing of the osteogenic superlot data may hint that hASC exhibiting minimal to no evidence of calcium accretion express cell physiologies preventing them from undergoing osteogenesis and/or accreting calcium. Therefore, it is critical that investigators utilizing pooled hASC superlots proceed with caution —acknowledging that the superlot cell populations have a higher level of heterogeneity than that of single donors, which can affect the outcome of studies.

Despite the skewed pre- and post-menopausal data, there is considerable value in employing superlots containing donor lines with differing potencies. The reasoning for selecting this range of potency levels within our cell lines was to begin to glean potency information of a "typical" hASC. Extending this thinking further, using superlots may facilitate prediction of the differentiation potential for an average patient's hASC. Since hASC are so extensively studied for their promise as an autologous cell source for tissue

replacement therapies, it is important to acquire practical data that can be more directly translated into the clinic. That is to say, every patient will not have hASC with a high level of multipotency or hASC that exhibit high proclivity towards the desired cell lineage. Through studying hASC superlot differentiation activity, investigators can begin to profile the average patient, and subsequently hone research approaches to address limitations of the hASC cell source.

In addition to using a superlot approach to characterize the "typical" patient hASC population, we thought it necessary to highlight the extreme differences amongst hASC donor cell differentiation potential. This is not only clinically relevant information, but suggests that as investigators we should evaluate reported data with a critical eye. In the future it may be necessary to develop a classification system to identify predictors of differentiation potential. Though some work has been done profiling hASC using cell-surface markers (*8*, *131*) and microarray surveys of gene expression (*113*, *151*) and micro-RNA profiles (*138*), this data has not been extensively correlated with hASC potency. In addition, it is important to consider the *in vivo* differentiation capacity of hASC. This study describes a method to consider donor specific effects on hASC differentiation, towards the goal of clinically employing them in tissue engineering applications, however we only consider their *in vitro* differentiation capacity. The differentiation behavior of hASC derived from donors of a specific age, and that of superlots will need to be further investigated to elucidate the valid application of this data within the *in vivo* model systems.

According to our data, which displays a high degree of donor-to-donor variability, regardless of age, we suggest that a method for baseline characterization of hASC be

reported along with donor patient data. Stark differences were observed amongst the relative differentiation capacities of pre-, peri- and post-menopausal age groups and the trends were contrary to what was expected, showing the youngest group expressing the highest proclivity for adipogenic differentiation and the oldest group expressing the highest proclivity for osteogenesis (Figure 6.7). These findings are consistent with other human and animal ASC studies exhibiting a decrease in adipogenesis with age (*142*, *143*). Interestingly, our osteogenesis results showing increased calcium accretion in the post-menopausal age group is consistent with work in human mesenchymal stem cells (hMSC) derived from osteoporotic post-menopausal donors (*145*). However, the effect of age on hASC differentiation, particularly osteogenesis, has been largely debated in the literature (*135*, *138*, *140*, *142*).

In addition to variations in hASC potency with age, hASC also exhibit age related changes in total DNA and protein content with age, following 14 days of osteogenic differentiation (Figure 6.8). Generally, pre-menopausal hASC have the highest DNA content following 14 days of osteogenesis, while post-menopausal cells had the highest level of protein. This may in part explain the lowered level of osteogenesis as this may indicate higher proliferation in hASC derived from younger patients, thus slowing the lineage commitment process, while hASC derived from post-menopausal donors slow their proliferation as evidenced by a relatively lowered DNA content (Figure 6.8a,c). This is further corroborated by the fact that hASC derived from post-menopausal donors exhibit relatively higher total protein values than pre- and peri-menopausal cell lines following 14 days of osteogenesis, which may be indicative of increased extracellular matrix production, a hallmark of osteogenesis (Figure 6.8b, d). It is important to note, that when hASC are

cultured under expansion media for up to 12 days, the proliferation profile amongst age groups does not vary drastically (Figure 6.4), suggesting that these changes are specifically related to hASC developing the osteogenic phenotype.

Our data, suggest that there may be age-related changes in hASC potency, which are likely related to physiological changes associated with menopause. It should be noted that with the limitations of our study, and our currently catalogued cell-bank, we only grouped our age-matched superlots based on the average purported age of menopausal phases, and supplied patient information did not include menopausal information. With that general information, we do hypothesize that these hASC potency changes may be related to the physiological changes in the body such as a lowering of bone density and osteoblast/osteoclast activity already known to affect women following menopause (*152*). However, we propose that to generate more informative age-related studies in the future, it would be valuable to acquire female patient information on menopausal phase. Having this information would allow hASC studies to report more definitive results on the differentiation potential of hASC and further the capacity and limitations of their therapeutic applications. Though there is a strong relationship between menopausal phase and bone density and physiology, the age-matched hASC superlot approach proposes a streamlined tactic to predicting the behavior of tissue-engineered constructs of other musculoskeletal tissues such as cartilage, tendon and muscle. In the case of other tissues, it may be useful to cluster the ages of the donors around critical developmental phases for a given tissue and/or even to develop specific donor patient criteria to select for characteristics beneficial to a particular lineage. This study is the first step in building this approach.

It should be noted that this study focuses on *in vitro* behavior of superlots, however it is unclear whether superlots can predict hASC differentiation when used in studies in which hASC are implanted *in vivo.* Exploring the use of superlots supports the goal of utilizing hASC for autologous tissue replacements, although the cells are derived from many patients and there is potential for an immune response. Nonetheless, their potential to streamline hASC studies and increase throughput is clear and thus their *in vivo* characterization may be a critical next step to validating their efficacy.

One final caveat to this study, and a majority of hASC studies in the literature that should be noted, is that hASC are largely sourced from overweight to severely obese patients. The hASC in our cell banks are obtained from discarded tissue derived from abdominoplasty, panniculectomy or liposuction tissue. Though all three procedures are technically cosmetic surgery, we do not have patient body mass index (BMI) or weight data and thus little indication of the patient's health status. It is likely that hASC derived from healthy patients will exhibit a very different differentiation profile from those derived from severely obese patients (*130*, *153*). Other sources of variation may include the specific medical procedure with which the tissue was obtained, however it is likely that patient physiology may have the greatest influence. This may partially explain the high level of donor-to-donor variation across age groups. Understanding the source of the differential hASC potencies is essential to applying hASC in clinical procedures.

In conclusion, we have described a method for generating age-matched pooled donor cell lines to produce hASC superlots containing cells from four to five donors. We have demonstrated that the hASC can proliferate and differentiate in these pooled donor cell

environments and that they exhibit the combined average osteogenic and adipogenic differentiation levels of each donor cell line. Further, we highlight the high degree of donor-to-donor variation in differentiation capability that occurs amongst donor cell lines and suggest superlots may be a way to circumvent this issue when generating experimental data. We do, however, suggest that researchers proceed with caution in determining whether their particular study is best suited for analyses using individual donor hASC cell lines or hASC superlots. Either approach will depend, of course, on the particular scientific question being asked. That being said, we propose that hASC superlots are a powerful tool to study hASC, and may provide an efficient way to increase data throughput to facilitate hASC use in clinical applications.

6.5 Acknowledgements

The authors would like to thank Dr. Liliana Mellor for her technical expertise. They would also like to acknowledge their funding sources: NIH/NIBIB grant R03EB008790 (EGL), NIH/NCRR10KR51023 (EGL), NC TraCS 10KR51023 (EGL), NSF/CBET1133427 (EGL) and the NSF Graduate Research Fellowship Program (JCB).

6.6 Summary

Human adipose-derived stem cells (hASC) are now a prevalent source of adult stem cells for studies in tissue engineering and regenerative medicine. However, researchers utilizing hASC in their investigations often encounter high levels of donor-to-donor variability in hASC differentiation potential. Because of this, conducting studies with this primary cell type can require extensive resources to generate statistically significant data. We

present a method to generate pooled donor cell populations, termed “superlots” containing cell populations derived from 4-5 age-clustered donors. The goal of generating these superlots was: 1) to increase experimental throughput, 2) to utilize assay resources more efficiently, and 3) to begin to establish global hASC differentiation behaviors that may be associated with donor age. With our superlot approach, we have validated that pooled donor cell populations exhibit proliferative activity representing combined behavior of each individual donor cell line. Further, the superlots also exhibit differentiation levels roughly approximating the average combined differentiation levels of each individual donor cell line. Further, we established that high donor-to-donor variability exists between pre-, peri-, and post-menopausal age groupings and that proliferation and differentiation characteristics can vary widely, independent of age. Interestingly, we did observe that cell lines derived from post-menopausal donors demonstrated a relatively high proclivity for osteogenic differentiation and a relatively lowered proclivity for adipogenic differentiation as compared to cells derived from pre- and peri-menopausal donors.

In general, superlots effectively represented the average differentiation behavior of each of their contributing cell populations and could provide a powerful tool for increasing experimental throughput to more efficiently utilize resources when studying hASC differentiation.

CHAPTER 7 Conclusions

7.1 Conclusions

In this dissertation we have reviewed current relevant studies summarizing the state of adipose stem cell research towards musculoskeletal tissue engineering with a particular focus on osteogenesis and bone tissue engineering applications. Further we have summarized current, relevant work in the field of primary cilia biology as it pertains to stem cell differentiation, chemosensing and mechanotransduction. We presented three separate studies elucidating different aspects of hASC differentiation ranging from a fundamental loss of function study, to an observational study to a global study of general hASC behavior. We have established primary cilia as mediators of chemically induced osteogenic differentiation in hASCs as well and specialized mechanosensitive structures in adipogenic and osteogenic hASCs. Additionally, we have aimed to highlight differences in hASC multipotency based on source donor age, but we have also revealed complicated challenges which underscore barriers to using hASCs in clinical applications.

From this body of work it is clear that primary cilia are involved in the fundamental processes of hASC differentiation, and the cilium may be a novel therapeutic target in manipulating hASC differentiation behavior. It is possible that with further research, the cilium structure may be a potential biomarker indicative of cell potency and/or mechanosensitivity. However, their frequency of expression is difficult to predict in different cell populations, which remains a gap in our understanding of this structure.

In validating the proof of principle for using superlots in hASC studies, we inadvertently revealed the often difficult to predict age-related behavior of hASC differentiation. While superlots are a powerful tool in creasing experiment throughput and circumventing the need to interpret data with a high level of variability due to differences in donor cell populations, we have discovered the double-edged sword in this type of experimental approach. While it is valuable to researchers to pre-select multipotent hASC lines to understand fundamental differentiation processes, a large group of hASCs are being left behind and there is a dearth of knowledge regarding their lack of multipotency in culture. In turn, these donors are then in a way are excluded from the very technologies we hope patients will benefit from in the future. It may be important for investigators to take a step back and evaluate hASCs from a broader perspective in order to assess their feasibility of use across patient populations.

7.2 Recommendations of Future Work

Within the scope of this dissertation, the studies presented utilized hASC models under monolayer culture. However it is will known that few cell types grow in monolayer in the body and osteogenic and adipogenic cell types are suspended in a 3-dimensional (3D) extracellular matrix space. Further, though monolayer culture is a direct easy to use experimental model, many studies suggest that cell behavior is drastically different when cultured in a 3D environment and these investigators caution others on the absolute relevance of monolayer culture studies.

When considering efforts towards engineering hASC-derived tissue replacements, it is critical to consider the geometry in which one hopes to fill the void of diseased tissue. In

the context of all three studies presented here, repeating the studies within a 3D culture model would be valuable and relevant research in understanding hASC differentiation behavior within a 3D environment. Moreover, observing cilia expression under 3D culture is a very understudied area of research and may inform researchers on the relevance of 2D cilia work to simulating the *in vivo* chemical and mechanical environment.

Lastly, the industry standard for evaluating hASC multipotency is generally performed in standard tissue culture plates, with the exception of chondrogenic validation which is typically performed in pellet cell culture. Regardless, some critics have brought up the missing link between *in vitro* and *in vivo* hASC differentiation behavior. There is a major void in our knowledge about how *in vitro* multipotency truly correlates with successful maintenance of a particular hASC-derived tissue phenotype *in vivo*, so there is a critical need to develop improved methods to reliable predict the outcome of *in vivo* transplantation of hASCs. The crux of this work will likely rely on the development of standardized 3D culture methods.

As tissue engineers it is paramount that we continue to forge ahead with a multidisciplinary approach to generating engineering tissue replacements with the eventual goal of applying autologous cell-based treatment methods in the clinic. However, while it is necessary to pursue fundamental studies on hASC phenotypic development and methods best manipulate and harness hASC multipotency, it is also necessary to maintain a broader perspective on the common goal of generating personalized medical treatments. As such it is important to consider the spectrum of the patient population we wish to serve, and take this into account when choosing which lines to study for tissue engineering applications and

consider the physiology of those cells which yield negative results in conjunction with the multipotent ones we already study. Acquiring detailed patient data in combination and publishing this information along with our research findings is critical to accelerating the use of hASC technologies within the clinic.

REFERENCES

1. P. A. Zuk *et al.*, Human adipose tissue is a source of multipotent stem cells. *Molecular biology of the cell* **13**, 4279–4295 (2002).

2. P. A. Zuk *et al.*, Multilineage cells from human adipose tissue: implications for cell-based therapies. *Tissue Eng* **7**, 211–228 (2001).

3. J. C. Bodle, A. D. Hanson, E. G. Loboa, Adipose-Derived Stem Cells in Functional Bone Tissue Engineering: Lessons from Bone Mechanobiology. *Tissue Engineering Part B: Reviews* **17**, 195–211 (2011).

4. V. Singla, The Primary Cilium as the Cell's Antenna: Signaling at a Sensory Organelle. *Science* **313**, 629–633 (2006).

5. A. Liu, Mouse intraflagellar transport proteins regulate both the activator and repressor functions of Gli transcription factors. *Development* **132**, 3103–3111 (2005).

6. B. K. Yoder, Role of Primary Cilia in the Pathogenesis of Polycystic Kidney Disease. *Journal of the American Society of Nephrology* **18**, 1381–1388 (2007).

7. S. H. Bernacki, M. E. Wall, E. G. Loboa, *Methods in Cell Biology* (Elsevier, 2008), pp. 257–278.

8. T. Rada, R. L. Reis, M. E. Gomes, Distinct Stem Cells Subpopulations Isolated from Human Adipose Tissue Exhibit Different Chondrogenic and Osteogenic Differentiation Potential. *Stem Cell Rev and Rep* **7**, 64–76 (2010).

9. A. J. Katz, A. Tholpady, S. S. Tholpady, H. Shang, R. C. Ogle, Cell Surface and Transcriptional Characterization of Human Adipose-Derived Adherent Stromal (hADAS) Cells. *STEM CELLS* **23**, 412–423 (2005).

10. L. Aust *et al.*, Yield of human adipose-derived adult stem cells from liposuction aspirates. *Cytotherapy* **6**, 7–14 (2004).

11. J. M. Gimble, F. Guilak, Adipose-derived adult stem cells: isolation, characterization, and differentiation potential. *Cytotherapy* **5**, 362–369 (2003).

12. B. Strem *et al.*, Expression of cardiomyocytic markers on adipose tissue-derived cells in a murine model of acute myocardial injury. *Cytotherapy* **7**, 282–291 (2005).

13. P. DiMuzio, T. Tulenko, Tissue engineering applications to vascular bypass graft

development: The use of adipose-derived stem cells. *Journal of Vascular Surgery* **45**, A99–A103 (2007).

14. R. D. Sumanasinghe, J. A. Osborne, E. G. Loboa, Mesenchymal stem cell-seeded collagen matrices for bone repair: Effects of cyclic tensile strain, cell density, and media conditions on matrix contraction in vitro. *J. Biomed. Mater. Res.* **88A**, 778–786 (2009).

15. A. D. Hanson *et al.*, Osteogenic Effects of Rest Inserted and Continuous Cyclic Tensile Strain on hASC Lines with Disparate Osteodifferentiation Capabilities. *Ann Biomed Eng* **37**, 955–965 (2009).

16. D. M. Raab-Cullen, M. P. Akhter, D. B. Kimmel, R. R. Recker, Bone response to alternate-day mechanical loading of the rat tibia. *J Bone Miner Res* **9**, 203–211 (1994).

17. S. H. Cartmell, B. D. Porter, A. J. Garcia, R. E. Guldberg, Effects of medium perfusion rate on cell-seeded three-dimensional bone constructs in vitro. *Tissue Eng* **9**, 1197–1203 (2003).

18. A. S. Goldstein, T. M. Juarez, C. D. Helmke, M. C. Gustin, A. G. Mikos, Effect of convection on osteoblastic cell growth and function in biodegradable polymer foam scaffolds. *Biomaterials* **22**, 1279–1288 (2001).

19. G. P. Thomas, A. J. el Haj, Bone marrow stromal cells are load responsive in vitro. *Calcif Tissue Int* **58**, 101–108 (1996).

20. T. Yoshikawa, S. A. Peel, J. R. Gladstone, J. E. Davies, Biochemical analysis of the response in rat bone marrow cell cultures to mechanical stimulation. *Biomed Mater Eng* **7**, 369–377 (1997).

21. Mechanobiology of mandibular distraction osteogenesis: experimental analyses with a rat model. **34**, 336–343 (2004).

22. S. R. Buchman *et al.*, Unique rodent model of distraction osteogenesis of the mandible. *Ann Plast Surg* **49**, 511–519 (2002).

23. D. F. J. Ward *et al.*, Mechanical strain enhances extracellular matrix-induced gene focusing and promotes osteogenic differentiation of human mesenchymal stem cells through an extracellular-related kinase-dependent pathway. *Stem Cells Dev* **16**, 467–480 (2007).

24. C. A. Simmons *et al.*, Cyclic strain enhances matrix mineralization by adult human mesenchymal stem cells via the extracellular signal-regulated kinase (ERK1/2) signaling pathway. *Journal of Biomechanics* **36**, 1087–1096 (2003).

25. J. Mauney *et al.*, Mechanical Stimulation Promotes Osteogenic Differentiation of Human Bone Marrow Stromal Cells on 3-D Partially Demineralized Bone Scaffolds In Vitro. *Calcif Tissue Int* **74**, 458–468 (2004).

26. A. IGNATIUS *et al.*, Tissue engineering of bone: effects of mechanical strain on osteoblastic cells in type I collagen matrices. *Biomaterials* **26**, 311–318 (2005).

27. E. M. Kearney, E. Farrell, P. J. Prendergast, V. A. Campbell, Tensile Strain as a Regulator of Mesenchymal Stem Cell Osteogenesis. *Ann Biomed Eng* **38**, 1767–1779 (2010).

28. G. J. Pazour, G. B. Witman, The vertebrate primary cilium is a sensory organelle. *Current Opinion in Cell Biology* **15**, 105–110 (2003).

29. N. Santos, J. F. Reiter, P. Satir, J. F. Fallon, Eds. Building it up and taking it down: The regulation of vertebrate ciliogenesis. *Dev. Dyn.* **237**, 1972–1981 (2008).

30. A. Malone *et al.*, Primary cilia mediate mechanosensing in bone cells by a calcium-independent mechanism. *PNAS* **104**, 13325 (2007).

31. V. Marion *et al.*, Transient ciliogenesis involving Bardet-Biedl syndrome proteins is a fundamental characteristic of adipogenic differentiation. *PNAS* **106**, 1820 (2009).

32. C. A. Clement *et al.*, The primary cilium coordinates early cardiogenesis and hedgehog signaling in cardiomyocyte differentiation. *Journal of Cell Science* **122**, 3070–3082 (2009).

33. W. A. Abou Alaiwi, S. T. Lo, S. M. Nauli, Primary Cilia: Highly Sophisticated Biological Sensors. *Sensors* **9**, 7003–7020 (2009).

34. J. Slough, L. Cooney, M. Brueckner, Monocilia in the embryonic mouse heart suggest a direct role for cilia in cardiac morphogenesis. *Dev. Dyn.* **237**, 2304–2314 (2008).

35. S. C. Goetz, P. J. R. Ocbina, K. V. Anderson, *Chapter 10 - The Primary Cilium as a Hedgehog Signal Transduction Machine* (Elsevier, First edition. 2009), pp. 199–222.

36. P. Satir, L. B. Pedersen, S. T. Christensen, The primary cilium at a glance. *Journal of Cell Science* **123**, 499–503 (2010).

37. J. Zhou, Polycystins and Primary Cilia: Primers for Cell Cycle Progression. *Annu. Rev. Physiol.* **71**, 83–113 (2009).

38. J. R. Forman, S. Qamar, E. Paci, R. N. Sandford, J. Clarke, The Remarkable Mechanical Strength of Polycystin-1 Supports a Direct Role in

Mechanotransduction. *Journal of Molecular Biology* **349**, 861–871 (2005).

39. N. S. Murcia *et al.*, The Oak Ridge Polycystic Kidney (orpk) disease gene is required for left-right axis determination. *Development* **127**, 2347–2355 (2000).

40. J. T. Eggenschwiler, K. V. Anderson, Cilia and Developmental Signaling. *Annu. Rev. Cell Dev. Biol.* **23**, 345–373 (2007).

41. P. Tummala, E. J. Arnsdorf, C. R. Jacobs, The Role of Primary Cilia in Mesenchymal Stem Cell Differentiation: A Pivotal Switch in Guiding Lineage Commitment. *Cel. Mol. Bioeng.* **3**, 207–212 (2010).

42. S. T. Christensen, S. F. Pedersen, P. Satir, I. R. Veland, L. Schneider, *The Primary Cilium Coordinates Signaling Pathways in Cell Cycle Control and Migration During Development and Tissue Repair* (Elsevier Inc., ed. 1, 2008), pp. 261–301.

43. H. A. Praetorius, K. R. Spring, A PHYSIOLOGICAL VIEW OF THE PRIMARY CILIUM. *Annu. Rev. Physiol.* **67**, 515–529 (2005).

44. S. Nonaka *et al.*, Randomization of left–right asymmetry due to loss of nodal cilia generating leftward flow of extraembryonic fluid in mice lacking KIF3B motor protein. *Cell* **95**, 829–837 (1998).

45. P. Satir, The role of axonemal components in ciliary motility. *Comparative Biochemistry and Physiology Part A: Physiology* **94**, 351–357 (1989).

46. C. E. Farnum, N. J. Wilsman, Axonemal positioning and orientation in three-dimensional space for primary cilia: What is known, what is assumed, and what needs clarification. *Dev. Dyn.* **240**, 2405–2431 (2011).

47. S. S. SOROKIN, Centrioles and the formation of rudimentary cilia by fibroblasts and smooth muscle cells. *J Cell Biol* **15**, 363–377 (1962).

48. H. Goto, A. Inoko, M. Inagaki, Cell cycle progression by the repression of primary cilia formation in proliferating cells. *Cell. Mol. Life Sci.* **70**, 3893–3905 (2013).

49. A. M. Nguyen, C. R. Jacobs, Emerging role of primary cilia as mechanosensors in osteocytes. *Bone* **54**, 196–204 (2013).

50. D. A. Hoey, D. J. Kelly, C. R. Jacobs, A role for the primary cilium in paracrine signaling between mechanically stimulated osteocytes and mesenchymal stem cells. *Biochemical and Biophysical Research Communications* **412**, 182–187 (2011).

51. J. B. Kouri, S. A. Jiménez, M. Quintero, A. Chico, Ultrastructural study of chondrocytes from fibrillated and non-fibrillated human osteoarthritic cartilage.

Osteoarthritis and Cartilage **4**, 111–125 (1996).

52. J. Irianto, G. Ramaswamy, R. Serra, M. M. Knight, Depletion of chondrocyte primary cilia reduces the compressive modulus of articular cartilage. *Journal of Biomechanics* **47**, 579–582 (2014).

53. C. L. Thompson, J. P. Chapple, M. M. Knight, Primary cilia disassembly down-regulates mechanosensitive hedgehog signalling: a feedback mechanism controlling ADAMTS-5 expression in chondrocytes. *Osteoarthritis and Cartilage* **22**, 490–498 (2014).

54. H. A. Praetorius, K. R. Spring, Bending the MDCK Cell Primary Cilium Increases Intracellular Calcium. *Journal of Membrane Biology* **184**, 71–79 (2001).

55. H. A. Praetorius, J. Frokiaer, S. Nielsen, K. R. Spring, Bending the Primary Cilium Opens Ca2+-sensitive Intermediate-Conductance K+ Channels in MDCK Cells. *Journal of Membrane Biology* **191**, 193–200 (2003).

56. A. D. Egorova, K. Van der Heiden, R. E. Poelmann, B. P. Hierck, Differentiation. *Differentiation* **83**, S56–S61 (2012).

57. A. D. Egorova *et al.*, Lack of Primary Cilia Primes Shear-Induced Endothelial-to-Mesenchymal Transition. *Circulation Research* **108**, 1093–1101 (2011).

58. M. R. Sarkisian, S. M. Guadiana, Influences of Primary Cilia on Cortical Morphogenesis and Neuronal Subtype Maturation. *The Neuroscientist* (2014), doi:10.1177/1073858414531074.

59. Y.-G. Han *et al.*, Hedgehog signaling and primary cilia are required for the formation of adult neural stem cells. *Nature neuroscience* **11**, 277–284 (2008).

60. A. W. Ettinger *et al.*, Proliferating versus differentiating stem and cancer cells exhibit distinct midbody-release behaviour. *Nature Communications* **2**, 503–12 (1AD).

61. W.-H. Lien, E. Fuchs, Wnt some lose some: transcriptional governance of stem cells by Wnt/β-catenin signaling. *Genes & Development* **28**, 1517–1532 (2014).

62. J. C. McIntyre, C. L. Williams, J. R. Martens, Smelling the roses and seeing thelight: gene therapy for ciliopathies. *Trends in Biotechnology* **31**, 355–363 (2013).

63. S. Kim, B. D. Dynlacht, Assembling a primary cilium. *Current Opinion in Cell Biology* **25**, 506–511 (2013).

64. P. S. Mathieu, E. G. Loboa, Cytoskeletal and Focal Adhesion Influences on

Mesenchymal Stem Cell Shape, Mechanical Properties, and Differentiation Down Osteogenic, Adipogenic, and Chondrogenic Pathways. *Tissue Engineering Part B: Reviews* **18**, 436–444 (2012).

65. M. Knippenberg *et al.*, Adipose tissue-derived mesenchymal stem cells acquire bone cell-like responsiveness to fluid shear stress on osteogenic stimulation. *Tissue Eng* **11**, 1780–1788 (2005).

66. A. J. Engler, S. Sen, H. L. Sweeney, D. E. Discher, Matrix Elasticity Directs Stem Cell Lineage Specification. *Cell* **126**, 677–689 (2006).

67. A. W. Holle *et al.*, In situ mechanotransduction via vinculin regulates stem cell differentiation. *STEM CELLS* **31**, 2467–2477 (2013).

68. S. M. Nauli *et al.*, Polycystins 1 and 2 mediate mechanosensation in the primary cilium of kidney cells. **33**, 129–137 (2003).

69. A. K. T. Wann, M. M. Knight, Primary cilia elongation in response to interleukin-1 mediates the inflammatory response. *Cell. Mol. Life Sci.* **69**, 2967–2977 (2012).

70. K. Gardner, S. P. Arnoczky, M. Lavagnino, Effect of in vitro stress-deprivation and cyclic loading on the length of tendon cell cilia in situ. *J. Orthop. Res.* **29**, 582–587 (2010).

71. J. C. Bodle *et al.*, A. Asakura, Ed. Primary Cilia: The Chemical Antenna Regulating Human Adipose-Derived Stem Cell Osteogenesis. *PLoS ONE* **8**, e62554 (2013).

72. H. Hu, Sequential roles of Hedgehog and Wnt signaling in osteoblast development. *Development* **132**, 49–60 (2004).

73. M. Plaisant *et al.*, Activation of Hedgehog Signaling Inhibits Osteoblast Differentiation of Human Mesenchymal Stem Cells. *STEM CELLS* **27**, 703–713 (2009).

74. C. A. Clement *et al.*, TGF-β Signaling Is Associated with Endocytosis at the Pocket Region of the Primary Cilium. *CellReports* **3**, 1806–1814 (2013).

75. Z. Xiao *et al.*, Cilia-like Structures and Polycystin-1 in Osteoblasts/Osteocytes and Associated Abnormalities in Skeletogenesis and Runx2 Expression. *Journal of Biological Chemistry* **281**, 30884–30895 (2006).

76. J. Zhang, R. Lipinski, J. Gipp, A. Shaw, W. Bushman, Hedgehog pathway responsiveness correlates with the presence of primary cilia on prostate stromal cells. *BMC developmental biology* **9**, 50 (2009).

77. B. Song, C. J. Haycraft, H.-S. Seo, B. K. Yoder, R. Serra, Development of the post-natal growth plate requires intraflagellar transport proteins. *Developmental Biology* **305**, 202–216 (2007).

78. E. Koyama *et al.*, Conditional Kif3a ablation causes abnormal hedgehog signaling topography, growth plate dysfunction, and excessive bone and cartilage formation during mouse skeletogenesis. *Development* **134**, 2159–2169 (2007).

79. S. R. McGlashan, C. J. Haycraft, C. G. Jensen, B. K. Yoder, C. A. Poole, Articular cartilage and growth plate defects are associated with chondrocyte cytoskeletal abnormalities in Tg737orpk mice lacking the primary cilia protein polaris. *Matrix Biology* **26**, 234–246 (2007).

80. J. M. Lehman *et al.*, P. Satir, J. F. Fallon, Eds. The Oak Ridge Polycystic Kidney mouse: Modeling ciliopathies of mice and men. *Dev. Dyn.* **237**, 1960–1971 (2008).

81. C. J. Haycraft *et al.*, Intraflagellar transport is essential for endochondral bone formation. *Development* **134**, 307–316 (2007).

82. S. R. McGlashan, E. C. Cluett, C. G. Jensen, C. A. Poole, P. Satir, J. F. Fallon, Eds. Primary cilia in osteoarthritic chondrocytes: From chondrons to clusters. *Dev. Dyn.* **237**, 2013–2020 (2008).

83. C. POOLE *et al.*, **Confocal analysis of primary cilia structure and colocalization with the Golgi apparatus in chondrocytes and aortic smooth muscle cells.** *Cell Biology International* **21**, 483–494 (1997).

84. C. A. Poole, Z. J. ZHANG, J. M. Ross, The differential distribution of acetylated and detyrosinated alpha‐tubulin in the microtubular cytoskeleton and primary cilia of hyaline cartilage chondrocytes. *J Anat* **199**, 393–405 (2001).

85. C. G. Jensen *et al.*, Ultrastructural, tomographic and confocal imaging of the chondrocyte primary cilium in situ. *Cell Biology International* **28**, 101–110 (2004).

86. E. N. Kiprilov *et al.*, Human embryonic stem cells in culture possess primary cilia with hedgehog signaling machinery. *J Cell Biol* **180**, 897–904 (2008).

87. L. Schneider *et al.*, PDGFRαα Signaling Is Regulated through the Primary Cilium in Fibroblasts. *Current Biology* **15**, 1861–1866 (2005).

88. I. R. Veland *et al.*, M. Katoh, Ed. Inversin/Nephrocystin-2 Is Required for Fibroblast Polarity and Directional Cell Migration. *PLoS ONE* **8**, e60193 (2013).

89. D. R. Rich, A. L. Clark, Chondrocyte primary cilia shorten in response to osmotic challenge and are sites for endocytosis. *Osteoarthritis and Cartilage* **20**, 923–930

(2012).

90. R. M. Delaine-Smith, A. Sittichokechaiwut, G. C. Reilly, Primary cilia respond to fluid shear stress and mediate flow-induced calcium deposition in osteoblasts. *The FASEB Journal* **28**, 430–439 (2014).

91. H. Wang *et al.*, S. Agarwal, Ed. Polycystin-1 Mediates Mechanical Strain-Induced Osteoblastic Mechanoresponses via Potentiation of Intracellular Calcium and Akt/β-Catenin Pathway. *PLoS ONE* **9**, e91730 (2014).

92. Y. Huan, J. Van Adelsberg, Polycystin-1, the PKD1 gene product, is in a complex containing E-cadherin and the catenins. **104**, 1459–1468 (1999).

93. L. Geng *et al.*, Identification and localization of polycystin, the PKD1 gene product. **98**, 2674 (1996).

94. G. Pazour, Chlamydomonas IFT88 and Its Mouse Homologue, Polycystic Kidney Disease Gene Tg737, Are Required for Assembly of Cilia and Flagella. *The Journal of Cell Biology* **151**, 709–718 (2000).

95. A. M. Malone *et al.*, Primary cilia mediate mechanosensing in bone cells by a calcium-independent mechanism. *Proceedings of the National Academy of Sciences* **104**, 13325–13330 (2007).

96. S. McCullen *et al.*, *Application of low frequency AC electric fields via interdigitated electrodes: effects on cellular viability, cytoplasmic calcium, and osteogenic differentiation of human adipose-derived stem cells* (2010).

97. M. Knippenberg *et al.*, Adipose tissue-derived mesenchymal stem cells acquire bone cell-like responsiveness to fluid shear stress on osteogenic stimulation. *Tissue Eng* **11**, 1780–1788 (2005).

98. R. A. Meyer, M. H. Meyer, L. S. Phieffer, D. M. Banks, Delayed union of femoral fractures in older rats: decreased gene expression. *BMC musculoskeletal disorders* **2**, 2 (2001).

99. G. Rawadi, B. Vayssière, F. Dunn, R. Baron, S. Roman Roman, BMP‐2 controls alkaline phosphatase expression and osteoblast mineralization by a Wnt autocrine loop. *Journal of Bone and Mineral Research* **18**, 1842–1853 (2003).

100. A. Robert *et al.*, The intraflagellar transport component IFT88/polaris is a centrosomal protein regulating G1-S transition in non-ciliated cells. *Journal of Cell Science* **120**, 918–918 (2007).

101. M. Kottgen *et al.*, TRPP2 and TRPV4 form a polymodal sensory channel complex.

The Journal of Cell Biology **182**, 437–447 (2008).

102. Z. S. Xiao, L. D. Quarles, Role of the polycytin-primary cilia complex in bone development and mechanosensing. *Annals of the New York Academy of Sciences* **1192**, 410–421 (2010).

103. M. H. Raymond, B. C. Schutte, J. C. Torner, T. L. Burns, M. C. Willing, Osteocalcin: genetic and physical mapping of the human gene BGLAP and its potential role in postmenopausal osteoporosis. *Genomics* **60**, 210–217 (1999).

104. W. Tsuji, Adipose-derived stem cells: Implications in tissue regeneration. *WJSC* **6**, 312 (2014).

105. J. M. Dugan, S. H. Cartmell, J. E. Gough, Uniaxial cyclic strain of human adipose-derived mesenchymal stem cells and C2C12 myoblasts in coculture. *Journal of Tissue Engineering* **5** (2014), doi:10.1177/2041731414530138.

106. J. Puetzer, J. Williams, A. Gillies, S. Bernacki, E. G. Loboa, The Effects of Cyclic Hydrostatic Pressure on Chondrogenesis and Viability of Human Adipose- and Bone Marrow-Derived Mesenchymal Stem Cells in Three-Dimensional Agarose Constructs. *Tissue Engineering Part A* **19**, 299–306 (2013).

107. R. Ogawa, D. P. Orgill, G. F. Murphy, S. Mizuno, Hydrostatic Pressure–Driven Three-Dimensional Cartilage Induction using Human Adipose-Derived Stem Cells and Collagen Gels. *Tissue Engineering Part A*, 1–28 (2014).

108. A. Hanson, M. Wall, B. Pourdeyhimi, E. Loboa, Effects of oxygen plasma treatment on adipose-derived human mesenchymal stem cell adherence to poly (L-lactic acid) scaffolds. *Journal of Biomaterials Science, Polymer Edition* **18**, 1387–1400 (2007).

109. C. Ciobanasu, B. Faivre, C. Le Clainche, Integrating actin dynamics, mechanotransduction and integrin activation: The multiple functions of actin binding proteins in focal adhesions. *European Journal of Cell Biology* **92**, 339–348 (2013).

110. M. D. Treiser *et al.*, Cytoskeleton-based forecasting of stem cell lineage fates. *Proceedings of the National Academy of Sciences* **107**, 610–615 (2010).

111. K. A. Kilian, B. Bugarija, B. T. Lahn, M. Mrksich, Geometric cues for directing the differentiation of mesenchymal stem cells. *Proceedings of the National Academy of Sciences* **107**, 4872–4877 (2010).

112. R. D. Sumanasinghe, S. H. Bernacki, E. G. Loboa, Osteogenic differentiation of human mesenchymal stem cells in collagen matrices: effect of uniaxial cyclic tensile strain on bone morphogenetic protein (BMP-2) mRNA expression. *Tissue Eng* **12**, 3459–3465 (2006).

113. A. Charoenpanich *et al.*, Microarray Analysis of Human Adipose-Derived Stem Cells in Three-Dimensional Collagen Culture: Osteogenesis Inhibits Bone Morphogenic Protein and Wnt Signaling Pathways, and Cyclic Tensile Strain Causes Upregulation of Proinflammatory Cytokine Regulators and Angiogenic Factors. *Tissue Engineering Part A* **17**, 2615–2627 (2011).

114. A. W. James, Review of Signaling Pathways Governing MSC Osteogenic and Adipogenic Differentiation. *Scientifica* **2013**, 1–17 (2013).

115. C. T. Rubin *et al.*, Adipogenesis is inhibited by brief, daily exposure to high-frequency, extremely low-magnitude mechanical signals. *PNAS* **104**, 17879–17884 (2007).

116. B. Sen *et al.*, Mechanical Loading Regulates NFATc1 and -Catenin Signaling through a GSK3 Control Node. *Journal of Biological Chemistry* **284**, 34607–34617 (2009).

117. M. G. Hossain *et al.*, Compressive force inhibits adipogenesis through COX-2-mediated down-regulation of PPARγ2 and C/EBPα. *JBIOSC* **109**, 297–303 (2010).

118. A. M. Greiner, H. Chen, J. P. Spatz, R. Kemkemer, P. Aspenstrom, Ed. Cyclic Tensile Strain Controls Cell Shape and Directs Actin Stress Fiber Formation and Focal Adhesion Alignment in Spreading Cells. *PLoS ONE* **8**, e77328 (2013).

119. R. Kaunas, Hsu, Deguchi, Sarcomeric model of stretch-induced stress fiber reorganization. *CHC*, 13 (2010).

120. B. B. Nathwani, C. H. Miller, T. Yang, Morphological Differences of Primary Cilia Between Human Induced Pluripotent Stem Cells and Their Parental Somatic Cells. *Stem cells and ...* (2013), doi:10.1089/scd.2013.0162.

121. M. Lavagnino, S. P. Arnoczky, K. Gardner, In situ deflection of tendon cell-cilia in response to tensile loading: an in vitro study. *J. Orthop. Res.* **29**, 925–930 (2011).

122. J. Swift *et al.*, Nuclear lamin-A scales with tissue stiffness and enhances matrix-directed differentiation. *Science* **341**, 1240104–1240104 (2013).

123. K. N. Dahl, A. Kalinowski, Nucleoskeleton mechanics at a glance. *Journal of Cell Science* **124**, 675–678 (2011).

124. X. Qu *et al.*, Biomaterials. *Biomaterials* **34**, 9812–9818 (2013).

125. A. Pitaval, Q. Tseng, M. Bornens, M. Thery, Cell shape and contractility regulate ciliogenesis in cell cycle-arrested cells. *The Journal of Cell Biology* **191**, 303–312 (2010).

126. R. J. McMurray, A. Wann, C. L. Thompson, J. T. Connelly, Surface topography regulates wnt signaling through control of primary cilia structure in mesenchymal stem cells. *Scientific reports* (2013), doi:10.1038/srep03545.

127. A. Levy, S. Enzer, N. Shoham, U. Zaretsky, A. Gefen, Large, but not Small Sustained Tensile Strains Stimulate Adipogenesis in Culture. *Ann Biomed Eng* **40**, 1052–1060 (2011).

128. S. Perrini *et al.*, A. Vergani, Ed. Differences in Gene Expression and Cytokine Release Profiles Highlight the Heterogeneity of Distinct Subsets of Adipose Tissue-Derived Stem Cells in the Subcutaneous and Visceral Adipose Tissue in Humans. *PLoS ONE* **8**, e57892 (2013).

129. J. C. Bodle *et al.*, Age-Related Effects on the Potency of Human Adipose-Derived Stem Cells: Creation and Evaluation of Superlots and Implications for Musculoskeletal Tissue Engineering Applications. *Tissue Engineering Part C: Methods*, 140501115341005 (2014).

130. M. Roldan, M. Macias-Gonzalez, R. Garcia, F. J. Tinahones, M. Martin, Obesity short-circuits stemness gene network in human adipose multipotent stem cells. *The FASEB Journal* **25**, 4111–4126 (2011).

131. P. C. Baer *et al.*, Comprehensive Phenotypic Characterization of Human Adipose-Derived Stromal/Stem Cells and Their Subsets by a High Throughput Technology. *Stem Cells and Development* **22**, 330–339 (2013).

132. F. Guilak, H. Awad, B. Fermor, H. Leddy, J. Gimble, Adipose-derived adult stem cells for cartilage tissue engineering. *Biorheology* **41**, 389 (2004).

133. A. Noer, A. L. Sørensen, A. C. Boquest, P. Collas, Stable CpG hypomethylation of adipogenic promoters in freshly isolated, cultured, and differentiated mesenchymal stem cells from adipose tissue. *Molecular biology of the cell* **17**, 3543–3556 (2006).

134. S. Güven *et al.*, Validation of an Automated Procedure to Isolate Human Adipose Tissue–Derived Cells by Using the Sepax ®Technology. *Tissue Engineering Part C: Methods* **18**, 575–582 (2012).

135. W. Wu, L. Niklason, D. M. Steinbacher, The Effect of Age on Human Adipose-Derived Stem Cells. *Plastic and Reconstructive Surgery* **131**, 27–37 (2013).

136. P. P. Carvalho *et al.*, Undifferentiated human adipose-derived stromal/stem cells loaded onto wet-spun starch-polycaprolactone scaffolds enhance bone regeneration: Nude mice calvarial defect in vivostudy. *J. Biomed. Mater. Res.*, n/a–n/a (2013).

137. N.-C. Cheng, B. T. Estes, T.-H. Young, F. Guilak, Genipin-Crosslinked Cartilage-

Derived Matrix as a Scaffold for Human Adipose-Derived Stem Cell Chondrogenesis. *Tissue Engineering Part A* **19**, 484–496 (2013).

138. E. U. Alt *et al.*, Aging alters tissue resident mesenchymal stem cell properties. *Stem Cell Research* **8**, 215–225 (2012).

139. B. Levi, M. T. Longaker, Concise Review: Adipose-Derived Stromal Cells for Skeletal Regenerative Medicine. *STEM CELLS* **29**, 576–582 (2011).

140. A. Sepe, T. Tchkonia, T. Thomou, M. Zamboni, J. L. Kirkland, Aging and Regional Differences in Fat Cell Progenitors – A Mini-Review. *Gerontology* **57**, 66–75 (2011).

141. H. Mizuno, M. Tobita, A. C. Uysal, Concise Review: Adipose‐Derived Stem Cells as a Novel Tool for Future Regenerative Medicine. *STEM CELLS* **30**, 804–810 (2012).

142. D.-C. Ding, H.-L. Chou, W.-T. Hung, H.-W. Liu, T.-Y. Chu, Human adipose-derived stem cells cultured in keratinocyte serum free medium: Donor's age does not affect the proliferation and differentiation capacities. *Journal of Biomedical Science* **20**, 1–1 (2013).

143. S.-C. Huang *et al.*, Mechanical strain modulates age-related changes in the proliferation and differentiation of mouse adipose-derived stromal cells. *BMC Cell Biol* **11**, 18 (2010).

144. L. Labusca, F. Zugun-Eloae, G. Shaw, Isolation and Phenotypic Characterisation of Stem Cells from Late Stage Osteoarthritic Mesenchymal Tissues. *Current Stem Cell ...* (2012).

145. A. Charoenpanich *et al.*, Cyclic Tensile Strain Enhances Osteogenesis and Angiogenesis in Mesenchymal Stem Cells from Osteoporotic Donors. *Tissue Engineering Part A*, 130919062927003 (2013).

146. S. Kikuta *et al.*, Osteogenic Effects of Dedifferentiated Fat Cell Transplantation in Rabbit Models of Bone Defect and Ovariectomy-Induced Osteoporosis. *Tissue Engineering Part A*, 130515073255002 (2013).

147. A. M. Cheung, R. Chaudhry, M. Kapral, C. Jackevicius, G. Robinson, Perimenopausal and Postmenopausal Health. *BMC Women's Health* **4**, S23 (2004).

148. B. L. Riggs, S. Khosla, L. J. Melton, Sex steroids and the construction and conservation of the adult skeleton. *Endocrine reviews* **23**, 279–302 (2002).

149. H. Park *et al.*, Three-dimensional hydrogel model using adipose-derived stem cells

for vocal fold augmentation. *Tissue Engineering Part A* **16**, 535–543 (2009).

150. L. Zhu, A. I. Skoultchi, Coordinating cell proliferation and differentiation. *Current Opinion in Genetics & Development* **11**, 91–97 (2001).

151. R. Torensma *et al.*, The Impact of Cell Source, Culture Methodology, Culture Location, and Individual Donors on Gene Expression Profiles of Bone Marrow-Derived and Adipose-Derived Stromal Cells. *Stem Cells and Development* **22**, 1086–1096 (2013).

152. R. Sapir-Koren, G. Livshits, Is interaction between age-dependent decline in mechanical stimulation and osteocyte–estrogen receptor levels the culprit for postmenopausal-impaired bone formation? *Osteoporos Int* **24**, 1771–1789 (2012).

153. L. De Girolamo *et al.*, Stemness and osteogenic and adipogenic potential are differently impaired in subcutaneous and visceral adipose derived stem cells (ASCs) isolated from obese donors. *Int J Immunopathol Pharmacol* **26**, 11–21 (2013).

Appendix

Appendix A

Other Relevant Publications

Mathieu P S, Bodle J C, Loboa E G. *Primary cilium mechanotransduction of tensile strain in 3D culture: Finite element analyses of strain amplification caused by 10% tensile strain applied to a primary cilium embedded in a collagen matrix.* J Biomech. 2014 Jun 27;47(9):2211-7.

Relevant Presentations

Bodle, J C and Loboa, E G. *A Bottom-Up Approach to Tissue Engineering: siRNA Knockdown Techniques, Primary Cilia and Adipose Stem Cells.* Silpakorn University, Nakhon Pathom, Thailand, January 2014. Guest lecture for seminar course "Selected Topics in Genetics". (Guest Lecturer)

Bodle, J C; Williams, R B; Atchison, L J; Bernacki, S H; and Loboa, E G *Does Primary Cilia Structure Morphology Indicate Adipose Stem Cell Lineage Commitment?* North Carolina Tissue Engineering and Regenerative Medicine Annual Meeting Conference and Innovation Summit, Winston-Salem, NC, October 2013 (Poster)

Bodle, J C; Williams. R B; Veland, I R; Christensen, S T; Loboa, E G. *Primary Cilia on the Differentiating Adipose Derived Stem Cell: Investigating Regenerative Mechanisms on the Cell Level*. Biomedical Engineering Society Annual Meeting, Seattle, WA, September 2013 (Poster)

Bodle, J C; Williams, R B; Rubenstein, C D; and Loboa, E G. *Adipose Stem Cell Primary Cilia Exhibit Conformational Changes in Response to Chemical and Mechanical Stimulation.* Nordic Cilia and Centrosome Network Annual Meeting, Sigtuna, Sweden, January 2013 (Podium)

Bodle, J C; Williams, R B; Matthieu, P S; Rubenstein, C D; Charoenpanich, A; Bernacki, S H; and Loboa, E G. *Primary Cilia on Adipose-Derived Stem Cells in 3D culture: What is the Structure/Function Relationship?* Biomedical Engineering Society Annual Meeting, Atlanta, GA, October 2012 (Podium)

Bodle, J C; Williams, R B; Rubenstein, C D; Charoenpanich, A; Bernacki, S H; and Loboa, E G. *Primary Cilia: Does Cilium Architecture Predict Lineage Specification in Adipose-Derived Stem Cells?* TERMIS-World Congress, 2012, Vienna, Austria, September 2012 (Podium)

Bodle, J C; Phillips, M E; Rubenstein, C D; Qi, J; Banes, A J; Bernacki, S H; and Loboa, E G. *Primary Cilia: Dynamic Chemosensors Controlling Adipose Stem Cell Osteogenesis.* Orthopedic Research Society Annual Meeting, San Francisco, CA, February 2012 (Poster)

Bodle, J C; Rubenstein, C D; Phillips, M E; Charoenpanich, A; Bernacki, S H; and Loboa, E G. *Primary Cilia Exhibit 2D and 3D Sensitivity to Substrate Environment: Implications for Adipose Stem Cells in Musculoskeletal Tissue Engineering*. Orthopedic Research Society Annual Meeting, San Francisco, CA, February 2012 (Poster)

Bodle, J C; Williams J M; Phillips, M E; SooHoo, J R; Sakhare, A R; Bernacki, S H; Loboa, E G. *Novel Tensile Strain Bioreactor for Analysis of Primary Cilia-Extracellular Matrix Interactions in Adipose-Derived Stem Cells.* TERMIS-NA 2011 Annual Conference, Houston, TX, December 2011 (Poster)

Bodle, J C; Phillips, M E; Rubenstein, C D; Charoenpanich, A; Bernacki, S H; and Loboa, E G. *Primary Cilia Modulate Induction of Osteogenic Differentiation in Adipose-derived Stem Cells.* Biomedical Engineering Society Annual Meeting, Hartford, CT, October 2011 (Podium)

Bodle, J C; Sakhare, A R; Qi, J; Bernacki, S H; Banes, A J; Loboa, E G *The Primary Cilium: A Receptor Mediator of Osteogenesis in Human Adipose Derived Stem Cells?* TERMIS-NA 2010 Annual Conference, Orlando, FL, December 2010 (Poster)

Bodle J C; Rubenstein C D; Phillips M E; Bernacki S H; Loboa E G *Primary Cilia Critically Modulate Human Adipose Derived Stem Cell (hASC) Proliferation and Differentiation Signaling.* NCTERM Conference and Innovation Summit, Durham, NC November 2010. (Poster, Competition Finalist)

Bodle, J C; Sakhare, A R; Qi, J; Bernacki, S H; Banes, A J; Loboa, E G. *The Primary Cilium: A Potential Receptor Antenna in Human Adipose Stem Cells?* Biomedical Engineering Society Annual Meeting, Austin, TX, October 2010 (Podium)

Bodle J C; Sakhare A R; Vidt M E; SooHoo J R, Haslauer C M; McCulloch R C; Loboa E G. *Novel Tensile Strain Bioreactor for Culture of Three-Dimensional Tissue-Engineered Constructs.* Orthopedic Research Society Annual Meeting, New Orleans, LA, March 2010 (Poster)

Bodle J C; Sakhare A R; Qi J; Bernacki S H; Banes A J; Loboa E G *Primary Cilia: Potential Mechanotransducers in Human Adipose Derived Stem Cells?* NCTERM Conference and Innovation Summit, Winston-Salem, NC November 2009. (Poster)

Bodle, J C; Vidt M E; SooHoo J R, Haslauer C M; McCulloch R C, Loboa E G.

Tensile Strain Bioreactor with Force Feedback and Custom Incubator for Straining Cells in Three-Dimensional Culture. North Carolina Tissue
Engineering and Regenerative Medicine Conference and Innovation Summit, Durham, NC, October 2008. (Poster)

C-F Li, J.C. Bodle*, J.P. Hatton, M. Hughes-Fulford. *Activation and Regulation of Signal Transduction in Monocytes and their Correlation with Gravity.* Western Student Medical Research Forum, Carmel, CA, February 2007. (*Presenting Author, Podium)

Bodle JC, Tuin S, Charoenpanich A, McCullen S, Marvel S, Loboa EG (Mar 2014). *Functional tissue engineering: mechanobiology of adipose derived stem cells.* 18th Annual Regenerative Medicine Workshop. Hilton Head Island, SC.

Loboa, E.G. Bodle, J., Charoenpanich, A., Mathieu, P., Mohiti-Asli, M., Tuin, S., Williams, J. *Biomimetic Forces and Scaffolds to Control Human Stem Cell Fate.* The New Jersey Symposium on Biomaterials Science. New Brunskick, NJ October 2012.

Charoenpanich A; Bodle J C; McCullen S D; Pfeiler T W; Bernacki S H; Loboa E G, Human Adipose-Derived Stem Cells in Functional Bone Tissue Engineering. Translational Regenerative Medicine Forum, Washington DC, April 2011.